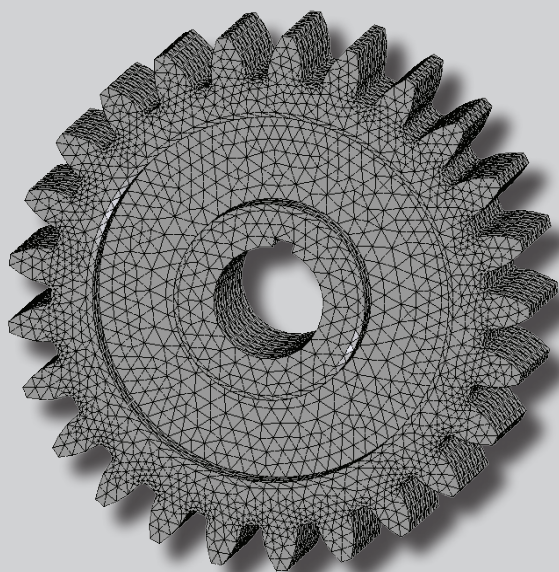




*Hubert Dębski, Jakub Gajewski
Józef Jonak, Grzegorz Ponieważ*

Selected issues of machine design



Lublin 2015

PODRECZNIKI

Selected issues of machine design

Podręczniki – Politechnika Lubelska



HUMAN CAPITAL
NATIONAL COHESION STRATEGY

EUROPEAN UNION
EUROPEAN
SOCIAL FUND



*Publication co-financed by the European Union
under the European Social Fund*

Hubert Dębski , Jakub Gajewski
Józef Jonak , Grzegorz Ponieważ

Selected issues of machine design



Politechnika Lubelska
Lublin 2015

Reviewers:

Dr. hab. inż. Paweł Drożdżel, prof. Politechniki Lubelskiej

Doc. Ing. Dana Stančková, PhD

Translation at the sole request of Lublin University of Technology



Free of charge publication.

The publication was prepared and published as a part of the project *Engineer with a warranty of quality – tailoring the course offer of the Lublin University of Technology to the requirements of the European labour market* (agreement number: UDA-POKL.04.01.01-00-041/13-00), co-financed by the European Social Fund, Human Capital Operational Programme, Submeasure 4.1.1.

Publication approved by the Rector of Lublin University of Technology

© Copyright by Lublin University of Technology 2015

ISBN: 978-83-7947-129-4

Publisher: Lublin University of Technology
ul. Nadbystrzycka 38D, 20-618 Lublin, Poland

Realization: Lublin University of Technology Library
ul. Nadbystrzycka 36A, 20-618 Lublin, Poland
tel. (81) 538-46-59, email: wydawca@pollub.pl
www.biblioteka.pollub.pl

Printed by : TOP Agencja Reklamowa Agnieszka Łuczak
www.agencjatop.pl

The digital version is available at the Digital Library of Lublin University of Technology: www.bc.pollub.pl
Circulation: 200 copies

Contens

Chapter I	Introduction to engineering graphics	7
Chapter II	Designing of screw mechanisms and gears	51
Chapter III	Method of finite elements in engineering applications.....	93
Chapter IV	Modern techniques of production accelerating.....	111

Chapter I

Introduction to engineering graphics

1. Introductory information

1.1. Formats of sheets

While choosing the size of a **drawing sheet**, one should comply with the norm PN – EN ISO 5457 which suggests that the original copy of a drawing should be made on the smallest sheet allowing to gain an indispensable clarity and resolution of the drawing.

The basic paper sheet is the sheet A4 with dimensions 210 mm x 297 mm after cutting. Dimensions of other cut sheets are given in the table 1.1.

Table 1.1. *Dimensions of drawing formats in mm (after cutting)*

Sheet marking	a2	b2
A0	841	1189
A1	594	841
A2	420	594
A3	297	420
A4	210	297

An indispensable element of the format is a label, placed in the right bottom corner of a drawing.

The formats of the sheets A0, A1, A2 and A3 are situated only horizontally, the sheet A4 is situated vertically.

A sheet should have the frame made with continuous line of the thickness of 0,7 mm, at the 5 mm distance from the line of cutting.

1.2. Drawing Lines

Kinds and widths of lines used in the machine technical drawing are based on the norm PN – ISO 128 – 24.

For drawing of elements one ought to use the lines of two widths, while the proportion between **thin and thick lines** should be 1:2, tab. 1.2.

Table 1.2. *Widths of drawing lines in mm*

Width of thin lines	0,13	0,18	0,25	0,35	0,5	0,7	1
Width of thick lines	0,25	0,35	0,5	0,7	1	1,4	2

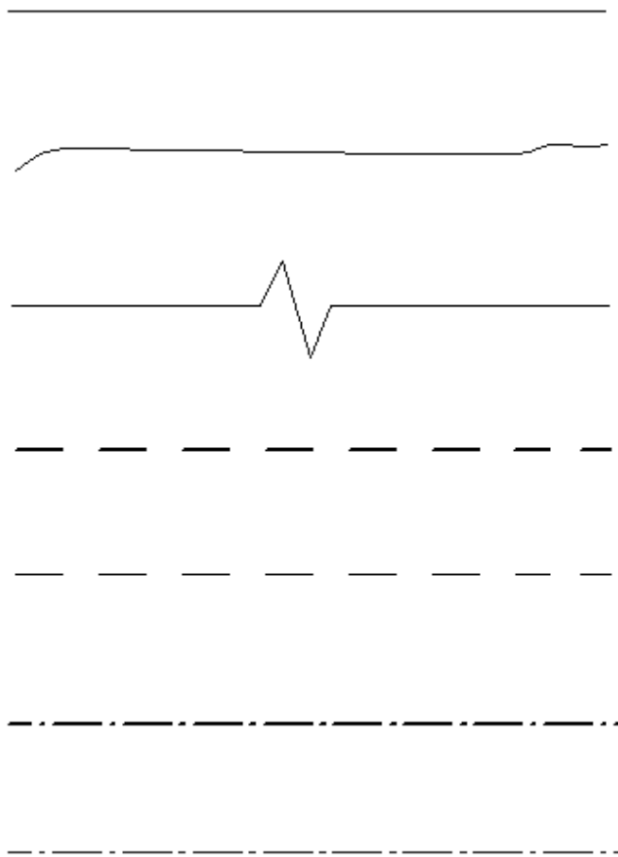
Below, the kinds of lines used in machine technical drawing, and their basic use have been outlined:

- **continuous thick line**; visible edges and contours of an object, contours of detail sections, contouring of drawings
- **continuous thin line**; dimension lines, auxiliary dimension lines, hatching of section field, outlines of superimposed sections,
- **wavy thin line**; used mainly with manual plotting, as partial ending, intermittent view or section, as line separating view from section,
- **thin zigzag line**; used mainly for automatic plotting, has the use like wavy thin line,
- **thick dash line**; for marking of admissible areas of surface processing
- **thin dash line**; invisible contours and edges,
- **thick line with long dash and dot**; for limiting the areas of surface processing; location of sections surface,
- **thin line with long dash and dot**; symmetry axes and surfaces, separating lines,
- **thin line with dash and two dots**; extreme position of moving parts.

Lines in the order of the above order have been presented in the pic. 1.1.

While drawing non-continuous lines one should make sure that:

- distance between the dashes or between dashes and points equals 4 widths of lines
- length of dashes for the line with dash and dot should be from 1- to 12 mm,
- length of dashes for the dash line should be from 3 to 6 mm,
- lines should start, cut across and end with dashes,
- for the circles to 12 mm, axes of symmetry should be drawn with thin continuous line.



Pic. 1.1. *Drawing lines*

1.3. Technical writing

Technical writing in technical drawing is regulated by the norms: PN – EN ISO 3098 - 0 , PN - EN ISO 3098 – 2 and PN – EN 3098 – 5

Values of the **heights of the writing h**, specified by the norms are: 1,8; 2,5; 3,5; 5; 7; 10; 14;20 [mm].

One distinguishes:

- **writing of the kind A**, in which the width of the line of writing d is $d=1/14 h$,
- **writing of the kind B**, in which there is the dependency $d=1/10 h$.

Writing may be **straight** or **slanting** – with the gradient of 75° to the basis of a verse. Below is an example of technical slanting writing – pic. 1.2.

1.4. Scales

Objects in machine drawings may be considerably differentiated as regards measuring. It causes that one should use the **scale**, which is the quotient of line values from the drawing and real line values.

According to the norm PN-EN ISO5455, one should use the following scales:

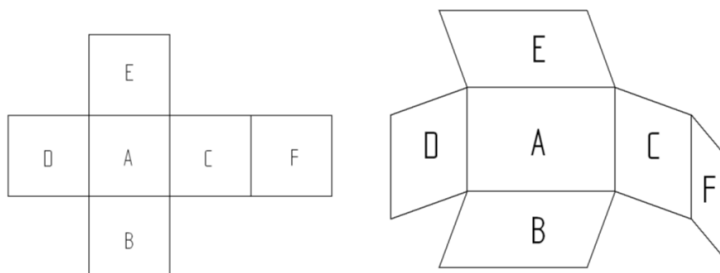
Increasing scale;	50:1; 20:1; 10:1; 5:1, 2:1,
Natural scale;	1:1,
Decreasing scale;	1:2; 1:20; 1:200; 1:2000, 1:5; 1:50; 1:500; 1:5000, 1:10; 1:100; 1:1000; 1:10000.

2. Patterning of geometrical shape of an object

2.1. Rectangle projecting with the European method

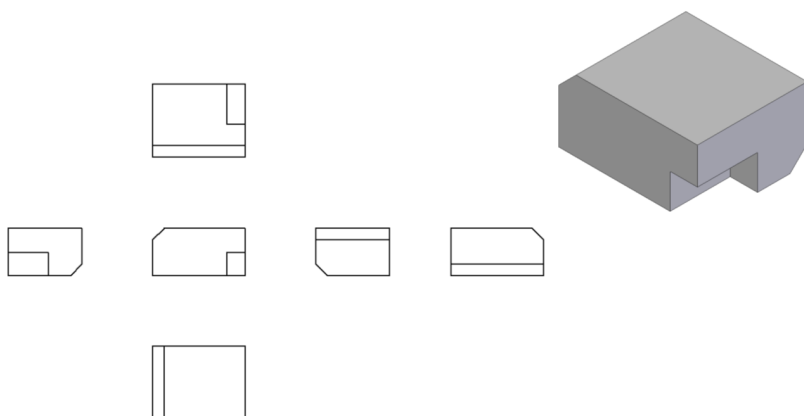
Rectangle projecting with the European method uses the Monge impinging rule. It is based on marking rectangle projections of solid element on six mutually perpendicular surfaces – projection planes. Through this one gets the following projections, pic. 2.1.:

- projection in the direction A – projection from the front, called the main projection
- projection in the direction B – projection from the above
- projection in the direction C – projection from the left
- projection in the direction D – projection from the right
- projection in the direction E – projection from the underneath
- projection in the direction F – projection from the back.



Pic. 2.1. *Rectangle projecting – projection planes*

In the pic. 2.2. the object patterned on six projection planes has been presented.



Pic. 2.2. *Patterning of the object in six mutually perpendicular projection planes*

It is assumed, that:

- number of projections should be limited to an indispensable minimum for unambiguous presentation and measuring of an object,
- the main projection – A – should present an object in usable or processing location, from the side presenting its highest number of details,
- if the usable location is different from the horizontal or the vertical one, the object is drawn in the location which makes most of its characteristic surfaces and axes horizontal or vertical in relation to the projection planes.

Projections of objects may be:

- views**; present the picture of an object while observation from the outside,
- sections**; presenting the surfaces or details of an object, partly or entirely covered by other elements of it.

In the starting phase of an object designing it is hard to predict the number of necessary projections, and what follows – the format of the sheet. Engineering practice suggests, however, to consider the need of using projections B and C before starting from the main projection A and, if need be, to do the further ones.

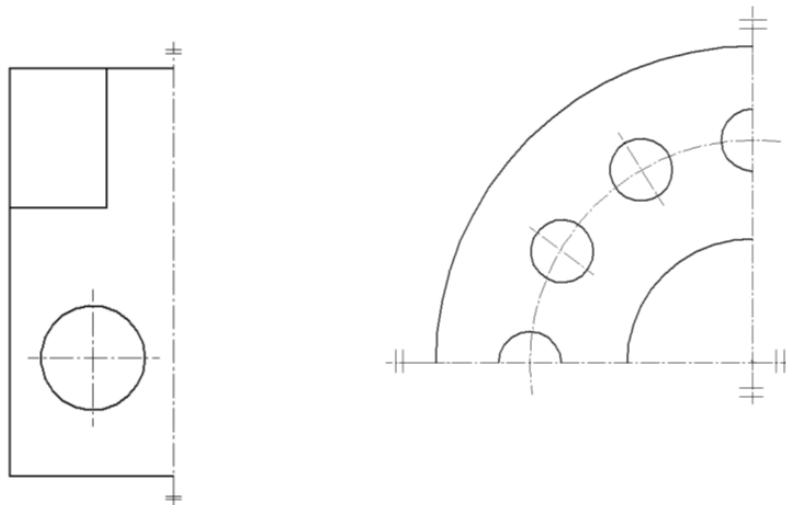
One should also remember about the possibilities of using the projections which are additional views or sections. They will be discussed in the further part of the script.

2.2. Views

The projection which most frequently takes the place of the main projection and specifies the highest number of characteristic traits of a patterned object is called the **basic view**.

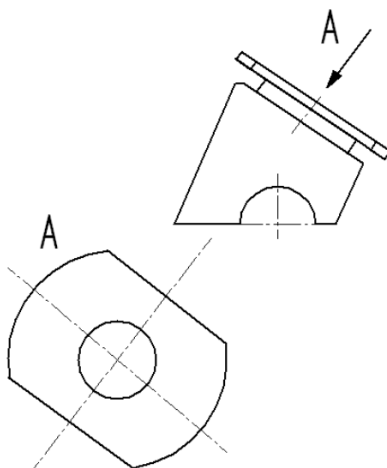
The picture of the object, presented entirely in the drawing, is called the **complete view**. However, when there is a need of showing a certain fragment of an element, one may use the **partial view**.

In the case of symmetrical objects of simple structures, one usually uses half-views or even quarter-views (pic. 3.3).



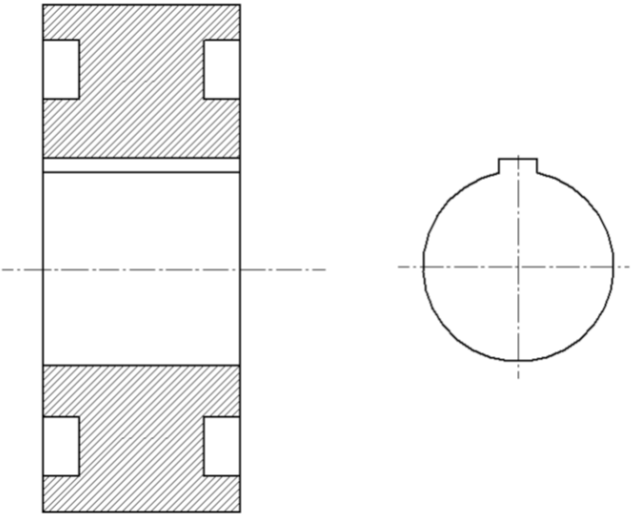
Pic. 2.3. *Patterning of symmetrical objects*

Aid view is used in the cases when one should present part of an object in non-parallel surface to any of basic surfaces of rectangular projection – pic. 3.4.

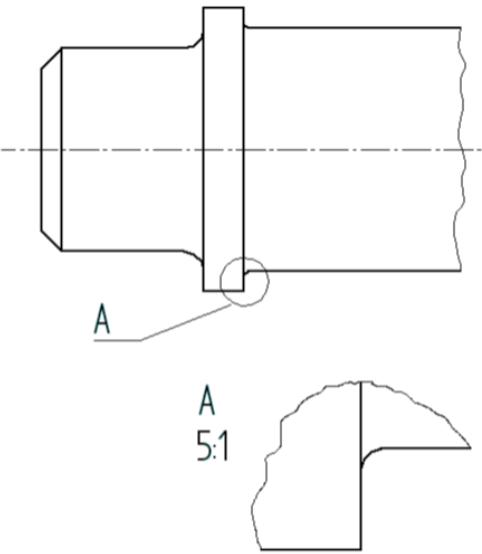


Pic. 2.4. *Aid view*

In specific cases, we also use the **partial views**, like it is shown in the pic. 2.5 and pic. 2.6 on an increased scale.



Pic. 2.5. *Partial view*



Pic. 2.6. *Partial view on an increased scale*

2.3. Sections

Sections are used when there is a necessity of showing geometrical shapes inside of an object, e.g. all kinds of openings. One gets them by cutting through an object with an imaginable cutting surface, eliminating part of the object in front of the surface and drawing flat figure lying within the **surface of section** and all the edges lying beside it.

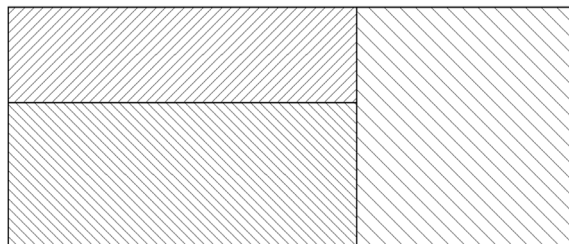
The division of sections may be made by using various criteria. Most frequently these are the characteristics of:

- **complexity of the surface of section, which is the number of surfaces,**
- **size of the area of an object covered with section.**

2.3.1. Marking of sections

The contouring of a flat figure lying directly within the cutting surface should be dashed with the thin continuous line in the gradient of 45° towards the horizontal line, specified most frequently by location of drawing table. In the specific cases it is possible to dash it in the gradient of 30° or 60° . The scale of dashing is adjusted according to the size of the dashed area of the section; the smaller it is, the smaller the distance between dashing lines is and the other way round. It is assumed that the size of scale is from 0,5 to 5 mm – pic. 3.7.

Section of an object in the case of using one cutting surface is presented in the pic. 3.9 and section with three parallel to each other surfaces is shown in pic. 3.10.



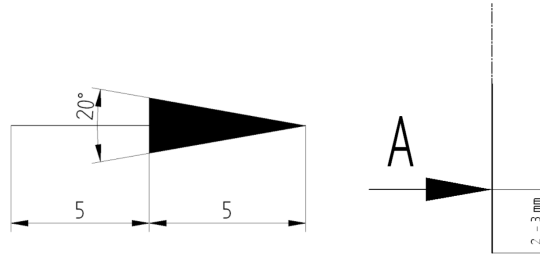
Pic. 2.7. *Dashing of sections*

Full marking of section includes:

- Specification of location of the cutting surface; most frequently in the form of thick line with long dash and dot, drawn beside the contours of an object and, if need be, completed with thin line with long dash and dot; in the case of straight sections, when the location of surface doesn't raise any doubts, there is no need to mark it,

- Specifying the direction of projecting in the form of arrows; in the case when the set of projections made with the European method is kept, and the section takes the place of one of the projections, there is no need to make additional letter markings, which are the capital letters of the Latin alphabet (letters I, O, Q, R, S, X – they are not used in technical drawing).

In the pic. 2.8 graphic tips for drawing and placing arrows are presented.



Pic. 2.8. *Graphic markings for section marking*

2.3.2. Kinds of sections

Taking into consideration the criteria of division of sections given in the pic. 2.3 below the examples of the most frequently used ones have been shown.

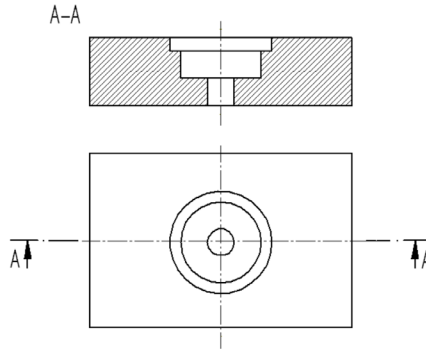
Depending on the used number of surfaces, we divide sections into **simple** – one surface, and **complex** – two or more surfaces.

Complex sections are divided into **gradual** – when the cutting surfaces are parallel to each other, and **broken** – if there is an obtuse angle between the surfaces.

Depending on the area covered with section, they are divided into **complete**, **partial** and **partitive** (called extractions).

Simple sections.

In the pic. 2.9 the element for which it is sufficient to use the simple section is presented. If the location of cutting surface is obvious, it is permissible not to mark it. However, one should always remember about drawing the edges lying beside the surface.

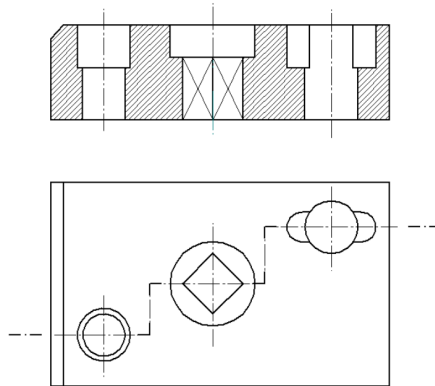


Pic. 2.9. *Simple section*

Complex sections

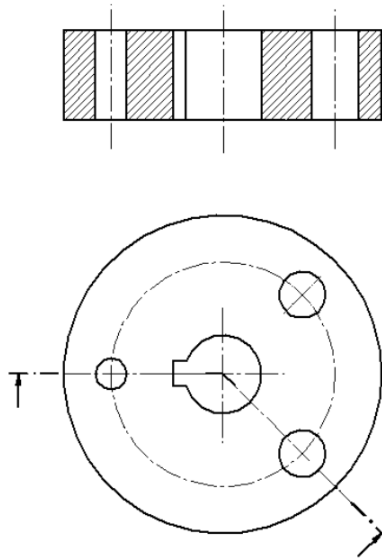
As it was mentioned above, complex sections occur when there was one or more cutting surface used for making the sections. However, while drawing this kind of section, elements presented on different surfaces join in in one - mutual.

In the pic. 2.10 the object is presented, the structure of which required the usage of the three cutting surfaces, mutually parallel. This section is called the **gradual section**. Location of cutting surfaces is completed here with the line with long dash and a dot. Moreover, one should pay attention to the fact, that the gradual section is obtained by bringing the sections placed closer or further from an observer to one surface.



Pic. 2.10. *Complex section – the gradual one*

The other kind of complex section is presented in the pic. 3.11. Cutting surfaces have been used here, the trails of which create the obtuse angle. This is the **broken section**.



Pic. 2.11. *Complex section – the broken one*

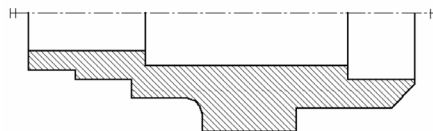
Complete sections

The sections presented in the pictures 2.9, 2.10 and 2.11 belong to the group of complete sections, because they present the full section of the whole object.

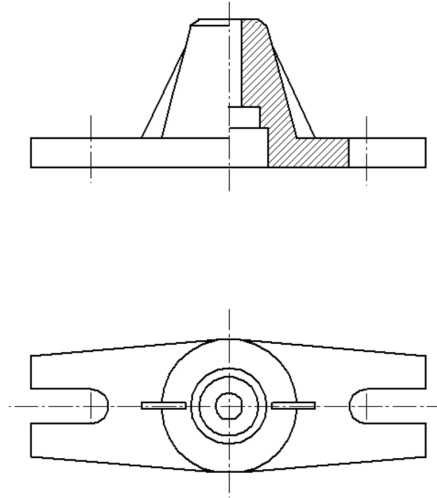
Partial sections

In the case of simple symmetrical objects or the ones of rotary shapes one may easily use the partial section presenting only a certain part of the object contouring. It allows for making graphical works much easier, while knowing the same information about the designed element.

In the pic. 2.12 the object in the projection being half-section was shown, and in the pic. 2.13 half-view and half-section is shown (projection A).



Pic. 2.12. *Rotary solid, half-view*

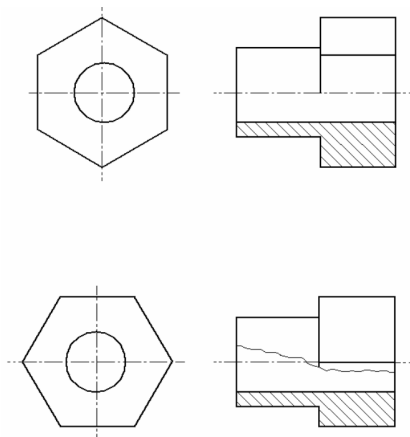


Pic.2.13. Projections of symmetrical object – half-view and half-section

In the case of the half-section, one should pay attention to the fact that according to the norm it may be the right or the left side of the projection. Symmetry of the object has been marked by drawing the segments of the thin continuous line on the axis (pic. 2.12).

It's worth adding that in engineering practice while patterning a rotary object in one projection, one draws it mainly in the half-view of the half-section, despite the fact that half-section is sufficient.

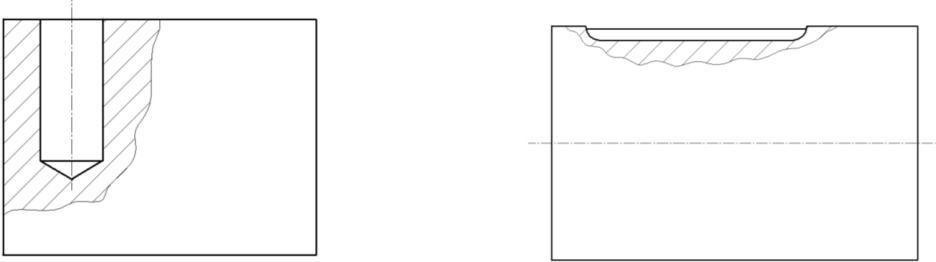
Using the sections presented in the pic. 2.13, one should make sure that the **visible edge** of an object doesn't stand the **line delimiting the half-view and the half-section** – pic. 2.14.



Pic. 2.14. Patterning of hexagons in various locations

Partitive sections.

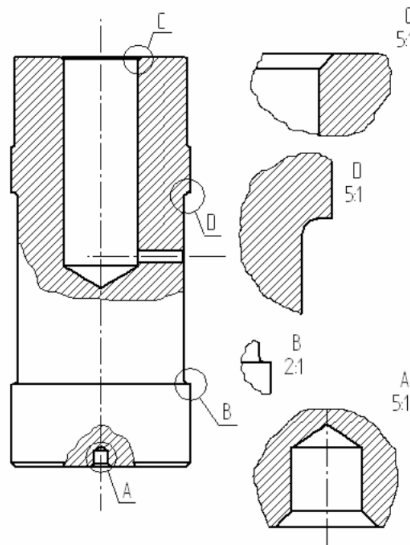
Partitive section, commonly called extraction, is used when there is a need of showing small interior details of an object, with no need of using the complete section. Drawn in the view of the object, it is separated with the wavy line (the thin one) – pic. 2.15.



Pic. 2.15. *Examples of using the partitive section (extraction)*

While using this type of section one should remember that the line limiting the section should never overlap with the line of contour or the edge of an object. If one is drawing several sections lying close to each other, it is best to join them together.

Sometimes there is a need of showing a detail of an object, in increased scale. Such case is presented in the pic. 2.16.



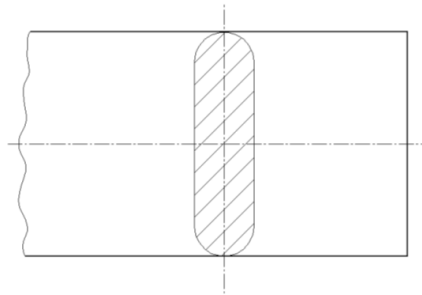
Pic. 2.16. *Partitive sections in increased scale*

2.3.3. Sections

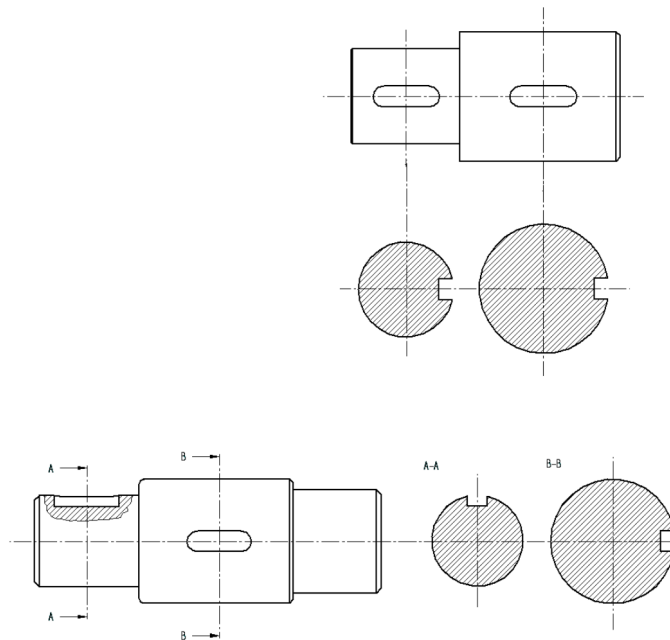
Section is the contour of a geometrical figure lying within the surface of cross section of an object, after bringing this surface to the surface of the made drawing (which is the rotation of 90°). The difference between section and section is based on the rule that in the case of section one doesn't draw the contours of views placed beside the surface of section.

Sections are divided into:

- **local sections** – pic. 2.17, drawn with the thin line in the view of an object,
- **detail sections** – pic. 2.18, drawn besides the view of an object.



Pic. 2.17. *Local section*

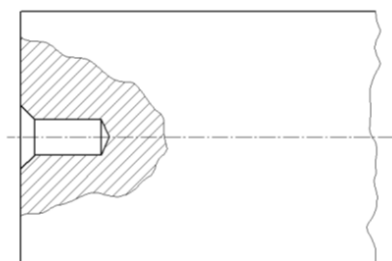


Pic. 2.18. *Detail sections*

2.4. Notices concerning drawing of views and sections

Below we will discuss the issues which one may encounter while patterning an object, and which are not included in the previous chapters.

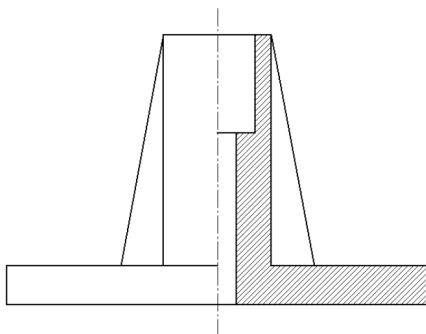
Generally, **full elements, including the ones of rotary shapes** are not presented. If there is a need of showing details, one should use the partitive sections, pic. 2.19.



Pic. 2.19. *Full object of rotary shapes*

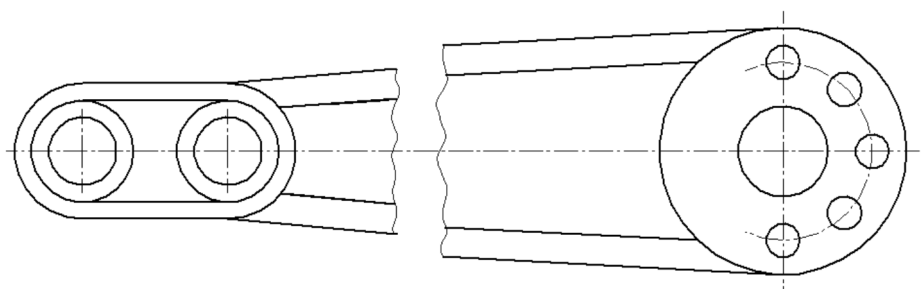
And that is how the elements like pegs, clinches, pivots, bolts, chocks, mortises, drawn in compounding drawings, are presented in views.

One shouldn't also draw **ribs, thin walls, arms of wheels** – pic. 2.20.



Pic. 2.20. *Element of rib type*

Long objects, which don't include any details which would require showing, may be shortened in their middle part, in the way shown in the pic. 2.21.



Pic. 2.21. *Drawing of long objects*

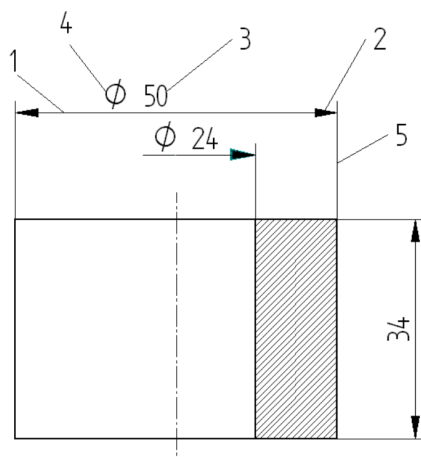
3. Notation of Dimensions

Most of the elements of machines are made of basic geometrical creations such as cylinder, sphere, cone or prism. They are usually slightly modified after processing, however it doesn't change their characteristic contour. This fact has essential influence on the notation of dimensions of a particular element.

3.1. Graphic rules of notation of dimensions

Notation of dimensions in the drawing requires locating of several graphic elements. These are:

- dimension line – 1
- mark of dimension line limitation – 2
- dimension number – 3
- dimension mark – 4
- aid dimension line – 5 (pic. 4.1)



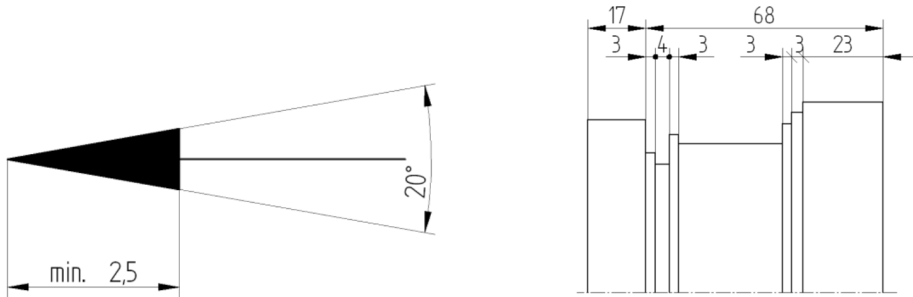
Pic. 3.1. *Graphic elements of dimensions notation*

Dimension lines are drawn as thin continuous lines, parallel to the edge of an object, in the distance not smaller than 10 mm from the line of its contour and 7 mm from the parallel dimension line. The rule is that these lines shouldn't cross each other.

Marks of dimension lines limitation are boltheads, the construction of which is discussed in the pic. 4.2a, and if there is no place, boltheads can be replaced by slanting dashes or by dots of about 1 mm in diameter – pic. 3.2b.

Auxiliary lines are drawn with thin continuous line, lengthened by about 2 mm beyond corresponding to them dimension lines, parallel to them.

Dimension numbers should be placed above the dimension lines, possibly in the middle. One should write them down so that they are legible in two locations of a sheet. One gives line dimensions in mm and angle dimensions in degrees, minutes and seconds.



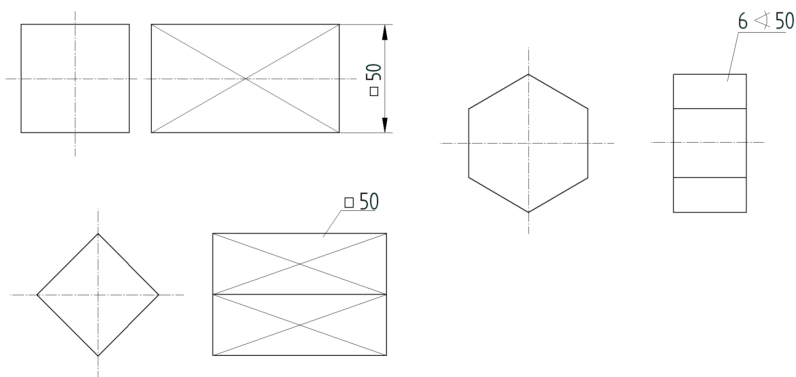
Pic. 3.2. Marks of dimension lines limitations

The use of proper **dimension marks** makes the measuring much easier; it limits the number of projections, which makes reading of a drawing easier.

The most frequently used dimension marks are:

- Ø – diameter; e.g. Ø100
- R – radius; e.g. R50,
- ' square; e.g. '100,
- 6 – hexagon; e.g. 6 100,
- SR – radius of sphere; e.g. SR100,
- SØ – diameter of sphere; e.g. SØ100,
- x – thickness of object presented in one projection; e.g. x 5,
- M – metric thread; e.g. M20.

One should pay attention especially to the difference between placing dimension marks of square and hexagon in the pic. 4.3.



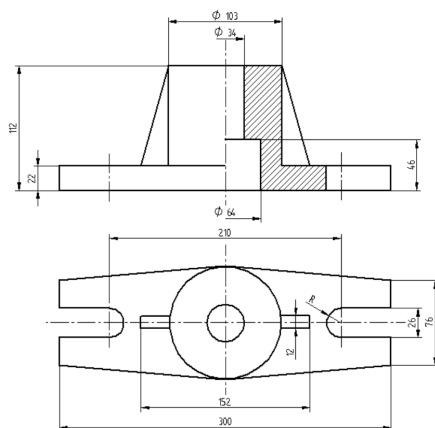
Pic. 3.3. *Measuring of hexagon and square*

3.2. General rules of measuring

When attempting to dimension, one should strictly obey the rules given above.

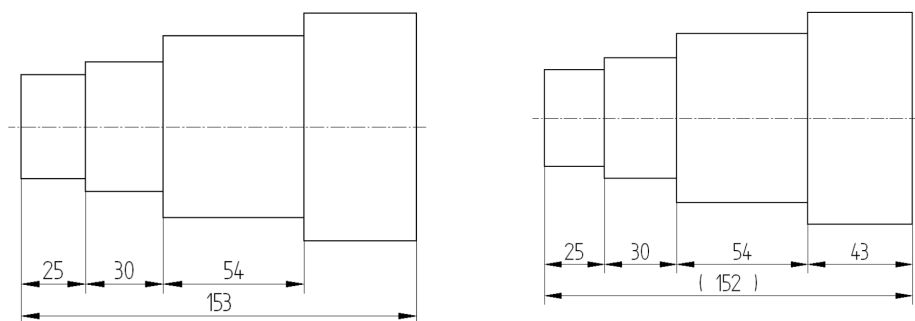
The **rule of necessary dimensions** orders to give only necessary dimensions on a drawing for unambiguous reconstruction of an element.

The **rule of non-repetition of dimensions** assumes that each of the dimensions is given in a drawing only one time. Giving the same dimension on several projections is a mistake. One should also make sure that a dimension is given there, where it is best readable and understandable. That is why, while having e.g. two projections of an element to choose from, one should dimension diameters on section – pic. 3.4.



Pic. 3.4. *Measuring (model UM)*

The **rule of open measuring chain** orders to omit one of the dimensions considered as the resultant in measuring chain. Then, we get open measuring chain. If the dimension makes reading of drawings easier, one may give it as auxiliary one, informative in brackets – pic. 3.5.



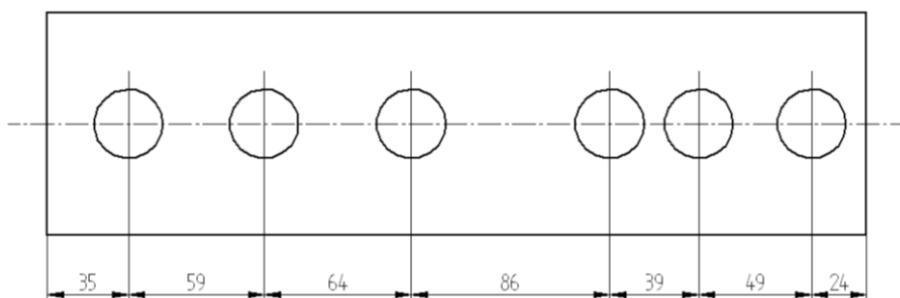
Pic. 3.5. *The rule of open measuring chain*

The **rule of obvious dimensions omission** orders to omit the obvious dimensions, such as e.g. angle dimensions equaling respectively 0° and 90° .

3.3. Kinds of measuring

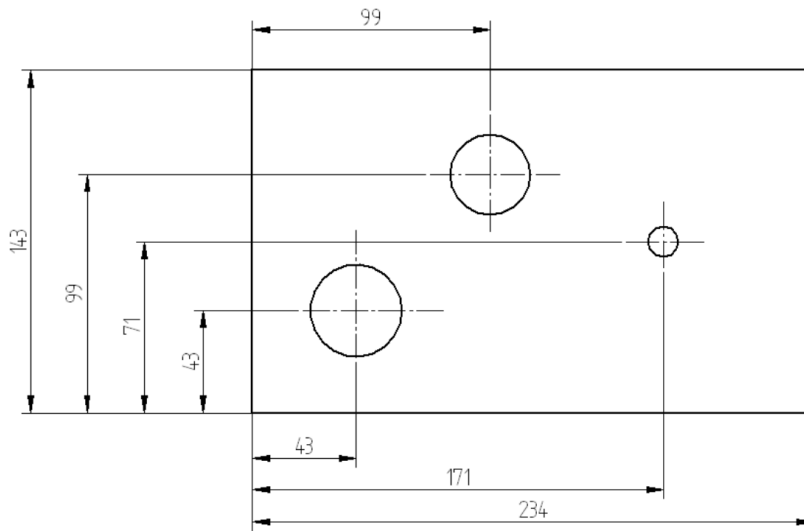
The following ways of measuring the objects are distinguished:

- **measuring in the serial system of dimensions**, based on giving dimensions one after another; this way is used when attention is paid to precision of mutual location of the neighboring geometrical elements of an object – pic. 3.6,



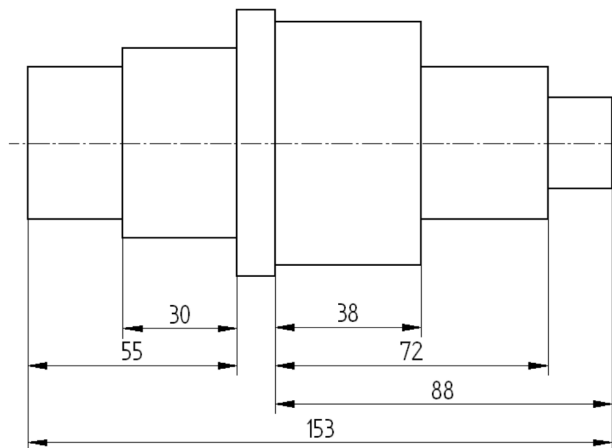
Pic. 3.6. *Measuring in serial system*

- **measuring in parallel system of dimensions**, is based on one measuring base; this way is used when there is a necessity of precise location of geometrical elements of an object towards one measuring base – pic. 3.7,



Pic. 3.7. *Measuring in parallel system*

- **measuring in mixed system of dimensions** is a mixture of serial and parallel measuring – pic. 3.8,



Pic. 3.8. *Measuring in mixed system*

4. Marking of Surface Roughness

Roughness, which is a geometrical structure of worked surfaces, is described usually with the aid of parameter R_a , specified as arithmetic mean of absolute values of profile's deviation from average line in the range of elementary segment.

In the picture the value of roughness has been presented in micrometers.

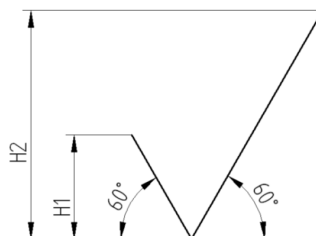
Normalized, advisable by the norm values of the parameter R_a are given in the table 5.1.

Table 5.1. *Advisable values of parameter R_a [μm]*

R_a [μm]	R_a [μm]	R_a [μm]
400	12,5	0,40
200	6,3	0,20
100	3,2	0,100
50	1,6	0,050
25	0,80	0,025

4.1. Marks of roughness

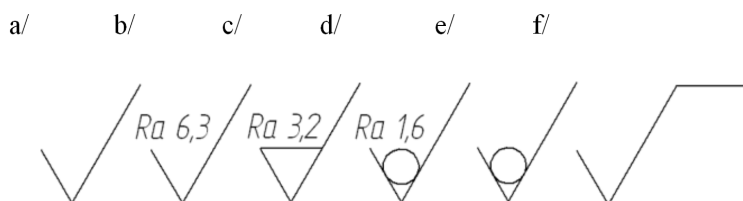
The basic **graphic mark** used for marking roughness in the drawing is made of two segments of the continuous of various length, inclined in the angle of 60° to the line which marks the surface – pic. 5.1.



Pic. 4.1. *The basic graphic mark of roughness*

The heights H^1 and H^2 are adjusted depending on the height of writing in the drawing sheet.

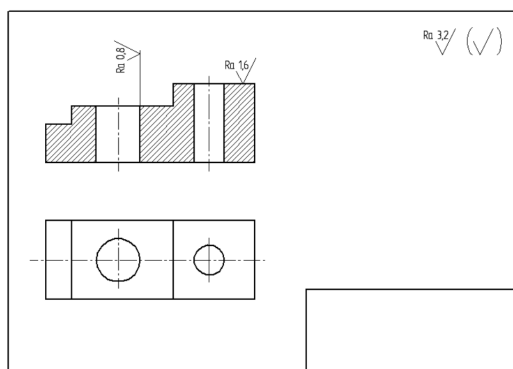
For marking roughness graphic symbols presented in the pic. 5.2 ought to be used.



Pic. 4.2. *Graphic symbols of marking the roughness*

The mark in the pic. 5.2a is used for marking several surfaces of an object, most frequently in collective markings of roughness.

In the pic. 5.2b the mark used when an expected roughness of a surface is gotten without removing or with removing a layer of material was shown. The mark in the pic. 5.2c is used when an expected roughness of surface is gotten only with removing a layer of material; in the pic. 5.2d without removing a layer of material. Another mark, 5.2e, is used when one should keep roughness from the previous technological process or for metallurgic making, e.g. raw cast. The last mark is used for giving detailed characteristics of surface's roughness. Marks of roughness should be placed in the right upper corner of a drawing, according to the pic. 5.3, in the distance from 5 to 10 mm from frame.



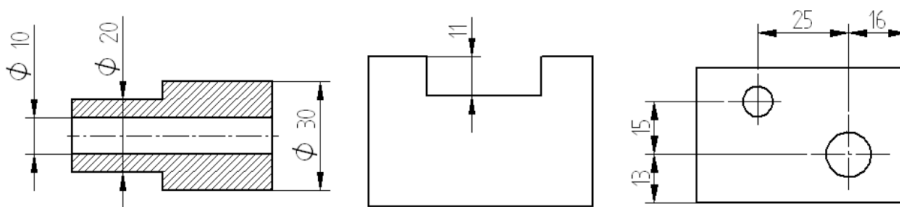
Pic. 4.3. *Placing of mark of roughness in drawings*

5. TOLERANCES AND FITS

5.1. Tolerances of line dimensions

Tolerating is based on specifying the range of values of permissible deviations from the **nominal dimension**.

Dimensions specifying a patterned object may be divided into: **external dimensions** (e.g. external diameters) – pic. 6.1a, **internal** (e.g. internal diameters) – pic. 6.1a, **mixed** pic. 6.1b and **intermediate** – pic. 6.1c.



Pic. 5.1 Kinds of dimensions

As regards precision of making an element, dimensions may be divided into: **free, theoretical** and **tolerated**.

Free dimensions are the ones for which there is no need to specify the deviation. **Theoretical dimensions** are also specified without giving deviations, they are usually dimensions for adjusting tools or tests. **Tolerated dimensions** are the ones for which deviations have been specified.

The dimension towards which the deviations are specified is the **nominal dimension** N – pic. 6.2.

Upper side dimension B (B_o is specified for internal dimension and B_w for external dimension) it is the highest permissible value of the tolerated dimension.

Lower side dimension B (A_o is specified for internal dimension and A_w for external dimension) it is the lowest permissible value of the tolerated dimension.

Upper deviation (ES for internal dimension and es for external dimension) it is the remainder of upper side dimension and nominal dimension.

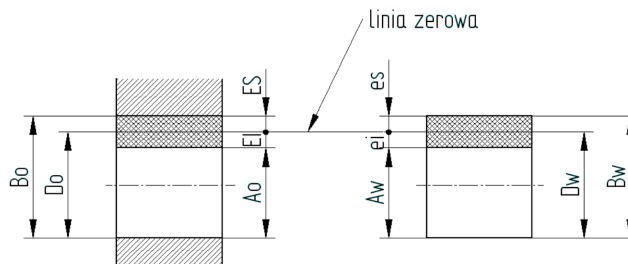
$$ES = es = B - N$$

Lower deviation (EI for internal dimension and ei for external dimension) it is the remainder between lower side dimension and nominal dimension.

$$EI = ei = A - N$$

The **area of tolerance T** is the area included in between upper and lower side dimension.

$$T = B - A = es - ei = ES - EI$$



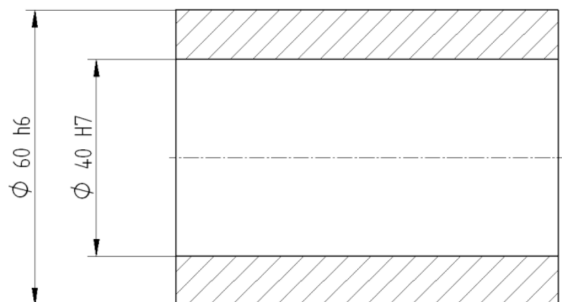
Pic. 5.2. Marks of location of dimensions, deviations and tolerances

The following can be distinguished:

- **normal tolerating**
- **free tolerating**

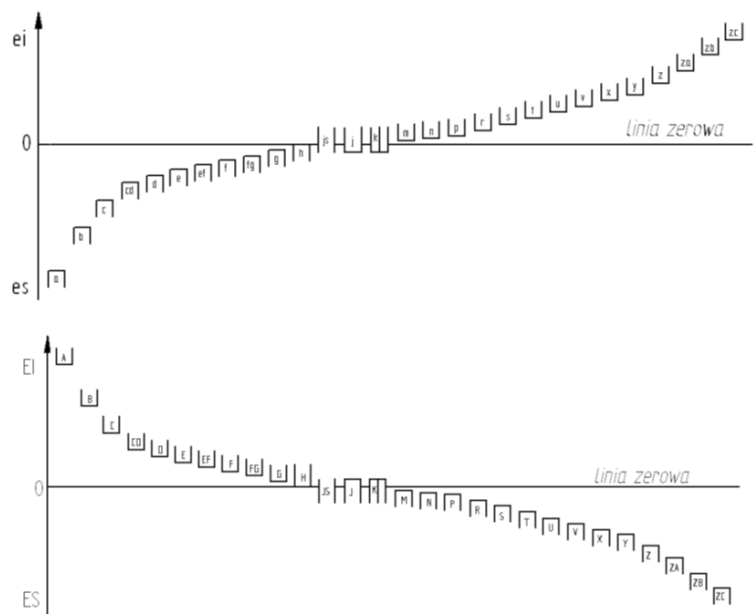
Normal tolerating is based on giving deviations based on set of tolerances included in proper norms. **Free tolerating** is based on giving deviations not connected with any conditions included in norms.

The example of marking dimensions' normal tolerating is presented in the pic. 5.3.



Pic. 5.3. Drawing notation of normal tolerating

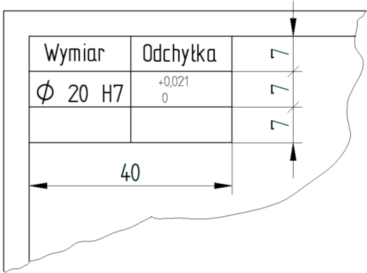
Letter symbols placed next to the dimension number specify the location of area of tolerance towards the baseline. Distribution of basic deviations and their letter symbols are presented in the pic. 5.4.



Pic. 5.4. *Distribution of basic deviations for shafts and openings*

In the notation of tolerated dimensions in the pic. 5.3, the numbers by the letters – h6, H7 – signify class of precision of making. There are 20 obligatory precision classes: 01; 0; 1; 2 ... 18, in order of decreasing precision.

The values of deviations read from the norms, indicated always in mm, are noted in table placed in the left upper corner of a drawing, as shown on the pic. 5.5.



Pic. 5.5. *Table of deviations placed in a drawing*

5.2. Fits of elements

One specifies **fit** as a way of co-operation of parts co-operating with each other: **shaft** (in conventional meaning of external dimension) and **opening** (in conventional meaning of internal dimension).

We distinguish the following fits:

- **loose**
- **tight**
- **mixed**

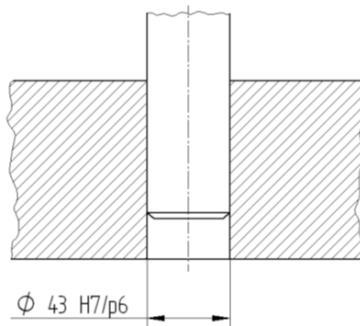
Loose fit occurs when the area of toleration of a shaft lies under the area of toleration of an opening. **Tight fit** occurs when the area of toleration of a shaft lies above the area of toleration of an opening; **mixed fit** – when these areas overlap completely or partially.

In a general structure of machines we commonly use the following fits:

- **on the basis of continuous opening – H**
- **on the basis of continuous shaft – h**

The first one of them is privileged. In case of the opening, the location of which is specified by the letter H, we adjust the toleration of shaft from the norms so as to provide the assumed co-operation of these elements.

The notation of fit used in drawings is presented in the pic. 5.6.



Pic. 5.6. The notation of fit

5.3. Tolerating of shape and location

The norm PN - 87/M – 01145 specifies the rules of **tolerance of shape and location**. The notation used in drawings should include:

- mark of kind of tolerance,
- number value of tolerance.

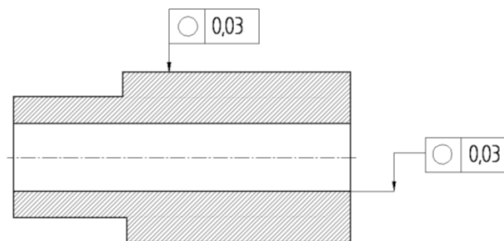
In the pic. 5.7 there is a notation of:

- **tolerance of shape:**
 - a) rectilinearity – pi. 5.7a,
 - b) flatness – pic. 5.7b,
 - c) roundness – pic. 5.7c,
 - d) cylindricity – pic. 5.7d,
- **tolerance of location:**
 - e) parallelism – pic. 5.7e,
 - f) perpendicularity – pic. 5.7f,
 - g) inclination – pic. 5.7g,
 - h) coaxiality – pic. 5.7h,
 - i) symmetry – pic. 5.7i,
 - j) position – pic. 5.7j,
- **tolerance of shape and location of:**
 - k) squareness – pic. 5.7k,
 - l) complete beating – pic. 5.7l,
 - m) shape of a given contour – pic. 5.7m,
 - n) shape of marked surface– pic. 5.7.

a)	b)	c)	d)	e)	f)	g)
—	▭	○	⊥	∥	⊥	∠
⊙	≡	⊕	↗	↗	⌒	⌒
h)	i)	j)	k)	l)	m)	n)

Pic. 5.7. Graphic signs for notation of tolerance, shape and location

The way of notation of shape and location in drawings is presented in the pic. 5.8.



Pic. 5.8. Notation of tolerance and shape in drawing

Notices for design classes

Signs of tolerance, shape and location should be written in with the height of writing $h = 3,5$ mm, height of frame should be $2h = 7$ mm

6. Connections

6.1. Thread connections

Thread connections belong to the group of disjoint connections.

Threads are characterized by the following values:

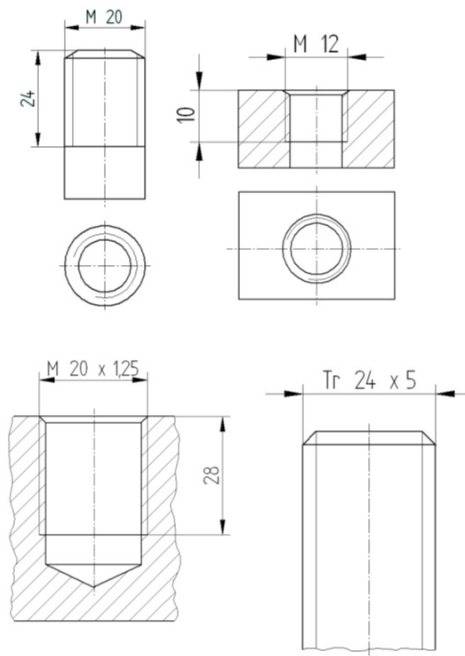
- diameter of a thread
- scale
- shape of a thread's contour – triangular, rectangular, trapezoidal symmetrical and non-symmetrical, round.

All kinds of threads are drawn in the same way, completing the dimensions with normalized marks.

One of the most frequently used threads is the **metrical thread** (of triangular contour) marked with the letter **M**.

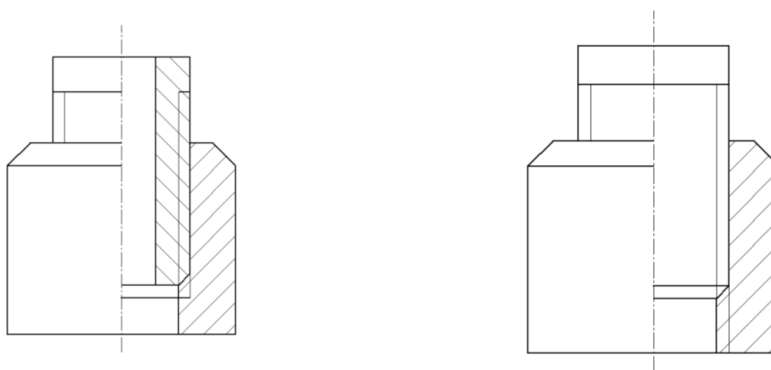
Elements with threads are drawn with simplification, patterning the bottoms of furrows with the continuous thin line, the peaks of a thread's ledges with the continuous thick line and ends of threads with continuous thick line, transversal towards the axis of a thread – pic. 6.1.

Distance from the thin line to the thick line equals the height of a thread, and is not smaller than 0,8 mm. In projection on surface perpendicular to the axis of a thread, one marks the thread by drawing continuous thin line for $\frac{3}{4}$ of a circle. This line shouldn't start or end on axes of symmetry.

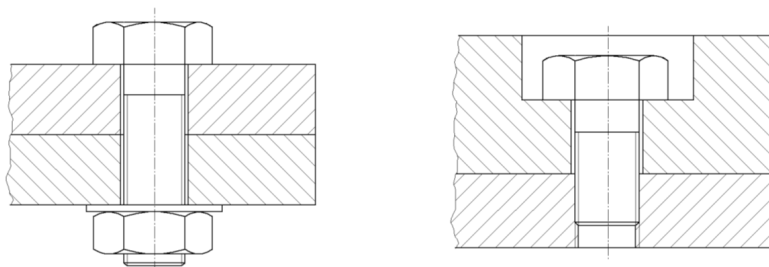


Pic. 6.1. *Elements with metric and trapezoidal symmetrical threads*

Examples of thread connections are presented in the pic. 7.2 and the pic. 7.3.



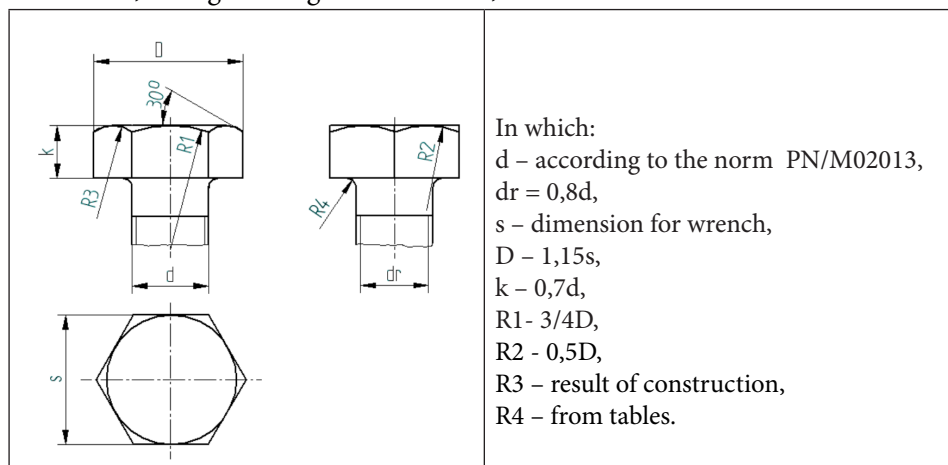
Pic. 6.2. *Thread connection*



Pic. 6.3. *Examples of thread connections*

While patterning the thread connections, one draws them so that the external thread always covers the internal thread.

Heads of threads should be drawn according to the pic. 6.4. In the same way one draws nuts, taking the height of nut $w = 0,8 d$.

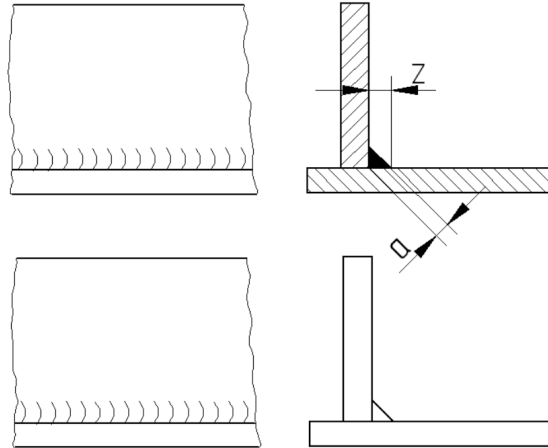


Pic. 6.4. *Drawing of heads of hexagonal screws*

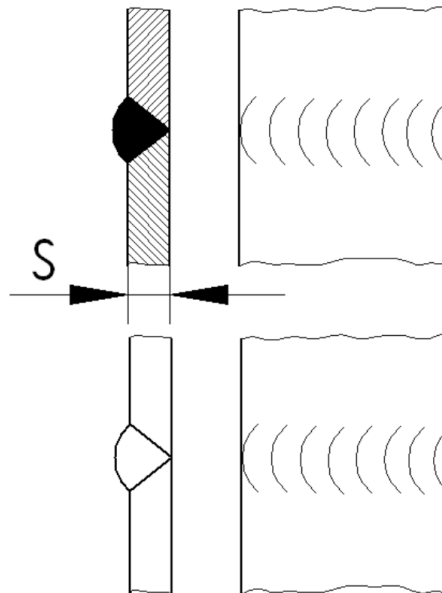
6.2. Welded connections

Welded connections belong to disjoint connections, in which the fundamental joining element is a weld. There are dozen or so various kinds of welds. One may draw welded connections in simplified way or in conventional way. While patterning the welded connection in the simplified way, in view, in projection from the side of weld's face, one marks it by drawing a row of perpendicular to each other arches with continuous thin line. In projection from the front, one draws contour

of elements of connection and of the weld with continuous thick line. In section, the weld is to be blackened. In the pic. 6.5 there is a spandrel weld and in the pic. 6.6 the front weld with characteristic dimensions is shown.

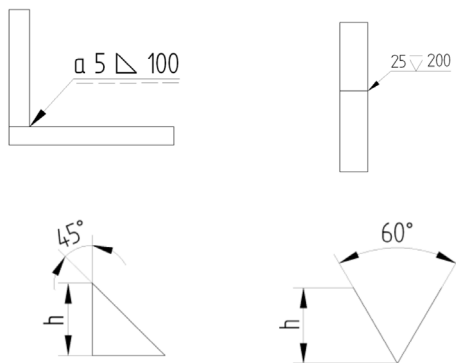


Pic. 6.5. *Spandrel weld*



Pic. 6.6. *Front weld*

While using the conventional way of patterning of welded connection, one assumes that the weld specified with a proper graphic mark is known, and that is why one doesn't draw it. The location of the weld, its shape and dimensions are given in the way presented below in the pic. 6.7.



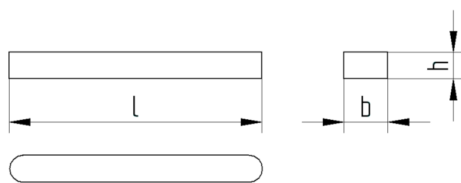
Pic. 6.7. *Measuring of spandrel and front weld, graphic marks*

The line of correspondence should be drawn with continuous thin line ended with an arrowhead which should touch the weld, most often from the front side. The graphic mark of weld should be drawn on the shelf of marking line. Characteristic dimensions of cross section of the weld should be written on the left from the mark, while for the front welds it is the value s , and for the spandrel welds there are values a or z . On the right side of the mark of weld one places the dimensions of profile section of the weld, its length. The identifying line (dashed one) drawn under the marking line specifies the location of weld towards the placed dimension. The location and measuring shown in the pic. 6.7 is the one most often used.

6.3. 7.3. Inlet connection

Inlet connections belong to the group of disjoint connections. One distinguishes prism, shuttle, suppository symmetrical and suppository non-symmetrical inlets.

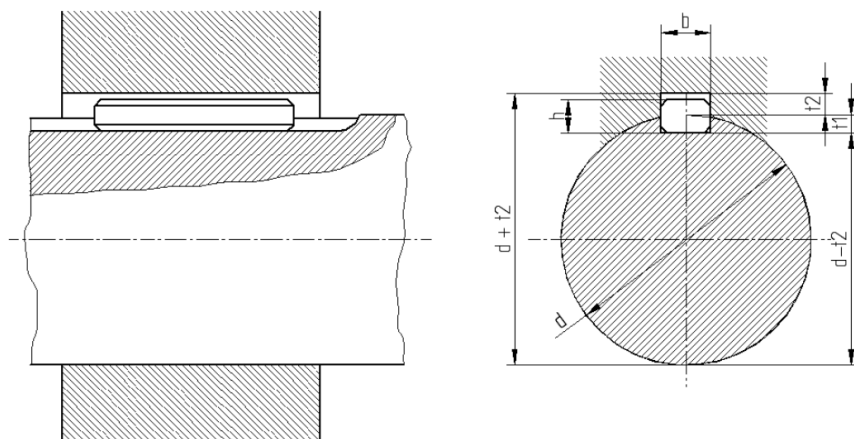
In the pic. 6.8 the prism inlet of A type is presented.



In which: b – width, h - height, l – length

Pic. 6.8. *Prism inlet*

The connection with the use of inlet is presented in the pic. 6.9.



Pic. 6.9. *Inlet connection*

Inlets are measured in the simplified way. From the contour of inlet one draws the line of correspondence and the marking line, above which one writes in, for prism inlets:

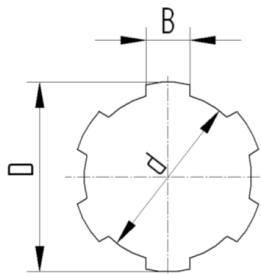
- prism inlet
- letter sign meaning the type of inlet
- values of width, height and length
- number of a proper norm

This notation has the following form: **Prism inlet A 12 x 8 x 56 PN/M-85005**

6.4. Splined connections

Splined connections belong to the group of disjoint connections. They provide the connection by properly shaped inlets. One distinguishes parallel splins and evolvent splins.

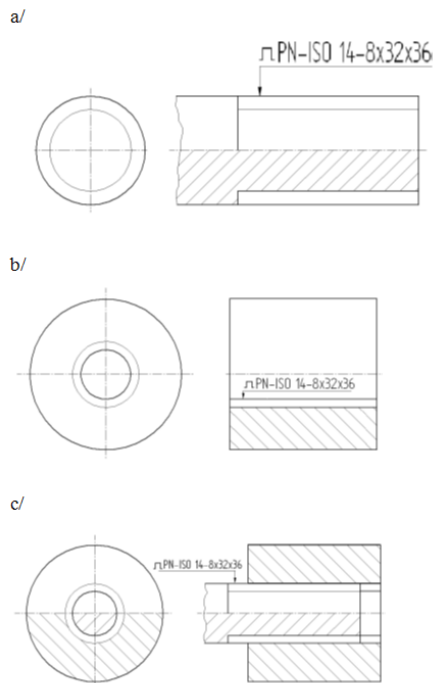
The example of a parallel splin is presented in the pic. 6.10.



In which:
 d – internal diameter,
 D – external diameter,
 B – width of splin.

Pic. 6.10. *Contour of splined shaft*

Elements of spline connector and the connector itself are drawn with simplification, in the way presented in the pic 6.11



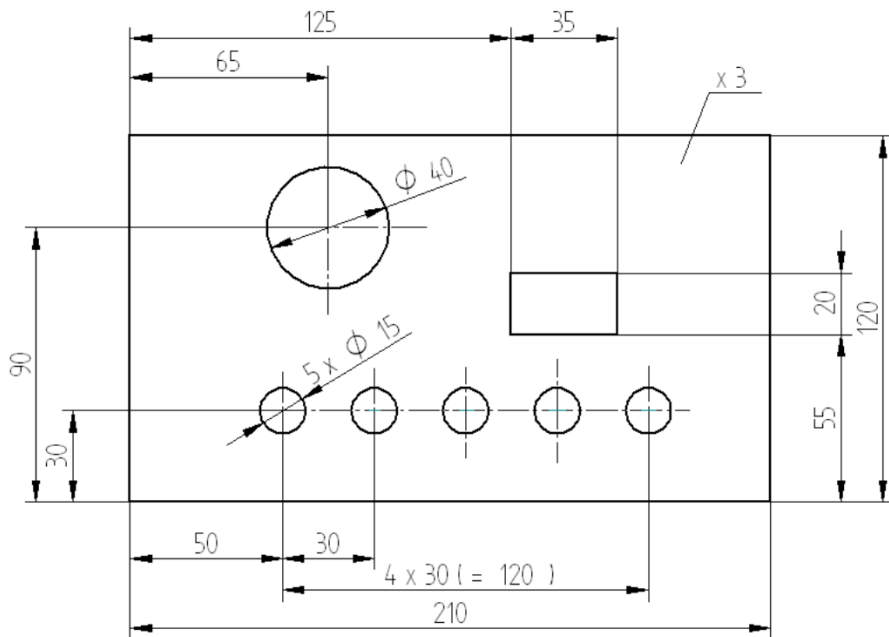
Pic. 6.11. *Elements and spline connectors: a) shaft, b) hub, c) connector*

Measuring of an element of spline connector includes the following markings:

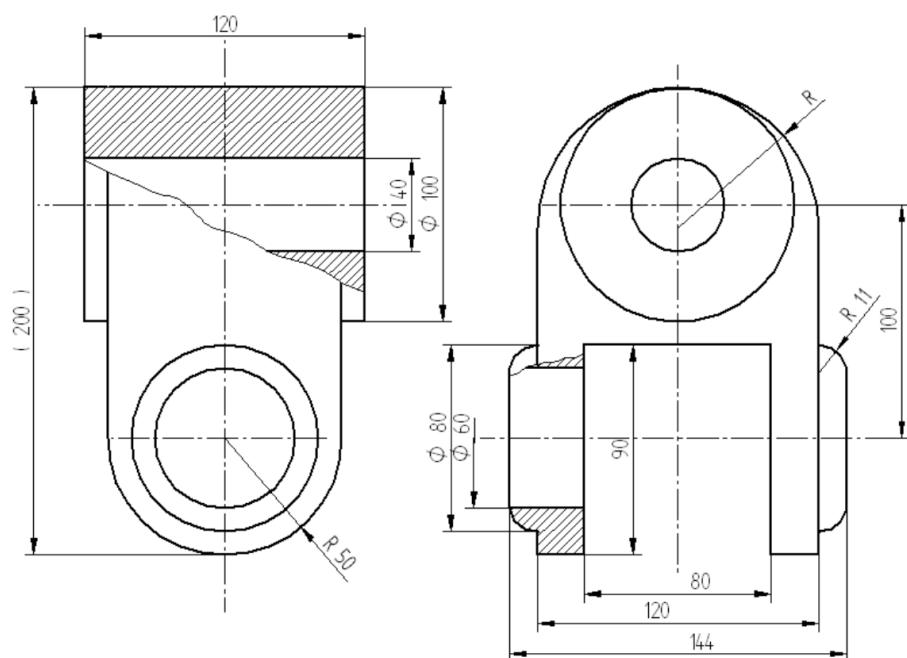
- graphic mark of spline,
- number of the norm PN – ISO 14,
- number of splines – e.g. 8,
- dimension of internal diameter– e.g. 32,
- dimension of external diameter – e.g. 36.

The above mentioned values are compliant with the norm.

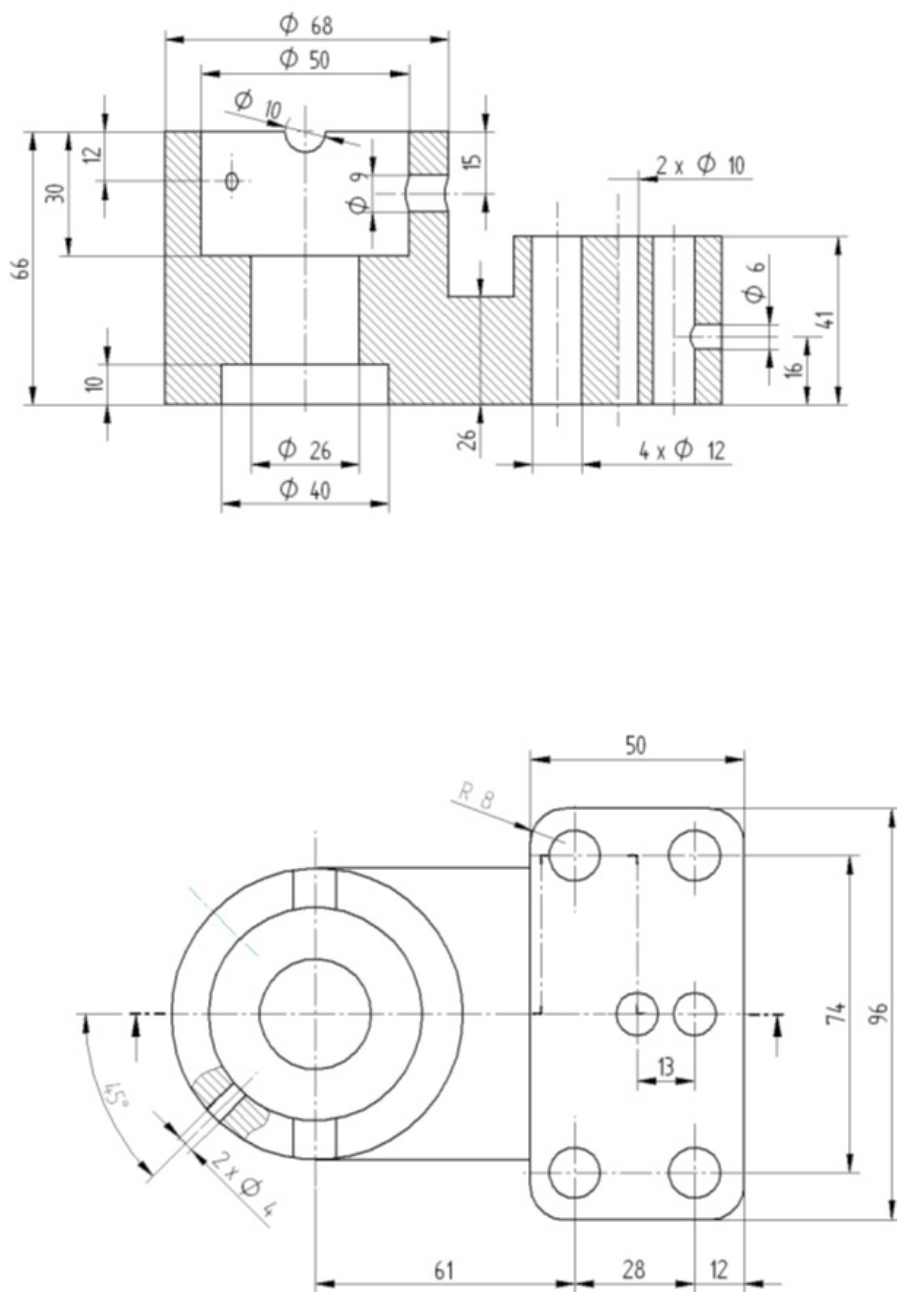
7. Example Solutions of Subjects of Design Exercises



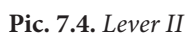
Pic. 7.1. PH plate

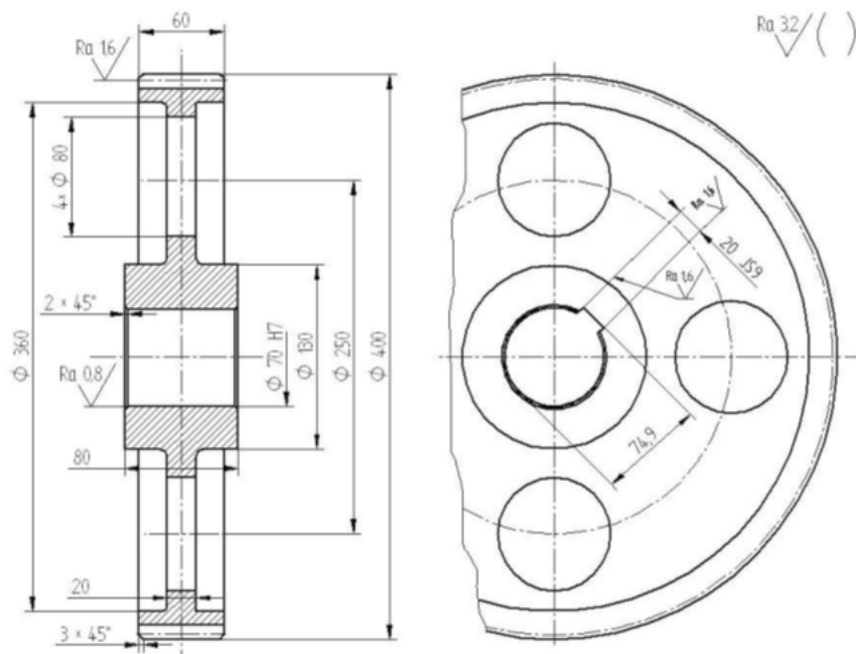


Pic. 7.2. *UC model*



Pic. 7.3. UO model





Number of cogs	z	79
Normal module	m	5
Angle of contour	α	20
Coord. of height of the cog	y	1
Coord. of dislocation of contour	x	0
Class of precision		7
Scale diameter	d	395
Height of the cog	h	8,5

Pic. 7.6. Gear

Literature

1. Bajkowski J.: *Bases of notation of construction* Publishing house of Warsaw University of Technology, Warsaw 2005 (*Podstawy zapisu konstrukcji* Oficyna Wydawnicza Politechniki Warszawskiej, Warszawa 2005).
2. Bober A., Dudziak M.: *Notation of construction* Scientific Press of the PWN, Warsaw 1999 (*Zapis konstrukcji*. Wydawnictwo Naukowe PWN, Warszawa 1999).
3. Dobrzański T.: *Machine technical drawing*. Scientific and technical Presses, Warsaw 2004 (*Rysunek techniczny maszynowy*. Wydawnictwa Naukowo Techniczne, Warszawa 2004).
4. Lewandowski T.: *Technical drawing for mechanics*. School and Pedagogical Press (SPP), Warsaw 2003 (*Rysunek techniczny dla mechaników*. WSiP, Warszawa 2003).
5. Polish Norms. *Technical Drawing and Machine Technical Drawing*. (Polskie Normy. *Rysunek Techniczny i Rysunek Techniczny Maszynowy*).

Chapter II

Designing of screw mechanisms and gears

1. Designing of screw lift

Screw lift designed with drive through the screw. Basic guidelines of construction include:

- working load of the lift 20kN
- height of lifting 300mm
- welded construction of the corpus
- movable crown (korona ruchoma) enabling nut's(nakrętka) rotary towards the screw
- pole triggered drive.

1.1. Calculation of the diameter of core of the screw and adjustment of thread

Assuming that material of the screw is steel C35 of the following resistance parameters: $k_{cj} = 85\text{MPa}$, $k_{gj} = 75\text{MPa}$, $k_{gj} = 115\text{MPa}$.

In the considered case of the screw lift the core of the screw is loaded with axial force arousing the squeezing stresses and with the twining moment arousing the twining stress. However, taking into consideration a considerable length of the screw, the resistance to buckling decides, above all, about its resistance. Thus, we can write down the resistance condition:

$$\sigma_c = \frac{Q}{A} \leq k_w = \frac{R_w}{x_w}$$

In which:

Q – axin load of the lift,
 A – area of the section of the screw's core,
 R_w – limit of resistance to buckling,
 x_w – safety factor on buckling.

With regards to a considerable height of lifting and the character of screw's fixing (one end placed in the nut, the other one free) we may assume that slimness of the screw will be bigger than the limit slimness, so for calculations of the lift we can use the Euler formula:

$$R_w = \frac{\pi^2 E}{s^2}$$

In which:

E – Young's module, we assume it for steel 210000MPa,
 s – slimness expressed through the formula,

$$s = \frac{l_s}{0,25d_3}$$

l_s – free (buckling) length including height of lifting and height of crown, also the place remained for the drive and way of fixing the screw,
 d_3 – diameter of the screw's core.

In the analyzed calculation example, the whole length of twined screw with the crown equals:

$$l = H + H_k$$

in which:

H – the assumed height of lifting
 H_k – height of the crown

We assume that the height of crown will be $H_k = 60\text{mm}$, so the free length will be:

$$l_s = 2l = 2(H + H_k) = 720 \text{ mm}$$

After transforming the Euler's formula we'll get the formula allowing to mark the diameter of the screw's core:

$$d_3 = \sqrt[4]{\frac{64x_w Q l_s^2}{\pi^3 E}}$$

Assuming that the buckling safety factor $x_w = 5$, we'll get the diameter of the core:

$$d_3 = \sqrt[4]{\frac{64 \cdot 5 \cdot 20000 \cdot 720^2}{\pi^3 \cdot 210000}} = 26,71 \text{ mm}$$

On the basis of the norm PN-ISO 2904+A:1996 we adjust the trapezoidal symmetrical thread **Tr34×6** of the following geometrical parameters:

$$d = 34,00 \text{ mm}, d_3 = 27,00 \text{ mm}, D_1 = 28,00 \text{ mm}, D_4 = 35,00 \text{ mm}, P = 6 \text{ mm}.$$

We calculate the slimness for the assumed thread and compare the received result with the value of limit slimness (Table 1.2):

$$s = \frac{l_s}{0,25d_3} = \frac{720}{0,25 \cdot 27} = 106,67$$

For the assumed material of the screw, the limit slimness is $s_{gr} = 90$, so the condition of applicability has been met:

$$s = 106,67 > s_{gr} = 90$$

Table 1.1 *Trapezoidal metrical threads (PN-ISO 2904+A:1996)*

Nominal size d	Scale P	Diameter of the screw's thread d₃	Internal diameter D₁	External diameter D₄
10	1,5	8,20	8,50	10,30
	2	7,50	8,00	10,50
12	2	9,50	10,00	12,50
	3	8,50	9,00	12,50
14	2	11,50	12,00	14,50
	3	10,50	11,00	14,50
16	2	13,50	14,00	16,50
	4	11,50	12,00	16,50
18	2	15,50	16,00	18,50
	4	13,50	14,00	18,50
20	2	17,50	18,00	20,50
	4	15,50	16,00	20,50

22	3	18,50	19,00	22,50
	5	16,50	17,00	22,50
	8	13,00	14,00	23,00
24	3	20,50	21,00	24,50
	5	18,50	19,00	24,50
	8	15,00	16,00	25,00
26	3	22,50	23,00	26,50
	5	20,50	21,00	26,50
	8	17,00	18,00	27,00
28	3	24,50	25,00	28,50
	5	22,50	23,00	28,50
	8	19,00	20,00	29,00
30	3	26,50	27,00	30,50
	6	23,00	24,00	31,00
	10	19,00	20,00	31,00
32	3	28,50	29,00	32,50
	6	25,00	26,00	33,00
	10	21,00	22,00	33,00
34	3	30,50	31,00	34,50
	6	27,00	28,00	35,00
	10	23,00	24,00	35,00
36	3	32,50	33,00	36,50
	6	29,00	30,00	37,00
	10	25,00	26,00	37,00
38	3	34,50	35,00	38,50
	7	30,00	31,00	39,00
	10	27,00	28,00	39,00
40	3	36,50	37,00	40,50
	7	32,00	33,00	41,00
	10	29,00	30,00	41,00
44	3	40,50	41,00	44,50
	7	36,00	37,00	45,00
	12	31,00	32,00	45,00
46	3	42,50	43,00	46,50
	8	37,00	38,00	47,00
	12	33,00	34,00	47,00

Source: The norm PN-ISO 2904+A:1996

Table 1.2. Values of material coordinates R_0 , R_1 , s_{gr}

Material	Symbol	R_0 MPa	R_1 MPa	s_{gr}
Coal steel, very soft	S185, C10, C15	303	1,29	112
Coal steel, soft	S235JR, S235JRG1, C20, C22, C30	310	1,19	105
Coal steel, middle hard	S275JR, E295, C35, C40, C45	335	0,62	90
Coal steel, very hard	E360, C55, C60	470	2,3	86

Source: Szewczyk K., *Thread connections (Połączenia gwintowe)*, Warszawa, Scientific Press of the PWN (Wydawnictwo Naukowe PWN), 1991

We calculate the buckling safety factor as follows:

$$R_w = \frac{\pi^2 E}{s^2} = \frac{\pi^2 \cdot 210000}{106,67^2} = 182,15 \text{ MPa}$$

$$\sigma_c = \frac{4Q}{\pi d_3^2} = \frac{4 \cdot 20000}{\pi \cdot 27^2} = 34,93 \text{ MPa}$$

$$x_w = \frac{R_w}{\sigma_c} = \frac{182,15}{34,93} = 5,21$$

The safety factor has achieved the value inconsiderably higher than the one assumed in the beginning, so we can say that the thread has been adjusted correctly.

1.2. Calculation of nut's dimensions

We assume that the material of nut – bronze CuSn10Pb10 is characterized by small fraction coefficient in cooperation with steel. We mark the height of the nut on the basis of condition of surface pressure on thread's pitches. With regard to mutual movement of the screw and the nut under considerable load of values of permissible stress we assume $p_{dop} = 12 \text{ MPa}$:

$$p = \frac{Q}{A} = \frac{4QP}{\pi(d^2 - D_1^2)H_n} \leq p_{dop}$$

In which:

H_n – is the height of nut,

D_1 – is the internal diameter of nut

After transforming and substituting the values, we mark the minimal height of nut resulting from the condition of surface stresses:

$$H_n \geq \frac{4QP}{\pi(d^2 - D_1^2)p_{dop}} = \frac{4 \cdot 20000 \cdot 6}{\pi(34^2 - 28^2) \cdot 12} = 34,23\text{mm}$$

With regard to necessity of providing a good cooperation between screw and nut, additionally there should be the so-called condition of good conduction met, on whose basis the height of nut should be:

$$H_n = (1,2 \div 1,5) \cdot d = (1,2 \div 1,5) \cdot 34 = 40,8 \div 51,0\text{mm}$$

Finally, we get the height of nut $H_n = 45\text{mm}$.

The external diameter of nut is marked through putting the same deformation of screw and nut while remembering that the above mentioned assumption will be real only in the case when the screw and the nut are squeezed at the same time. In order to meet the above assumption, there should be the following dependency:

$$\frac{1}{E_s A_s} = \frac{1}{E_n A_n}$$

In which:

E_s and E_n are the values of Young's module for materials of screw and nut ($E_s = 210000\text{MPa}$ for steel, $E_n = 100000\text{MPa}$ for bronze), then A_s and A_n are the areas of full sections of the screw and the nut.

After transforming, we'll get the dependency allowing to mark the diameter of external nut D_z :

$$E_s \frac{\pi d_3^2}{4} = E_n \frac{\pi(D_z^2 - D_4^2)}{4}$$

and on:

$$D_z = \sqrt{\frac{E_s}{E_n} d_3^2 + D_4^2} = \sqrt{\frac{210000}{100000} \cdot 27^2 + 35^2} = 52,49\text{mm}$$

We assume the external diameter of the nut $D_z = 54\text{mm}$.

1.3. Strength calculations of screw

We mark the moment of strength in thread connection while lifting the load, on the basis of the dependency:

$$M_s = 0,5Qd_s \operatorname{tg}(\gamma + \rho')$$

In which:

D_s – average diameter of screw and nut's cooperation

$$d_s = \frac{d + D_1}{2} = \frac{34 + 28}{2} = 31\text{mm}$$

γ – angle of the screw line's lifting

$$\operatorname{tg}\gamma = \frac{P}{\pi d_s} = \frac{6}{\pi \cdot 31} = 0,0616$$

$$\gamma = 3,53^\circ$$

ρ' – apparent angle of friction for the friction coordinate $\mu = 0,1$

$$\operatorname{tg}\rho' = \frac{\mu}{\cos \alpha_r} = \frac{0,1}{\cos 15^\circ} = 0,1035$$

$$\rho' = 5,91^\circ$$

By substituting the above data we'll get the value of the moment of strength in thread connection:

$$M_s = 0,5 \cdot 20000 \cdot 31 \cdot \operatorname{tg}(3,53^\circ + 5,91^\circ) = 51543 \text{ Nmm}$$

We mark stresses reduced in the core of screw; however, with regards to the fact that the basic condition during calculations is the buckling condition, one should expect that the marked values will be smaller than the permissible values.

$$\sigma_z = \sqrt{\sigma_c^2 + 3\tau_s^2} \leq k_{cj}$$

$$\sigma_c = 34,93\text{MPa}$$

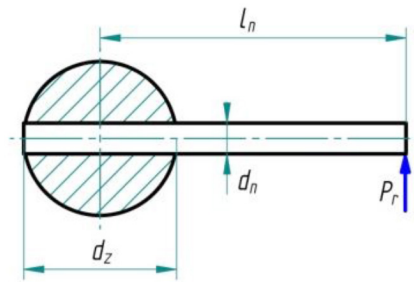
$$\tau_s = \frac{16M_s}{\pi d_3^3} = \frac{16 \cdot 51543}{\pi \cdot 27^3} = 13,34 \text{ MPa}$$

Thus, we can mark the value of reduced stresses:

$$\sigma_z = \sqrt{34,93^2 + 3 \cdot 13,34^2} = 41,88 \text{ MPa} < k_{cj} = 85 \text{ MPa}$$

1.4. Calculations of drive pole

We assume the force of arm on the level of 250N (from the range of values 200 ÷ 300). If we assume that between crown and screw we'll place a small ball, we may also assume that the value of the moment of friction between the ball and the nest is small in relation to the value of the moment of friction in the coils of thread. Thus, we can omit its value and while calculating the length of pole, we take into consideration only the moment M_5



Pic. 1.1. *The scheme of lift driving*

The length of pole (distance from the axin of screw) is marked on the basis of the dependency:

$$l_n = \frac{M_s}{P_r} = \frac{51543}{250} = 206 \text{ mm}$$

We assume the value $l_n = 205 \text{ mm}$.

Assuming the material of pole, steel C55, and assuming the diameter of the pole's placement in the range:

$$d_z = (1,1 \div 1,2) \cdot d = (1,1 \div 1,2) \cdot 34 = 37,2 \div 40,8 \text{ mm}$$

we assume the value $d_z = 40 \text{ mm}$.

The diameter of pole is marked from the condition for folding:

$$d_n = \sqrt[3]{\frac{32M_g}{\pi k_{gj}}}$$

In which:

$$M_g = P_r \cdot (l_n - 0,5d_z)$$

Thus, by substituting the values we get:

$$d_n = \sqrt[3]{\frac{32P_r(l_n - 0,5d_z)}{\pi k_{gj}}} = \sqrt[3]{\frac{32 \cdot 250 \cdot (205 - 0,5 \cdot 40)}{\pi \cdot 155}} = 14,48\text{mm}$$

And we assume the diameter of driving pole $d_n = 14,5\text{mm}$

In the end we check stresses in the nest of driving pole, one should remember to assume permissible stresses as permissible values for a lighter material.

$$p_{\max} = \frac{6M_s}{d_z^2 d_n} = \frac{6 \cdot 51543}{40^2 \cdot 14,5} = 13,4\text{MPa} < p_{dop} = 28\text{MPa}$$

1.5. Calculating of the basis

Assume constructing the internal diameter of the basis $D_{pw} = 90\text{mm}$ and the external diameter $D_{pz} = 150\text{mm}$, then mark the value of the basis' stress on the ground assuming $p_{dop} = 2\text{MPa}$ as the permissible values.

$$p = \frac{Q}{A} = \frac{4Q}{\pi(D_{pz}^2 - D_{pw}^2)}$$

$$p = \frac{4 \cdot 20000}{\pi(150^2 - 90^2)} = 1,77\text{MPa} < p_{dop} = 2\text{MPa}$$

The marked values of surface stresses on the ground are smaller than permissible values, thus the assumed constructing dimensions of the basis are to be considered as the correct ones.

1.6. Testing calculations of the corpus

Assuming that the corpus of lift will be made of steel pipe without seam (material S235JR) of the external diameter 56mm and thickness of wall 3mm, mark slimness of the pipe assuming that its length equals the height of lift, fully pulled out.

$$s = \frac{l_s}{i_x} = \frac{l_s}{0,25 \cdot \sqrt{D_{kz}^2 + D_{kw}^2}} = \frac{1440}{0,25 \cdot \sqrt{56^2 + 50^2}} = 76,7$$

With regard to the slimness being smaller than the limit slimness ($s_{gr} = 105$ - Table 2), thus the permanent buckling occurs there and the Tetmajer's formula should be used:

$$R_w = R_0 - R_1 s$$

For the assumed corpus the constants R_0 and R_1 takes the following values:

$$R_0 = 310 \text{ MPa}, \quad R_1 = 1,19 \text{ MPa}$$

After substitution one gets:

$$R_w = R_0 - R_1 s = 310 - 1,19 \times 76,7 = 218,7 \text{ MPa}$$

Marking of the buckling safety factor for the corpus of lift:

$$x_w = \frac{R_w}{\sigma_c} = \frac{R_w \pi (D_{kz}^2 - D_{kw}^2)}{4Q} = \frac{218,7 \cdot \pi \cdot (56^2 - 50^2)}{4 \cdot 20000} = 5,46$$

The calculated safety factor is bigger than the assumed at the beginning value and it is bigger than buckling safety factor for the screw, thus one may assume that the thickness of wall of the pipe has been fitted correctly. One should remember that in reality the value of buckling safety factor for the corpus is bigger than the marked one, which is beneficial, this difference results from the regard to the accepted simplifications of the model of calculations.

1.7. Testing calculations of placing the nut in nest

Assume that the nut will be placed in nest with tight fitting H7/s6 or H7/r6. Besides, assume that axis load will be moved through the surface of the nest of nut's bottom. The nut will be secured from rotation, with two longitudinal pegs.

Check the condition of nut's stresses on the bottom of the nest (permissible stresses for bronze CuSn10Pb10 $p_{dop} = 28\text{MPa}$), assuming the internal diameter of the nest $D_w = 36\text{mm}$ (for the thread **Tr34×6**):

$$p = \frac{4Q}{\pi(D_z^2 - D_w^2)} = \frac{4 \cdot 20000}{\pi(54^2 - 36^2)} = 15,72\text{MPa} < p_{dop} = 28\text{MPa}$$

Assuming two cylindrical pegs 4×18 on the basis of the norm PN-ISO8734:2003, we check resistance conditions for stresses and the cuttings of the pegs.

$$p = \frac{2M_s}{D_z d_k l_k} = \frac{2 \cdot 51543}{54 \cdot 4 \cdot 18} = 26,5\text{MPa} < p_{dop} = 28\text{MPa}$$

$$\tau_t = \frac{M_s}{D_z d_k l_k} = \frac{51543}{54 \cdot 4 \cdot 18} = 13,3\text{MPa} < k_{ij} = 61\text{MPa}$$

The pegs have been fitted correctly and they will secure net from rotation. An additional security from the rotary of net will be placing of the net in nest by using tight fit H7/s6 or H7/r6.

1.8. Testing calculations for security from full unscrewing of lift's screw

The screw of the lift should be secured from the possibility of full unscrewing from the net. One may use a washer of the external diameter 45mm, tightened with the aid of screw of left-twisting thread M10LH. The screw should enable load of stretching force of the value equaling to the lifted load Q .

$$\sigma_r = \frac{4Q}{\pi d_3^2} = \frac{4 \cdot 20000}{\pi \cdot 8,160^2} = 382,45\text{MPa}$$

Thus we may use the screw M10LH×35 of the class of mechanical features 8.8 for which the limit of plasticity is $Re = 640\text{MPa}$.

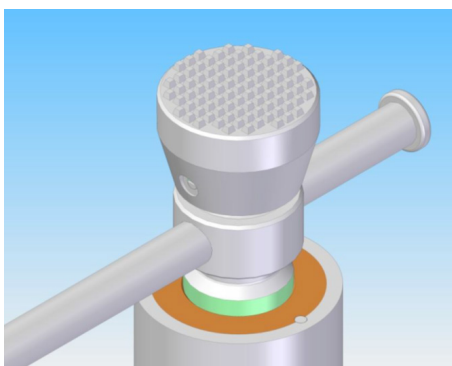
1.9. Screw lift with drive through the screw – model 3D

In the pictures 1.2 and 1.3 the 3D model of the calculated before screw lift with drive through the screw has been presented. In the next picture 1.4 the fragment of unveiled upper part of the lift is shown; there are visible screws securing the crown

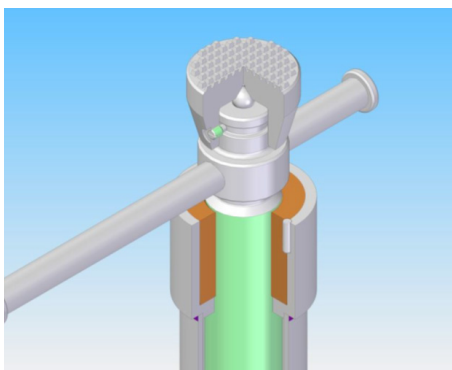
from sliding off the screw and cylindrical pegs securing the net from rotary in the nest. Pic. 1.5 presents the lower part of lift in section, there is a visible washer and the screw securing the main screw from full unscrewing of the net. One should remember that the securing screw has the opposite thread in relation to the main screw.



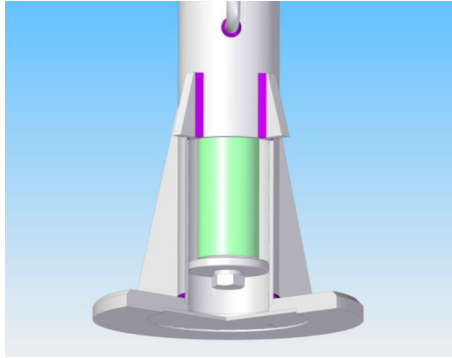
Pic. 1.2. *Screw lift with drive through the screw – 3D model*



Pic. 1.3. *The view of upper part of the lift*



Pic. 1.4. *Section of the upper part of the lift*



Pic. 1.5. *Lower part of the lift – securing washer*

2. Designing of reducer with cylindrical wheels with screw cogs

We design one-step reducer with cylindrical wheels with screw cogs. Introductory data for calculations:

- force by entering of transmission $N = 15\text{kW}$,
- rotary speed on entering $n_1 = 1000\text{obr/min}$,
- transmission ratio $u = 4 \pm 3\%$,
- hour durability $Lh = 12000\text{h}$.

2.1. Introductory selection of wheels' dimensions

With regard to a complicated character of conditions deciding on wheels' resistance, marking of dimensions on their basis is made highly difficult. Thus, making introductory calculations of wheels' dimensions seems to be necessary, while assuming lots of important parameters of cog wheel, and checking of resistance conditions and potential correcting of the assumed dimensions. The divisional diameter of the smaller wheel may be marked on the basis of the dependency [1]:

$$d_1 = 270 \sqrt[3]{\frac{N}{n_1 \psi Q_u} \cdot \frac{u+1}{u}} \quad [\text{mm}]$$

In which:

Q_u – rate of load,

ψ – relative width of cog wreath of pinion, $\psi = b/d_1$,

N – force located by the calculated pair of wheels [kW],

u – geometrical transmission ratio,

n_1 – rotary speed of pinion

The ratio of load Q_u is approximately proportional to stresses in the bottom of cog and to contact stresses. We may assume its values for transmission of general use dependently on the circuit speed of cog while assuming the use of alloy steel for carburizing [1]:

$$Q_u = \begin{cases} 3,46 - 6,92 \frac{N}{mm^2}, & \text{przy } v \leq 5 \text{ m/s} \\ 2,42 - 5,20 \frac{N}{mm^2}, & \text{przy } v > 5 \text{ m/s} \end{cases}$$

Relative width of cog wreath one may assume by the Table 2.1. Assuming introductory the value $Q_u = 6 \text{ N/mm}^2$ and $\psi = 0,75$ we'll get the divisional diameter of pinion:

$$d_1 = 270 \sqrt[3]{\frac{N}{n_1 \psi Q_u} \cdot \frac{u+1}{u}} = 270 \sqrt[3]{\frac{15}{1000 \cdot 0,75 \cdot 6} \cdot \frac{4+1}{4}} = 43,45 \text{ mm}$$

Table 2.1. Advisable values of relative width of pinion $\psi = b/d_1$

Location of wheels towards bearing	Hardness of cog's sides	
	HB \leq 350	HB $>$ 350
Symmetrical	0,80 – 1,40	0,40 – 0,90
Non-symmetrical	0,60 – 1,20	0,30 – 0,60
supporting	0,30 – 0,40	0,20 – 0,25

Source: Dziama A., Michniewicz M., Niedźwiedzki A., *Przekładnie zębate*, Warszawa, Wydawnictwo Naukowe PWN, 1989

The divisional diameter may be marked also on the basis of other dependency [2]:

$$d_1 = f_H \sqrt[3]{\frac{M_s K}{\psi \sigma_{HP}^2} \cdot \frac{u+1}{u}} \quad [\text{mm}]$$

In which:

$f_H = 770$ for the wheels of simple cogging

$f_H = 690$ for the wheels of diagonal cogging

M_s = turning moment of pinion

K – working coordinate, first we may assume the values of the range 1,3-1,7,

σ_{HP} – permissible contact stresses

σ_{Hlim} – contact exhaustion resistance, by assuming the use of wheel of alloy steel for carbonizing, the value = 1600 – 1630 MPa.

Substituting the assumed values for the above dependency we'll get:

$$d_1 = f_H \sqrt[3]{\frac{M_s K}{\psi \sigma_{HP}^2} \cdot \frac{u+1}{u}} = 690 \cdot \sqrt[3]{\frac{9550 \frac{15}{1000} \cdot 1,5}{0,75 \cdot (0,8 \cdot 1600)^2} \cdot \frac{4+1}{4}} = 41,56 \text{ mm}$$

We can notice that on the basis of both dependencies we've got the approximate values of divisional diameter and for the further calculations we can assume smaller value.

Using introductorily marked value of divisional diameter we may mark the distance between axes of wheels:

$$a = 0,5 d_1 (u+1)$$

Next, assuming the number of pinion's cogs z_1 and the angle of gradient of the line of cogs β we mark the nominal module:

$$m_n = \frac{2a}{z_1 (u+1)} \cos \beta$$

In which:

z_1 – number of cogs of the pinion (Table 2.2)

β – angle of cogs' gradient (advisable values $8 - 20^\circ$)

Table 2.2. *Advisable number of pinion's cogs*

Wheels' material	Transmission ratio			
	1	2	3	4
Improved steel HB < 230	32 – 60	29 – 55	25 – 50	22 – 45
Improved steel HB > 300	30 – 50	25 – 45	23 – 40	20 – 35
Carbonized steel	21 – 32	19 – 29	16 – 25	14 – 22
Note: use lower ranges with: $n_1 < 1000$ rotations/min, upper with: $n_1 > 3000$ rotations/min				

Source: Dziama A., Michniewicz M., Niedźwiedzki A., *Przekładnie zębate*, Warszawa, Wydawnictwo Naukowe PWN, 1989

Taking the values $z_1 = 19$ and $\beta = 15^\circ$, and next substituting in the formulae we'll get:

$$a = 0,5 d_1 (u+1) = 0,5 \cdot 41,56 \cdot (4+1) = 103,90 \text{ mm}$$

$$m_n = \frac{2a}{z_1(u+1)} \cos \beta = \frac{2 \cdot 103,09}{19 \cdot (4+1)} \cos 15^\circ = 2,10 \text{ mm}$$

Mark the number of cogs of big wheel, remembering that wheels don't have mutual aliquots:

$$z_2 = u \cdot z_1 = 4 \cdot 19 = 76$$

Take the normalized value of module (Table 2.3), number of cogs of the bigger wheel and then mark real transmission ratio:

$$m_n = 2,25 \quad z_2 = 77$$

$$u = \frac{z_2}{z_1} = \frac{77}{19} = 4,05$$

Table 2.3. Chosen normalized values of nominal modules m_n

Sequence	Nominal module m_n [mm]					
1	1	1,25	1,5	2	2,5	3
	4	5	6	8	10	12
2	1,125	1,375	1,75	2,25	2,75	3,5
	4,5	5,5	7	9	11	14

Source: Norm PN-ISO 54:2001

Table 2.4. Chosen lengths of axes of general purpose reducers a_w

Sequence	Axis distance a_w [mm]			
1	50	63	80	100
	125	160	200	225
2	56	71	90	112
	140	180	225	280

Source: Norm PN-M-88525:1993

After taking normalized value of module and number of cogs we mark the zero distance of axis again and take normalized real distance of axis a_w (Table 2.4).

$$a = \frac{m_n}{\cos \beta} \cdot \frac{z_1 + z_2}{2} = \frac{2,25}{\cos 15^\circ} \cdot \frac{19 + 77}{2} = 111,81 \text{ mm}$$

$$a_w = 112 \text{ mm}$$

We should remember that regarding resistance issues, it is very useful to conduct positive construction correction which allows to regulate the value of folding stresses by the bottom of cogs of both wheels. As long as it is possible, it is advisable to take the coordinate of contour dislocation for the smaller wheel $x_1 \approx 0,5$. In order to make conduction of positive correction of the type P possible, the zero distance of the axis should be smaller than the distance a_w of the value which equals approximately $0,5 m_n$. In the case when this value is higher than $1 m_n$, one should make the correction of the taken angle of gradient of cogs line or number of wheel's cogs z_2 . For further calculations, take the following parameters of transmission rate:

$$\begin{aligned} z_1 &= 19 \quad z_2 = 77 \\ m_n &= 2,25 \quad \beta = 13^\circ \\ \alpha_n &= 20^\circ \quad y_n = 1 \quad c^* = 0,25 \\ a_w &= 112 \text{ mm} \quad b = 35 \text{ mm} \end{aligned}$$

2.2. Calculations of the basic geometrical dimensions of transmission rate

Before proceeding to check resistance calculations, one should make construction correction, mark the wheel dimensions and press number.

The marked before zero distance of axis is:

$$a = \frac{m_n}{\cos \beta} \cdot \frac{z_1 + z_2}{2} = \frac{2,25}{\cos 13^\circ} \cdot \frac{19 + 77}{2} = 110,84 \text{ mm}$$

On the basis of the below dependency one marks rolling angle of press in the front surface a_{wt} :

$$a_w \cos \alpha_{wt} = a \cos \alpha_t$$

In which:

$$\operatorname{tg} \alpha_t = \frac{\operatorname{tg} \alpha_n}{\cos \beta} = \frac{\operatorname{tg} 20^\circ}{\cos 13^\circ} = 0,37354 \quad \alpha_t = 20,48^\circ$$

$$\cos \alpha_{wt} = \frac{a \cos \alpha_t}{a_w} = \frac{110,84 \cdot \cos 20,48^\circ}{112} = 0,92709 \quad \alpha_{wt} = 22,01^\circ$$

On the basis of the next dependency:

$$inv\alpha_{wt} - inv\alpha_t = 2 \frac{\sum x_t}{z_1 + z_2} \operatorname{tg} \alpha_t$$

One marks the sum of coordinates of contours in front surface:

$$\sum x_t = \frac{inv\alpha_{wt} - inv\alpha_t}{2 \operatorname{tg} \alpha_t} (z_1 + z_2) = \frac{0,020082 - 0,016043}{2 \cdot 0,37354} (19 + 77) = 0,519$$

While,

$$inv\alpha_{wt} = \operatorname{tg} \alpha_{wt} - \hat{\alpha}_{wt} = 0,020082$$

$$inv\alpha_t = \operatorname{tg} \alpha_t - \hat{\alpha}_t = 0,016043$$

Take the following coordinates of contour dislocation, then mark theirs values in nominal surface:

$$x_{t1} = 0,519 \quad x_{t2} = 0$$

$$x_{n1} = \frac{x_{t1}}{\cos \beta} = \frac{0,519}{\cos 13^\circ} = 0,533 \quad x_{n2} = 0$$

Calculate the apparent distance of axis and coordinate of heads shortening:

$$a_p = a + (x_{n1} + x_{n2}) m_n = 110,84 + (0,533 + 0) \cdot 2,25 = 112,039 \text{ mm}$$

$$k_t = \frac{a_p - a_w}{m_t} = \frac{a_p - a_w}{m_n} \cos \beta = \frac{112,039 - 112}{2,25} \cos 13^\circ = 0,017$$

The value of coordinate of heads shortening is small (smaller than 0,1), thus in the further calculations one may omit it, taking $kt = kn = 0$.

$$d_1 = \frac{m_n z_1}{\cos \beta} = \frac{2,25 \cdot 19}{\cos 13^\circ} = 43,87 \text{ mm}$$

$$d_2 = \frac{m_n z_2}{\cos \beta} = \frac{2,25 \cdot 77}{\cos 13^\circ} = 177,81 \text{ mm}$$

Diameters of heads:

$$\begin{aligned} d_{a1} &= m_n \left(\frac{z_1}{\cos \beta} + 2y_n + 2x_{n1} - 2k_n \right) = \\ &= 2,25 \cdot \left(\frac{19}{\cos 13^\circ} + 2 \cdot 1 + 2 \cdot 0,533 - 2 \cdot 0 \right) = 50,77 \text{ mm} \end{aligned}$$

$$\begin{aligned} d_{a2} &= m_n \left(\frac{z_2}{\cos \beta} + 2y_n + 2x_{n2} - 2k_n \right) = \\ &= 2,25 \cdot \left(\frac{77}{\cos 13^\circ} + 2 \cdot 1 + 2 \cdot 0 - 2 \cdot 0 \right) = 182,31 \text{ mm} \end{aligned}$$

Diameters of feet:

$$\begin{aligned} d_{f1} &= m_n \left(\frac{z_1}{\cos \beta} - 2y_n - 2c^* + 2x_{n1} \right) = \\ &= 2,25 \cdot \left(\frac{19}{\cos 13^\circ} - 2 \cdot 1 - 2 \cdot 0,25 + 2 \cdot 0,533 \right) = 40,65 \text{ mm} \end{aligned}$$

$$\begin{aligned} d_{f2} &= m_n \left(\frac{z_2}{\cos \beta} - 2y_n - 2c^* + 2x_{n2} \right) = \\ &= 2,25 \cdot \left(\frac{77}{\cos 13^\circ} - 2 \cdot 1 - 2 \cdot 0,25 + 2 \cdot 0 \right) = 172,18 \text{ mm} \end{aligned}$$

Diameters of rolling wheels:

$$\begin{aligned} d_{w1} &= 2a_w \frac{z_1}{z_1 + z_2} = 2 \cdot 112 \cdot \frac{19}{19 + 77} = 44,333 \text{ mm} \\ d_{w2} &= 2a_w \frac{z_2}{z_1 + z_2} = 2 \cdot 112 \cdot \frac{77}{19 + 77} = 179,667 \text{ mm} \end{aligned}$$

Calculating the front number of press:

$$\begin{aligned} \varepsilon_\alpha &= \frac{1}{2\pi} \left[z_1 (\operatorname{tg} \alpha_{a1} - \operatorname{tg} \alpha_{wt}) + z_2 (\operatorname{tg} \alpha_{a2} - \operatorname{tg} \alpha_{wt}) \right] \\ \alpha_{a1} &= \arccos \left(\frac{d_1 \cos \alpha_t}{d_{a1}} \right) = \arccos \left(\frac{43,87 \cdot \cos 20,48^\circ}{50,77} \right) = 35,96^\circ \end{aligned}$$

$$\alpha_{a2} = \arccos\left(\frac{d_2 \cos \alpha_t}{d_{a2}}\right) = \arccos\left(\frac{177,81 \cdot \cos 20,48^\circ}{182,31}\right) = 23,98^\circ$$

$$\varepsilon_\alpha = \frac{1}{2\pi} \left[19 \cdot (\operatorname{tg} 35,96^\circ - \operatorname{tg} 22,01^\circ) + 77 \cdot (\operatorname{tg} 23,98^\circ - \operatorname{tg} 22,01^\circ) \right] = 1,47$$

Calculating the after-jump number of press:

$$\varepsilon_\beta = \frac{b \sin \beta}{\pi m_n} = \frac{35 \cdot \sin 13^\circ}{\pi \cdot 2,25} = 1,11$$

Total number of press is:

$$\varepsilon = \varepsilon_\alpha + \varepsilon_\beta = 1,47 + 1,11 = 2,58$$

2.3. Testing strength calculations for surface exhaustion

Taking the pinion material: alloy steel for carbonizing 18CrNi8. Nominal contact stresses are marked on the basis of the dependency:

$$\sigma_{H0} = Z_E Z_H Z_\varepsilon Z_\beta \sqrt{\frac{F}{d_{w1} b} \cdot \frac{u+1}{u}}$$

In which:

F – peripheral force,

$$F = \frac{2M_s}{d_{w1}} = \frac{2 \cdot 9550 N}{d_{w1} n_1} = \frac{2 \cdot 9550 \cdot 15 \cdot 10^3}{44,333 \cdot 1000} = 6462,5 N$$

Z_E – material coordinate,

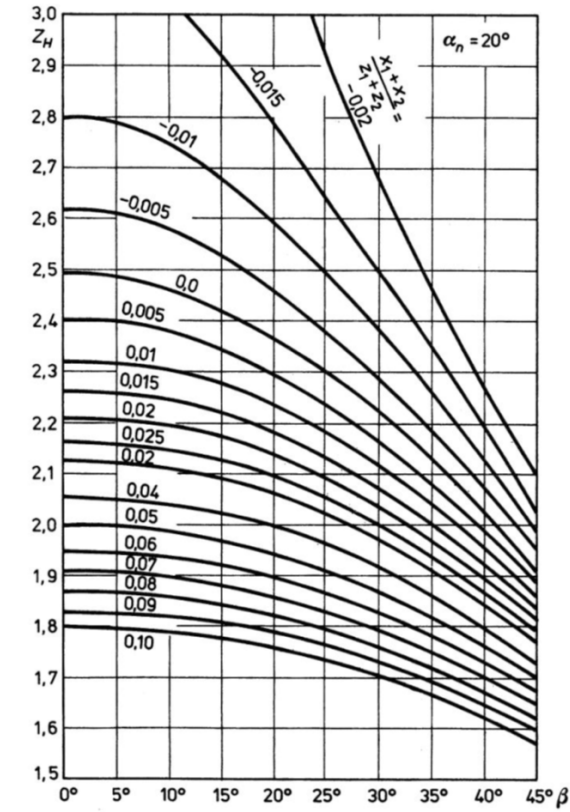
$$Z_E = \sqrt{\frac{1}{\pi \left(\frac{1-\nu_1^2}{E_1} + \frac{1-\nu_2^2}{E_2} \right)}}$$

In the case in which both wheels are made of steel, material coordinate is:

$$Z_E = 189,8 \text{ MPa}^{1/2}$$

Z_H – coordinate of geometry in the area of contact (Pic. 2.1),

$$Z_H = 2,35 \quad \frac{x_{n1} + x_{n2}}{z_1 + z_2} = 0,006$$



Pic. 2.1. Coordinate Z_H of geometry in the area of contact ($\alpha_n = 20^\circ$) [1]

Z_E – coordinate allowing for the influence of press number

$$Z_\varepsilon = \sqrt{\frac{4 - \varepsilon_\alpha}{3} (1 - \varepsilon_\beta) + \frac{\varepsilon_\beta}{\varepsilon_\alpha}} \quad \text{when } \varepsilon_\beta < 1$$

$$Z_\varepsilon = \sqrt{\frac{1}{\varepsilon_\alpha}} \quad \text{when } \varepsilon_\beta \geq 1$$

$$Z_{\varepsilon} = \sqrt{\frac{1}{\varepsilon_{\alpha}}} = \sqrt{\frac{1}{1,47}} = 0,825$$

Z_{β} – coordinate of cogs gradient.

$$Z_{\beta} = \sqrt{\cos \beta} = \sqrt{\cos 13^{\circ}} = 0,990$$

After substituting the coordinates one gets:

$$\sigma_{H0} = 189,8 \cdot 2,35 \cdot 0,825 \cdot 0,990 \cdot \sqrt{\frac{6462,5}{44,333 \cdot 35} \cdot \frac{4,05+1}{4,05}} = 830,2 \text{ MPa}$$

Real contact stress after allowing for the coordinate of exploitation:

$$\sigma_H = \sigma_{H0} \sqrt{K} = \sigma_{H0} \sqrt{K_A K_v K_{H\beta} K_{H\alpha}}$$

In which:

K – coordinate of exploitation

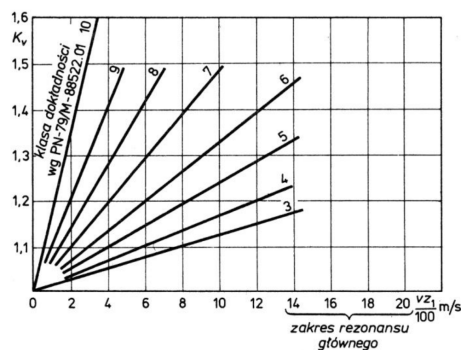
K_A – coordinate of usage (Table 2.5) $K_A = 1,25$,

K_v – coordinate of dynamic loads

Table 2.5. Values of coordinate of usage K_A

Character of changes on engine shaft				
	regular	moderate pulsation	medium pulsation	high pulsation
regular	1,00	1,25	1,50	1,75
moderate pulsation	1,10	1,35	1,60	1,85
medium pulsation	1,25	1,50	1,75	2,00
high pulsation	1,50	1,75	2,00	2,25

Source: Dietrich M., *Podstawy konstrukcji maszyn*, Warszawa, Wydawnictwa Naukowo-Techniczne, 1999

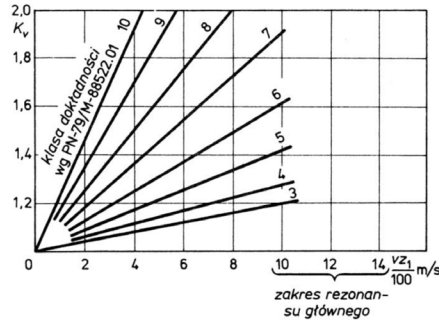


Pic. 2.2. Coordinate of dynamic loads K_v for screw wheels and $\varepsilon\beta > 1$ [1]

If $\varepsilon\beta < 1$, the coordinate of dynamic loads is marked according to the dependency;

$$K_v = K_{v\alpha} - \varepsilon_\beta (K_{v\alpha} - K_{v\beta})$$

Additionally, the value K_{valfa} is marked from the graph presented in the pic. 2.2, the value $K_{v\beta}$ is marked from the graph in the pic. 2.3.



Pic. 2.3. Coordinate of dynamic loads K_v , for simple wheels [1]

In our case $\varepsilon\beta > 1$, then for the parameter $v_z/100 = 0,44$ and 7th class of precision of making wheel the coordinate of dynamic loads is:

$$K_v = 1,02$$

$K_{H\beta}$ – coordinate of distribution of load along the cog, marked with simplified method [1] for the 7th class of precision of making:

$$K_{H\beta} = 1,23 + 0,18 \cdot \left(\frac{b}{d_1} \right)^2 + 0,61 \cdot 10^{-3} b$$

Marking the value of coordinate of load distribution along the cog for the taken before 7th class:

$$K_{H\beta} = 1,23 + 0,18 \cdot \left(\frac{35}{43,87} \right)^2 + 0,61 \cdot 10^{-3} \cdot 35 = 1,37$$

K_{Ha} – coordinate of load distribution along the segment of press. For wheels tempered superficially or to pierce, normally loaded, one takes:

$$K_{Ha} = 1$$

Substituting the marked values, we get the coordinate of exploitation and mark real contact stress:

$$K = K_A K_v K_{H\beta} K_{H\alpha} = 1,25 \cdot 1,02 \cdot 1,37 \cdot 1 = 1,75$$

$$\sigma_H = \sigma_{H0} \sqrt{K} = 830,2 \cdot \sqrt{1,75} = 1098,3 \text{ MPa}$$

The marked real stress for smaller wheel is smaller than the permissible value and while assuming the genre of material of smaller wheel before, it equals (Table 2.6):

$$\sigma_{HP} \approx 0,8 \cdot \sigma_{H\lim}$$

$$\sigma_{HP} \approx 0,8 \cdot 1630 \text{ MPa} = 1304 \text{ MPa}$$

Table 2.6. Resistance features of chosen materials for cogwheels

Kind of steel	Symbol	$\sigma_{H\lim}$ [MPa]	σ_{Flim} [MPa]	Hardness [HV]
Constricting steel of higher quality	C22	440	170	140
	C45	590	200	185
	C55	620	220	210
Alloy steel for heating improvement	34Cr2	650	270	260
	41Cr4	650	270	260
	42CrMo4	670	290	280
	34crNiMo6	770	320	310
Tempered superficially steel for improving	C45	1100	270	560
	41Cr4	1280	310	610
	42CrMo4	1360	350	650
Nitric steel for improving	C45	1100	350	400
	42CrMo4	1220	430	500
	42CrMo4	1220	430	550
Steel for carbonizing	C15	1600	230	720
	16MnCr5	1630	460	720
	20MnCr5	1630	480	720
	15CrNi6	1630	500	720
	18CrNi8	1630	500	740
	18CrNiMo7	1630	500	740

Source: Mazanek E. *Przykłady obliczeń z podstaw konstrukcji maszyn*, Warszawa, Wydawnictwa Naukowo-Techniczne, 2005

2.4. Testing strength calculations for exhaustion fracture

Nominal calculation stresses:

$$\sigma_{F0} = \frac{F}{bm_n} Y_{Fa} Y_{Sa} Y_\epsilon Y_\beta$$

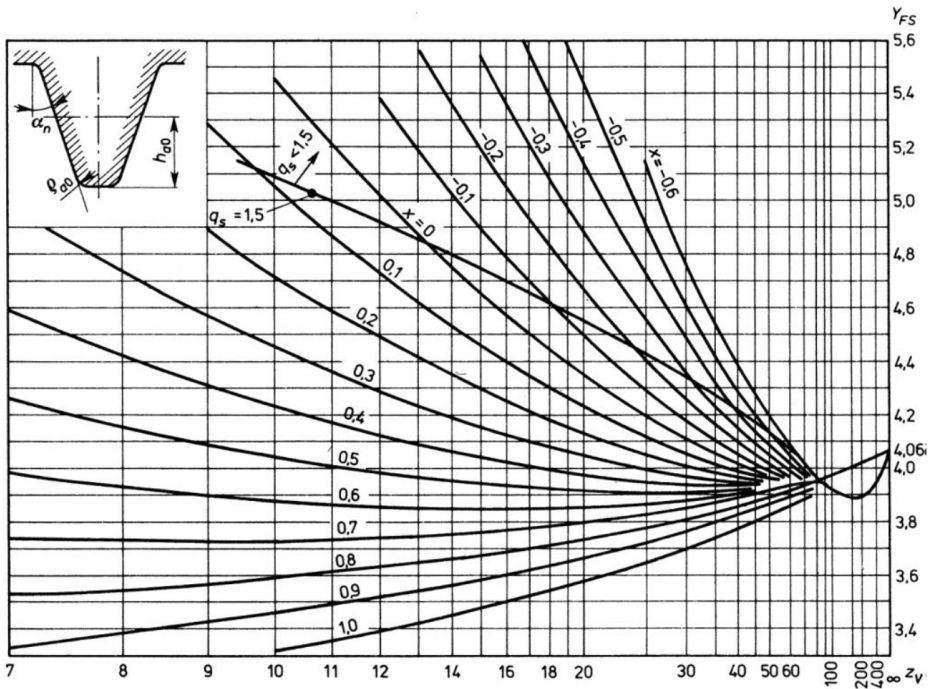
In which:

Y_{Fa} – cog shape coordinate

Y_{Sa} – notch working coordinate

On the basis of the graph (Pic. 2.4) for $x_{t1} = 0,519$ and for replacing number of cogs $z_{v1} = 20,8 \approx 21$ we mark the coordinate Y_{FS}

$$Y_{FS} = Y_{Fa} \cdot Y_{Sa} = 3,92$$



Pic. 2.4. Coordinate Y_{FS} ($\alpha_n = 20^\circ$, $y_n = 1$, $c^* = 0.25$) [1]

Y_E – press coordinate:

$$Y_{\varepsilon} = 0,25 + \frac{0,75}{\varepsilon_{\alpha}} \cos^2 \beta_b$$

$$\beta_b = \arctg(\cos \alpha_i \operatorname{tg} \beta)$$

Substituting the values, we'll get:

$$\beta_b = 12,20^\circ$$

$$Y_{\varepsilon} = 0,25 + \frac{0,75}{1,47} \cos^2 12,20^\circ = 0,737$$

Y_{β} – coordinate of cogs gradient influence:

$$Y_{\beta} = 1 - \varepsilon_{\beta} \frac{\beta}{120} = 1 - 1,11 \cdot \frac{13}{120} = 0,880$$

Mark nominal stresses and real stresses, taking the simplification $K_{F\beta} \approx K_{H\beta}$ or $K_{F\alpha} \approx K_{H\alpha}$

$$\sigma_{F0} = \frac{P}{bm_n} Y_{Fa} Y_{Sa} Y_{\varepsilon} Y_{\beta} = \frac{6462,50}{35 \cdot 2,25} \cdot 3,92 \cdot 0,737 \cdot 0,880 = 208,6 \text{ MPa}$$

$$\sigma_F = \sigma_{F0} K = 208,6 \cdot 1,75 = 365,1 \text{ MPa}$$

As we can see, the value of real stress is much higher than the permissible value, which while assuming the usage of alloy steel for carbonizing equals (Table 8):

$$\sigma_{FP} \approx 0,6 \cdot \sigma_{F\lim} = 0,6 \cdot 500 \text{ MPa} = 300 \text{ MPa}$$

In this case we have to increase the width of the wreath of cogwheel till the value $b = 43 \text{ mm}$ and make calculations of values of coordinates and values of stresses, which underwent change, again:

$$\varepsilon_{\beta} = 1,37 \quad \varepsilon = 2,84 \quad K_{H\beta} = 1,43 \quad K = 1,82 \quad Y_{\beta} = 0,852$$

$$\sigma_{H0} = 749,0 \text{ MPa} \quad \sigma_H = 1110,5 \text{ MPa}$$

$$\sigma_{F0} = 164,4 \text{ MPa} \quad \sigma_F = 299,2 \text{ MPa}$$

With regards to more favorable conditions of wheel working we may omit testing calculations, under the condition of making a wheel of the material of the values $\sigma_{Hlim}, \sigma_{Flim}$, approximate to the small wheel. Thus, we take alloy steel 15CrNi6 for carbonizing as the material.

2.5. Calculations of input rolling

We calculate forces appearing in mesh, taking into consideration the coordinate of K_A usage. Circuit force F :

$$F = \frac{2M_{s1}}{d_{w1}} = \frac{2 \cdot 179060}{44,333} = 8078,0\text{N}$$

$$M_{s1} = 9550 \frac{N}{n_1} \cdot K_A = 9550 \frac{15}{1000} \cdot 1,25 = 179,06\text{Nm} = 179060\text{Nmm}$$

Radius force F_r :

$$F_r = F \cdot \operatorname{tg} \alpha_{wt} = 8078,0 \cdot \operatorname{tg} 22,01^\circ = 3265,4\text{N}$$

Axis force F_x (taking in approximate $\beta_w = \beta$):

$$F_x = F \cdot \operatorname{tg} \beta = 8078,0 \cdot \operatorname{tg} 13^\circ = 1865,0\text{N}$$

The smaller wheel will be cut on input rolling, then for calculations of rolling we take the permissible values:

$$k_{go} = 114\text{MPa}, k_{sj} = 124\text{MPa}$$

Calculating of theoretical diameter of input pin:

$$d_{we} \geq \sqrt[3]{\frac{16 \cdot M_{s1}}{\pi \cdot k_{sj}}} = \sqrt[3]{\frac{16 \cdot 179060}{\pi \cdot 124}} = 19,39\text{mm}$$

For input pin, we take a spline of the dimensions 6x21x25 according to the norm PN-ISO14 of the length $l = 25$ mm and we check the condition of stresses, assuming permissible stresses for the hub $p_{dop} = 90\text{MPa}$.

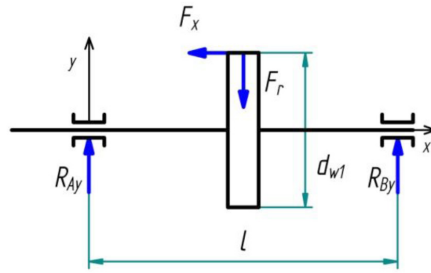
$$p = \frac{8M_{s1}}{(D^2 - d^2) \cdot l \cdot z \cdot \psi} = \frac{8 \cdot 179060}{(25^2 - 21^2) \cdot 25 \cdot 6 \cdot 0,75} = 69,20\text{MPa} < p_{dop}$$

We take the diameter of seal 28mm and nominal diameter of bearing in respective surfaces. Reactions in the surface XY is marked on the basis of moments equation towards any point:

$$l = b + 2 \cdot (15 \div 25 \text{mm}) = 43 + 2 \cdot 23,5 = 90 \text{mm}$$

We mark the values of forces reacting on bearing threads in respective surfaces. Reactions in the surface XY are marked on the basis of the equation of moments, towards any point:

$$\sum M_B = R_{Ay} \cdot l - F_x \cdot \frac{d_{w1}}{2} - F_r \cdot \frac{l}{2} = 0$$



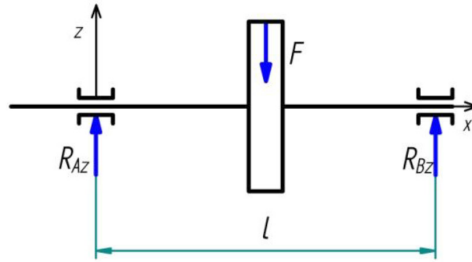
Pic. 2.5. Scheme of input rolling loading in the surface XY

$$R_{Ay} = \frac{F_x \cdot \frac{d_{w1}}{2} + F_r \cdot \frac{l}{2}}{l} = \frac{1865,0 \cdot \frac{44,333}{2} + 3265,4 \cdot 45}{90} = 2092,0 \text{N}$$

$$R_{By} = F_r - R_{Ay} = 3265,4 - 2092,0 = 1173,4 \text{N}$$

Similarly, we mark reactions in the surface XZ:

$$\sum M_B = R_{Az} \cdot l - F \cdot \frac{l}{2} = 0$$



Pic. 2.6. Scheme of input rolling loading in the surface XZ

$$R_{Az} = \frac{F}{2} = \frac{8078,0}{2} = 4039,0\text{N}$$

$$R_{Bz} = R_{Az} = 4039,0\text{N}$$

The values of resultant reactions R_A and R_B

$$R_A = \sqrt{R_{Ay}^2 + R_{Az}^2} = \sqrt{2092,0^2 + 4039,0^2} = 4548,6\text{N}$$

$$R_B = \sqrt{R_{By}^2 + R_{Bz}^2} = \sqrt{1173,4^2 + 4039,0^2} = 4206,0\text{N}$$

We mark the values of fracture moments in middle section of cogwheel in respective surfaces and the resultant moment:

$$M_{gy} = R_{Ay} \cdot \frac{l}{2} = 2092,0 \cdot \frac{90}{2} = 94140\text{Nmm}$$

$$M_{gz} = R_{Az} \cdot \frac{l}{2} = 4039,0 \cdot \frac{90}{2} = 181755\text{Nmm}$$

$$M_g = \sqrt{M_{gy}^2 + M_{gz}^2} = \sqrt{94140^2 + 181755^2} = 204688\text{Nmm}$$

Substitutive moment:

$$M_z = \sqrt{M_g^2 + \frac{3}{16} M_{s1}^2} = \sqrt{204688^2 + \frac{3}{16} 179060^2} = 218881\text{Nmm}$$

Checking the diameter of pinion's rolling:

$$d \geq \sqrt[3]{\frac{32 \cdot M_z}{\pi \cdot k_{go}}} = \sqrt[3]{\frac{32 \cdot 218881}{\pi \cdot 114}} = 26,94 \text{ mm}$$

Of course, the diameter of pinion's rolling has to be smaller than diameter of wheel's foot, thus the above calculations may be treated only as testing calculations.

2.6. Input rolling calculations

We assume the material of rolling 41Cr4 ($k_{go}=114\text{MPa}$, $k_{sj}=124\text{MPa}$) and mark turning moment, loading the input rolling from the dependency:

$$M_{s2} = M_{s2} \cdot \frac{z_2}{z_1} = 179060 \cdot 4,05 = 725193 \text{ Nmm}$$

We calculate theoretical diameter of input pin:

$$d_{wy} \geq \sqrt[3]{\frac{16 \cdot M_{s2}}{\pi \cdot k_{sj}}} = \sqrt[3]{\frac{16 \cdot 725193}{\pi \cdot 124}} = 31,00 \text{ mm}$$

For input pin, we take the spline of dimensions 8x32x38 according to the norm PN-ISO14 of the length $l=40\text{mm}$ and we check the surface stresses condition, assuming permissible stresses for hub:

$$p_{dop} = 90 \text{ MPa}$$

$$p = \frac{8M_{s2}}{(D^2 - d^2) \cdot l \cdot z \cdot \psi} = \frac{8 \cdot 725193}{(38^2 - 32^2) \cdot 40 \cdot 8 \cdot 0,75} = 57,56 \text{ MPa} < p_{dop}$$

We take the diameter of seal 42mm and nominal diameter of bearing in respective surfaces.

Values of reaction in the surface XY:

$$R_{Cy} = \frac{F_x \cdot \frac{d_{w2}}{2} + F_r \cdot \frac{l}{2}}{l} = \frac{1865,0 \cdot \frac{179,667}{2} + 3265,4 \cdot 45}{90} = 3494,2 \text{ N}$$

$$R_{Dy} = F_r - R_{Cy} = 3265,4 - 3494,2 = -228,8\text{N}$$

Values of reaction in the surface XZ:

$$R_{Cz} = \frac{F}{2} = \frac{8078,0}{2} = 4039,0\text{N}$$

$$R_{Dz} = R_{Cz} = 4039,0\text{N}$$

Values of resultant reactions R_C and R_D

$$R_C = \sqrt{R_{Cy}^2 + R_{Cz}^2} = \sqrt{3494,2^2 + 4039,0^2} = 5340,7\text{N}$$

$$R_D = \sqrt{R_{Dy}^2 + R_{Dz}^2} = \sqrt{228,8^2 + 4039,0^2} = 4045,5\text{N}$$

We mark the values of fracture moments in middle section of cogwheel in respective surfaces and the resultant moment:

$$M_{gy} = R_{Cy} \cdot \frac{l}{2} = 3494,2 \cdot \frac{90}{2} = 157239\text{Nmm}$$

$$M_{gz} = R_{Cz} \cdot \frac{l}{2} = 4039,0 \cdot \frac{90}{2} = 181755\text{Nmm}$$

$$M_g = \sqrt{M_{gy}^2 + M_{gz}^2} = \sqrt{157239^2 + 181755^2} = 240331\text{Nmm}$$

Regarding the domination of turning moment, we mark the substitutive moment from the dependency:

$$M_{zs} = \sqrt{\frac{16}{3} M_g^2 + M_{s2}^2} = \sqrt{\frac{16}{3} 240331^2 + 725193^2} = 913210\text{Nmm}$$

We calculate the diameter of rolling's pin in the place of big wheel location:

$$d \geq \sqrt[3]{\frac{16 \cdot M_{zs}}{\pi \cdot k_{sj}}} = \sqrt[3]{\frac{16 \cdot 913210}{\pi \cdot 124}} = 33,47\text{mm}$$

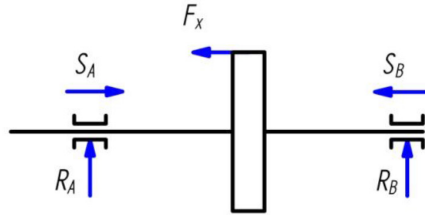
We take the spline 8x46x54 according to the norm PN-ISO14 of the length $l = 42\text{mm}$ (inconsiderably smaller than lengths of cogwheel, which is $b = 43\text{mm}$) and we check the condition for surface stresses.

$$p = \frac{8M_{s2}}{(D^2 - d^2) \cdot l \cdot z \cdot \psi} = \frac{8 \cdot 725193}{(54^2 - 46^2) \cdot 42 \cdot 8 \cdot 0,75} = 28,78 \text{ MPa} < p_{dop}$$

2.7. Calculations of input rolling bearing

Regarding the simplicity of building of the input rolling bearing set, we take cone bearings in the set "X". On the basis of SKF company catalogue and the assumed before diameter of bearing, we take bearings 32206 of the following construction parameters:

$$C = 50100 \text{ N} \quad C_0 = 57000 \text{ N} \quad X = 0,4 \quad Y = 1,6 \quad e = 0,37$$



Pic. 2.7. Scheme of load of bearings in the set "X" of input rolling

We mark the internal longitudinal forces in the bearings:

$$S_A = \frac{F_{rA}}{2Y} = \frac{R_A}{2Y} = \frac{4548,6}{2 \cdot 1,6} = 1421,4 \text{ N}$$

$$S_B = \frac{F_{rB}}{2Y} = \frac{R_B}{2Y} = \frac{4239,0}{2 \cdot 1,6} = 1324,7 \text{ N}$$

axis force F_x

$$F_x = 1865,0 \text{ N}$$

Analyzing the set of forces reacting on the rolling, we may state that:

$$S_A = 1421,4 \text{ N} < S_B + F_x = 1324,7 + 1865,0 = 3189,7 \text{ N}$$

So the bearing A is a bearing additionally loaded; the bearing B is the bearing with decreased load. Axis loads of bearings are as follows:

$$F_{aA} = S_B + F_x = 3189,7\text{N}$$

$$F_{aB} = S_B = 1324,7\text{N}$$

We mark substitutive dynamic loads of respective bearings:

$$P_A = XF_{rA} + YF_{aA} = 0,4 \cdot 4548,6 + 1,6 \cdot 3189,7 = 6923,0\text{N}$$

$$\frac{F_{aA}}{F_{rA}} = \frac{3189,7}{4548,6} = 0,70 > e = 0,37$$

$$P_B = XF_{rB} + YF_{aB} = 1 \cdot 4239,0 + 0 \cdot 1324,7 = 4239,0\text{N}$$

$$\frac{F_{aB}}{F_{rB}} = \frac{1324,7}{4239,0} = 0,31 < e = 0,35$$

Next, we mark hour resistances of bearings:

$$L_{hA} = \frac{10^6}{60 \cdot n_1} \left(\frac{C}{P_A} \right)^q = \frac{10^6}{60 \cdot 1000} \left(\frac{50100}{6923,0} \right)^{\frac{10}{3}} = 12218\text{h}$$

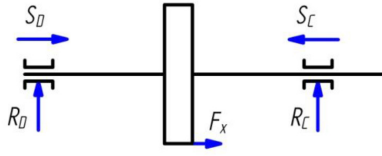
$$L_{hB} = \frac{10^6}{60 \cdot n_1} \left(\frac{C}{P_B} \right)^q = \frac{10^6}{60 \cdot 1000} \left(\frac{50100}{4239,0} \right)^{\frac{10}{3}} = 62675\text{h}$$

Required hour resistance of cog gear is 12000h, so the bearings have been fitted correctly.

2.8. Calculations of output rolling bearing

Similarly to input rolling, we take the cone bearings 32009 in the set “X”, of the following parameters:

$$C = 58300\text{N} \quad C_0 = 80000\text{N} \quad X = 0,4 \quad Y = 1,5 \quad e = 0,4$$



Pic. 2.8. Scheme of bearings loads in the set "X" of output rolling

We mark the internal longitudinal forces in bearings:

$$S_C = \frac{F_{rC}}{2Y} = \frac{R_C}{2Y} = \frac{5340,7}{2 \cdot 1,5} = 1780,2\text{N}$$

$$S_D = \frac{F_{rD}}{2Y} = \frac{R_D}{2Y} = \frac{4045,5}{2 \cdot 1,5} = 1348,5\text{N}$$

axis force F_x :

$$F_x = 1865,0\text{N}$$

Similarly to the previous case, analyzing the set of forces reacting on the rolling we may state that:

$$S_D + F_x = 1348,5 + 1865,0 = 3213,5\text{N} > S_C = 1780,2\text{N}$$

So the bearing C is a bearing additionally loaded; the bearing D is the bearing with decreased load. Axis loads of bearings are:

$$F_{aC} = S_D + F_x = 3213,5\text{N}$$

$$F_{aD} = S_D = 1348,5\text{N}$$

We mark substitutive dynamic loads of respective bearings:

$$P_C = XF_{rC} + YF_{aC} = 0,4 \cdot 5340,7 + 1,5 \cdot 3213,5 = 6956,5\text{N}$$

$$\frac{F_{aC}}{F_{rC}} = \frac{3213,5}{5340,7} = 0,60 > e = 0,4$$

$$P_D = XF_{rD} + YF_{aD} = 1 \cdot 4045,5 + 0 \cdot 1348,5 = 4045,5\text{N}$$

$$\frac{F_{aD}}{F_{rD}} = \frac{1348,5}{4045,5} = 0,33 < e = 0,4$$

Hour resistances of the bearings:

$$L_{hC} = \frac{10^6}{60 \cdot n_2} \left(\frac{C}{P_C} \right)^q = \frac{10^6}{60 \cdot 247} \left(\frac{58300}{6956,5} \right)^{\frac{10}{3}} = 80676\text{h}$$

$$L_{hD} = \frac{10^6}{60 \cdot n_2} \left(\frac{C}{P_D} \right)^q = \frac{10^6}{60 \cdot 247} \left(\frac{58300}{4045,5} \right)^{\frac{10}{3}} = 491443\text{h}$$

We may notice that hour resistances of the bearings exceed considerably the required hour resistance of the gear; however, the fitted bearings are cone bearings of the smallest dynamic mobility available, by the assumed diameter of bearing.

2.9. Marking of the amount of oil in gear

The oil in gear has two basic roles. It separates the cooperating surfaces from each other, decreasing the coordinate of friction and protecting the surfaces from seizure at the same time. By giving out the heat of friction, it makes cooling the cooperating surfaces possible. So one should provide a proper amount of oil in gear. We assume the use of oil and standard stickiness according to ISO VG100 whose amount we may mark approximately from the dependence [2]:

$$V = (3,5 \div 11) \cdot N \left(\frac{0,1}{z_1 \cos \beta} + \frac{0,03}{2 + \nu} \right) [\text{dm}^3]$$

In which:

N – nominal force of gear [kW]

$$\nu = \frac{\pi n_1 d_{w1}}{60} \quad - \text{ is circuit speed [m/s]}$$

Smaller values are taken in the case of one-step gears, the bigger ones in the case of multi-step gears.

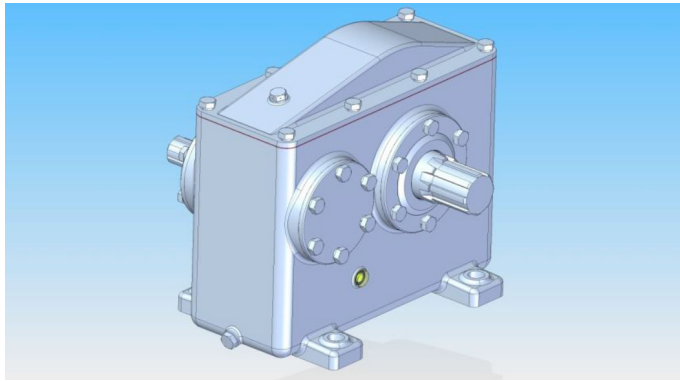
$$V = (3,5 \div 11) \cdot 15 \cdot \left(\frac{0,1}{19 \cdot \cos 13^\circ} + \frac{0,03}{2 + 2,32} \right) = 0,65 \div 2,78 \text{dm}^3$$

We assume $V = 1,0\text{dm}^3$, remembering at the same time that the corpus should be designed in the way so that the big wheel is sank in oil on the depth:

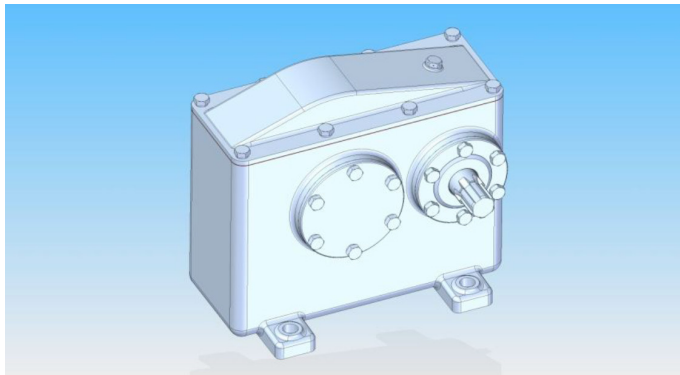
$$H = (1 \div 6) m_n$$

2.10. Cog gear with screw cogs – 3D model

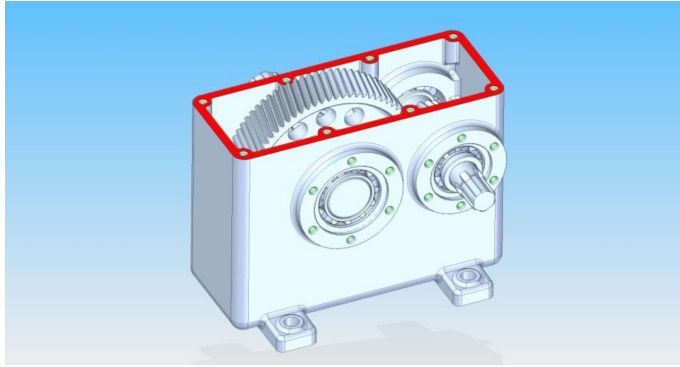
In the pic. 2.9 and 2.10 the model of cog gear with cog screws is shown, while in the pic. 2.11 and 2.12 the gear deprived of lid of corpus and side lids is presented.



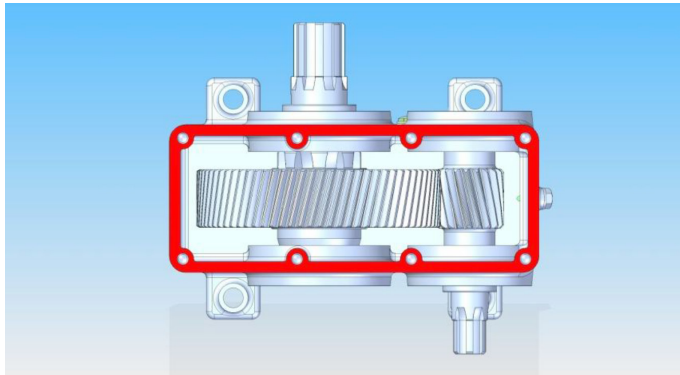
Pic. 2.9. *Cylindrical gear with screw cogs – view from output rolling*



Pic. 2.10. *Cylindrical gear with screw cogs – view from the side of input rolling*

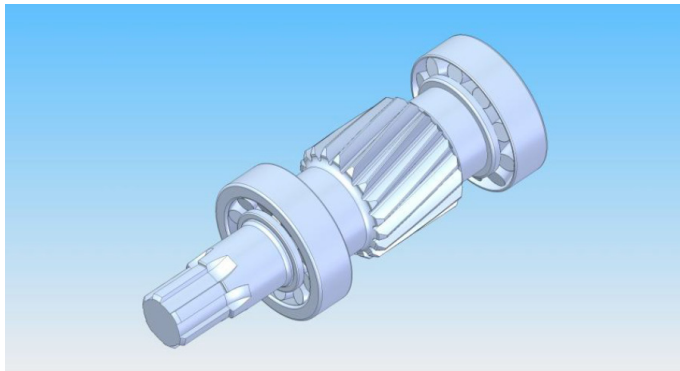


Pic. 2.11. *Cylindrical gear with screw cogs – view from the side of input rolling with the lids taken off*

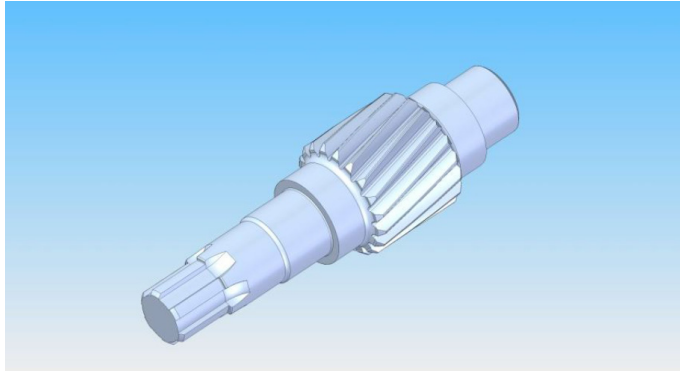


Pic. 2.12. *Cylindrical gear with screw cogs – view from the above, with the lids taken off*

In the picture 2.13 complete set of input rolling with cylindrical bearings on is shown; in the next picture (2.14) – input rolling is shown.

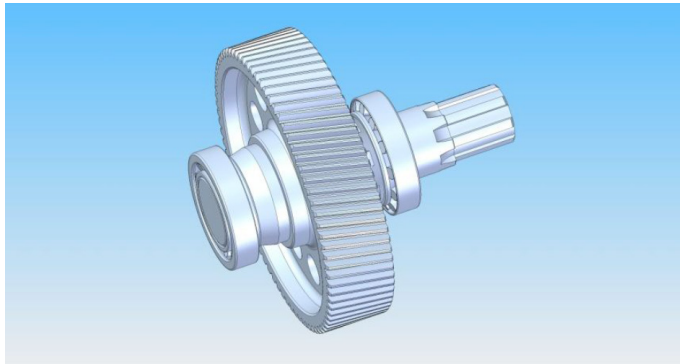


Pic.2.13. *Set of input rolling*



Pic. 2.14. *Input rolling of gear*

Picture 2.15 presents full set of output rolling with cogwheel, distance sleeve and bearings on.



Pic. 2.15. *Set of output rolling*

Literature

1. Dietrich M., *Podstawy konstrukcji maszyn*, Warszawa, Wydawnictwa Naukowo-Techniczne, 1999
2. Dziama A., Michniewicz M., Niedźwiedzki A., *Przekładnie zębate*, Warszawa, Wydawnictwo Naukowe PWN, 1989
3. Mazanek E., *Przykłady obliczeń z podstaw konstrukcji maszyn*, Warszawa, Wydawnictwa Naukowo-Techniczne, 2005
4. Szewczyk K., *Połączenia gwintowe*, Warszawa, Wydawnictwo Naukowe PWN, 1991
5. Norma PN-ISO 2904+A:1996, Gwinty trapezowe metryczne ISO. Wymiary nominalne.
6. PN-ISO 8734:2003, Kołki walcowe ze stali, hartowane lub z martenzytycznej stali nierdzewnej (kołki ustalające).
7. PN-EN ISO 4017:2011, Śruby z gwintem na całej długości z łbem sześciokątnym – Klasy dokładności A i B.
8. PN-M-85005:1970, Wpusty pryzmatyczne.
9. PN-ISO 14:1994, Połączenia wielowypustowe równoległe walcowe osiowane na średnicy wewnętrznej - Wymiary, tolerancje i sprawdzanie.
10. PN-ISO 54:2001, Przekładnie zębate walcowe ogólnego przeznaczenia oraz dla przemysłu ciężkiego – Moduły.
11. PN-M-88525:1993, Przekładnie i reduktory zębate walcowe ogólnego przeznaczenia - Podstawowe parametry.
12. PN-ISO 6336-1:2000, Przekładnie zębate walcowe. Obliczanie nośności kół. Podstawowe zasady i ogólne czynniki wpływające.
13. PN-ISO 6336-2:2000, Przekładnie zębate walcowe. Obliczanie nośności kół. Wytrzymałość zęba na zmęczenie stykowe (pitting).
14. PN-ISO 6336-3:2001, Przekładnie zębate walcowe. Obliczanie nośności kół. Wytrzymałość zęba na zginanie.
15. Katalog łożysk SKF <http://www.skf.com>

Table 2.7. Resistance tables of chosen constructing materials [MPa]

Material	Permissible stresses														
	k _r	k _{rj}	k _{rc}	k _g	k _{gj}	k _{go}	k _s	k _{sj}	k _{so}	k _t	k _{tj}	k _{to}	p	p _j	p _u
S235JR	125	90	55	135	79	44	75	52	26	67	34	19	90	54	27
S275JR	150	90	62	145	87	48	81	57	29	75	39	22	97	58	29
E295	165	100	62	162	105	58	90	69	34	87	46	25	109	66	33
E360	200	125	78	194	120	80	108	78	47	97	63	35	130	78	39
C10	99	54	30	118	70	40	66	47	24	59	32	18	89	50	25
C15	108	60	33	130	81	45	75	54	26	65	30	20	97	54	27
C20	117	65	36	140	86	49	78	58	29	70	39	22	105	60	30
C25	131	72	41	164	99	55	92	65	32	78	43	25	128	72	36
C35	172	85	47	205	115	64	115	75	38	103	51	28	155	87	43
C45	195	102	57	230	144	78	128	95	46	118	61	34	175	98	49
C55	220	112	66	260	155	85	145	102	51	132	67	40	200	112	58
C60	233	120	68	280	162	90	157	105	54	140	72	41	210	118	59
15Cr2	233	100	59	256	125	80	150	85	47	140	60	45	190	78	39
20Cr4	260	112	63	320	140	91	180	100	54	175	67	38	230	95	47
18CrMo4	330	135	80	360	172	109	205	115	65	200	81	48	285	108	54
15CrNi6	340	140	84	375	180	114	210	124	67	205	85	50	275	115	57
28Mn6	260	112	62	285	142	91	160	100	54	156	67	37	210	84	42
37MnSi5	325	125	75	355	160	102	200	112	61	195	75	45	260	104	52
41Cr4	360	140	84	395	175	114	220	124	67	215	84	47	275	109	55
200-400	116	60	36	128	72	41	72	49	29	69	36	22	125	65	32
230-450	128	67	40	140	78	46	78	54	32	77	40	24	138	72	36
270-480	160	79	49	170	92	55	98	65	39	96	47	29	170	89	44
EN-GJL-150	57	28	19	71	38	25	50	-	-	40	20	13	160	60	30
EN-GJL-250	86	41	28	118	59	38	87	-	-	60	29	20	240	90	46
EN-GJL-350	110	48	35	150	72	48	100	-	-	80	34	25	300	110	55
CuSn10Pb10	35	20	12	42	24	14	24	13	8	21	12	7	28	16	10
CuZn38Mn2Pb2	69	36	23	82	45	26	48	26	15	41	22	14	55	29	18
CuAl10Fe3Mn2	89	47	29	107	60	35	62	30	21	53	28	17	71	38	23

Source: Mazanek E. *Przykłady obliczeń z podstaw konstrukcji maszyn*, Warszawa, Wydawnictwa Naukowo-Techniczne, 2005

Chapter III

Method of finite elements in engineering applications

1. Introduction

The finite element method FEM is one of many approximate methods used for solving the issues of mechanics with usage of numerical procedures. With regard to its advantages it found its widest use from among other numerical methods, as e.g. BEM – boundary element method, or FDM – finite difference method, which were used more frequently than FEM before historically in practical solutions.

The conception of FEM assumes that each continuous area of physical model can be approximated with discrete model, consisting of finite number of elements and knots. Each element is described with the aid of continuous functions, called functions element shape, specifying physical values, such as dislocation, deformation, stress etc. defined in the knots of discrete model. This leads to the set of differential partitive equations (statics, dynamics), for which unambiguity of solution is obtained by filling the set of equations with starting and boundary conditions of discrete model. So carrying out the analysis with the use of FEM is based on approximation of continuous centre (real object) with discrete model; the process of calculations is solution of the discrete issue.

Analyses of resistance, thermal, exhaustion, internal vibrations and other issues are realized with the use of programming specified as CAE – Computer Aided Engineering. CAE programs allowing to realize numerical calculations are based on methods of solving discrete issues from which the most widely used is the finite-element method [1-3].

CAE programming is usually a system which consists of three modules: pre-processor, solver and postprocessor:

- **preprocessor** – it is a module of program (or an independent program) allowing to build discrete object model as well as to prepare calculation task. The general purpose of preprocessors is based on the possibility of building discrete model on the basis of geometrical object. Depending on CAE pro-

gramming, designer has the choice of more or less complex kinds of finite elements, techniques of generating and joining network of finite elements and the possibility of building mutual interactions between elements of model. It concerns also the library of available materials (or the possibility of entering materials defined by a user), and also formulating any sequences of boundary conditions and a model load. There is also a possibility of importing geometry (made in other CAD programs). In such situations, a user can make use of universal translators of geometry notation, such as among others: DXF, IGES, SAT, STP, STEP or direct translators destined for sending geometry notation between concrete programs.

- **solver** – it is a module of CAE program, with the aid of which the process of numerical calculations (calculation program) is realized. The use of a proper method of solution in calculations depends on specification of an analyzed issue and the size of set of equations. In the issues of construction resistance, one may most generally distinguish set of equations concerning:
 - construction statics
 - construction dynamics (the equation of movement)
 - geometrical non-linearity
 - material non-linearity (springiness-plastic issues)

While solving line issues, in which the Hook's law operates, usually for solving sets of equations, direct and iterative methods are used.

As the best known direct methods one may count the Gauss' method and the Cholesky method. Among iterative methods one uses stationary, scalar and cyclic methods.

When solving motion equations of discrete set, one commonly uses the following methods:

- for calculating the frequency of own vibrations: Ritz's method, methods of condensation, Stodola's method, method of subspace iterations
- in the case of movement equations of forced vibrations: method of direct integration, method of Fourier's transformation or modal method

For solving non-linear issues of FEM incremental calculation procedures are used, based on the method of changeable stiffness or the method of initial loads. Among methods of changeable stiffness one may distinguish the explicit method (called the Euler's integration "forward") and the Newton-Raphson method and modified method of Newton-Raphson [1-6]

The procedures of solving set of equations used in CAE systems are constantly developed and improved aiming at improvement of possibilities of solving more and more complicated issued and making the process of larger and larger calculations, with which we have to deal in contemporary calculation tasks, faster.

- **Postprocessor** – it is a module of CAE program allowing to edit results of made calculations. Contemporary processors have lots of possibilities of

graphic presentation of results, both in three-dimensional form and also in the form of graphs, tables or descriptions. Results of such values as: dislocation, stress, temperatures distribution etc. are presented usually in the form of colorful contour maps on the background of deformed model. A user has the possibility of visualization of results in most suitable form allowing to interpret them properly.

The development of modern numerical methods, especially in the scope of non-linear methods, causes that CAE programming is more and more frequently used, supporting engineering procedures in the process of designing in a wider and wider scope. In lots of cases making numerical simulations can replace conduction of more expensive and laborious scientific researches. Supporting the process of designing in the scope of numerical calculations allows to eliminate incorrect construction solutions, enlarging the possibility of getting optimal product.

2. The bases of FEM – linear and non-linear issues

Solving the problems of construction mechanics is based generally on linear physical and geometrical relations, characterizing with proportionality of dislocations to external loads. Mathematical models of systems lead to linear differential equations and in the case of discretization of an object, one gets a set of linear algebraic equations. Also the boundary and initial conditions are described with linear dependencies.

In reality, in case of non-linearities of constructions we deal almost from the beginning with loading process or after crossing a certain value of external load which may cause a low level of stresses. In such cases, for initial description of deformation scope one uses the linear notation. Formulating of issues leading to non-linear notations may be caused by many features, in construction working. As the most frequent ones we may indicate big dislocations or deformations of construction and non-linear characteristics of material, or of the knots put on the construction. According to the above, we distinguish generally two basic kinds of non-linearity: geometrically and physically non-linear issues [1-3].

2.1. Issues geometrically non-linear

In geometrically non-linear issues, relations between deformations and gradients of dislocations are non-linear. We deal with the use of non-linearity of this type in the cases of thin-wall load-bearing systems, slim constructions and the ones vulnerable to flexible bearing. These issues are connected also with the

occurrence of various types of imprecision (imperfection) as also loads of working destination dependent on deformation of a construction (tracking load). Examples of geometrical non-linearity may be also the issues of contact mechanics.

Formulating of non-linear mathematical models is a much more complex process than solving the issues based on linear theory of flexibility. The fundamental difference is the fact that in relation to non-linear equations one should distinguish the initial configuration of construction from the deformed construction, as well as the configuration of reference, to which we refer the calculated values. In linear processes, balance equations are noted for deformed configuration, which causes the omission of influence of geometry change on forces causing deformations, and what follows – the influence of deformation on balance conditions. In mechanics of construction, the simplified Lagrange's description is used for description of balance location [7].

The basic balance equation describing linear issues of deformable object statics, analyzed with the aid of finite element method can be noted as follows:

$$\{K\}\{U\} = \{P\} \quad (1)$$

In which:

$\{K\}$ – global matrix of a set stiffness

$\{P\}$ – knot forces vector

$\{U\}$ – knot dislocations vector

For description of geometrically non-linear issues in three-dimensional set, relations between deformations and dislocations are in the form [6]:

$$\{\varepsilon\} = \begin{bmatrix} \varepsilon_x \\ \varepsilon_y \\ \varepsilon_z \\ \gamma_{xy} \\ \gamma_{yz} \\ \gamma_{zx} \end{bmatrix} = \begin{bmatrix} \frac{\partial u}{\partial x} \\ \frac{\partial v}{\partial y} \\ \frac{\partial w}{\partial z} \\ \frac{\partial u}{\partial y} + \frac{\partial v}{\partial x} \\ \frac{\partial v}{\partial z} + \frac{\partial w}{\partial y} \\ \frac{\partial u}{\partial z} + \frac{\partial w}{\partial x} \end{bmatrix} + \begin{bmatrix} \frac{1}{2} \left(\left(\frac{\partial u}{\partial x} \right)^2 + \left(\frac{\partial v}{\partial x} \right)^2 + \left(\frac{\partial w}{\partial x} \right)^2 \right) \\ \frac{1}{2} \left(\left(\frac{\partial u}{\partial y} \right)^2 + \left(\frac{\partial v}{\partial y} \right)^2 + \left(\frac{\partial w}{\partial y} \right)^2 \right) \\ \frac{1}{2} \left(\left(\frac{\partial u}{\partial z} \right)^2 + \left(\frac{\partial v}{\partial z} \right)^2 + \left(\frac{\partial w}{\partial z} \right)^2 \right) \\ \left(\frac{\partial u}{\partial x} \right) \left(\frac{\partial u}{\partial y} \right) + \left(\frac{\partial v}{\partial x} \right) \left(\frac{\partial v}{\partial y} \right) + \left(\frac{\partial w}{\partial x} \right) \left(\frac{\partial w}{\partial y} \right) \\ \left(\frac{\partial u}{\partial y} \right) \left(\frac{\partial u}{\partial z} \right) + \left(\frac{\partial v}{\partial y} \right) \left(\frac{\partial v}{\partial z} \right) + \left(\frac{\partial w}{\partial y} \right) \left(\frac{\partial w}{\partial z} \right) \\ \left(\frac{\partial u}{\partial x} \right) \left(\frac{\partial u}{\partial z} \right) + \left(\frac{\partial v}{\partial x} \right) \left(\frac{\partial v}{\partial z} \right) + \left(\frac{\partial w}{\partial x} \right) \left(\frac{\partial w}{\partial z} \right) \end{bmatrix} \quad (2)$$

Or:

$$\{\varepsilon\} = \{\varepsilon_L\} + \{\varepsilon_{NL}\} \quad (3)$$

Linear deformations $\{\varepsilon_L\}$ Green's deformations and non-linear deformations $\{\varepsilon_{NL}\}$ are marks of higher level (squares, products of first derivatives), respectively towards the directions x, y, z .

What results from the above dependency is the fact that in non-linear issues the vector of deformations has been divided into linear part $\{\varepsilon_L\}$ – corresponding to infinitely small deformations, used in linear static analysis, and the non-linear part $\{\varepsilon_{NL}\}$ – allowing for non-linear deformations of a set.

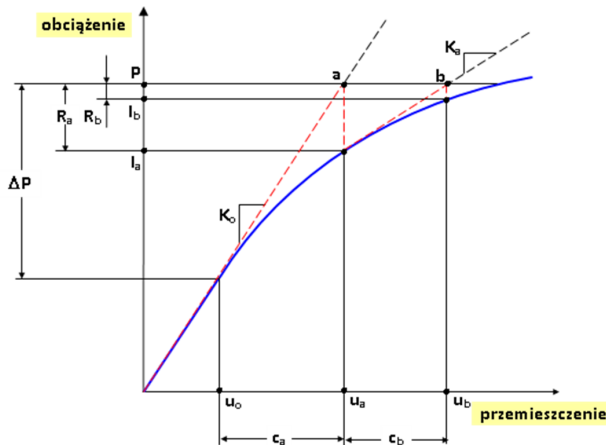
As a result, non-linear description of issues with the aid of finite elements method brings in a change of basic equation of statics (1) by adding non-linear part to the set of equations. As a result we obtain:

$$\{K\}\{U\} + f_N(U) = \{P\} \quad (4)$$

In which $f_N(U)$ is non-linear function of knot dislocations. Occurrence of this function makes solving of set equations, in which one uses iterative methods more complicated[5].

The most frequently used growth-iterative algorithm used in dislocation methods, giving precise results and providing fast gain of convergence in most of practical cases from the scope of mechanics of construction is the Newton – Raphson method [1,60].

The essence of Newton – Raphson method is presented in the picture 2.1, in which parameters occurring in the process of iteration are marked; a short description have been placed above in a simplified form.



Pic. 2.1. One-dimension interpretation of algorithm of the Newton – Raphson method

The basic formulation of balance equations in the N-R method may be put in a simple form as an equation [6]:

$$P - I = 0 \quad (5)$$

In which: P – generalized external force

I – generalized internal force

Elaborating on the left side of equation in the Taylor sequence (5) in surrounding of the point (u_a, P_a) we get:

$$P(u_a) - I(u_a) + \left\{ \frac{\partial P(u_a)}{\partial u} - \frac{\partial I(u_a)}{\partial u} \right\} c_b + \dots = 0 \quad (6)$$

With the next step we linearize the equation by eliminating all of parts of higher levels:

$$K_a c_b = P(u_a) - I(u_a) = R(u_a) \quad (7)$$

In which

$$K_a = \frac{\partial I(u_a)}{\partial u} - \frac{\partial P(u_a)}{\partial u} \quad \text{is the matrix of contact stiffness}$$

$$R(u_a) = P(u_a) - I(u_a) \quad \text{is residual force}$$

C_b – is the growth of dislocation. Upon solving the equation (7) we'll get:

$$c_b = (K_a)^{-1} R(u_a) \quad (8)$$

In which: $(K_a)^{-1}$ is the matrix opposite to K_a

The above description allows to formulate the algorithm of calculations for separate calculation step steered by the growth of load:

1. Loading of construction in growth way (growth 1)
2. Calculation of dislocation growth c_a on the basis of linear matrix of stiffness K_o and vector u_o and DP
3. Updating of configuration to u_a
4. Calculation of the value of internal forces I_a
5. Calculation of residual force R_a
6. If residual force R_a is very small, the construction is in moderation (implicit toleration in the program ABAQUS is specified so that the residual force is smaller than 0,5% of growth load DP . The program loads the construction with the next load growth (growth 2)

7. If iteration doesn't bring convergence (acceptable) solution, the program makes another iteration in order to gain convergence:
 - In updated configuration u_a comes formulating of contact stiffness matrix K_a and calculations of another dislocation growth c_b
 - New residual force R_b is compared to tolerations in order to make evaluation of whether the value u_b is convergent
 - The procedure repeats itself until the moment when residual force R_i doesn't decrease under the limit accepted previously.

The above algorithm is a description for the picture 1, in which the path of states of balance has been presented with continuous line. It results from the description that a basic drawback of the Newton – Raphson method is the necessity for creating and reversing the matrix of stiffness and solving a set of equations with new updated matrix of stiffness in each calculation step. It leads to a small efficiency of this method in solving large tasks and in issues in which non-symmetrical matrices of stiffness occur, such as: tracking external loads, or some inflexible issues. In these cases, aiming at increasing the efficiency of set of equations solution, one use relative growth-iterative methods, for which may we allow the simplified N-R method and the quasi – Newton method. The algorithm of calculations used in these methods is similar to the one used in the N-R method; the difference is the fact that the matrix of stiffness is marked only one time, at the beginning of iterative process [8, 9]. As a result, it simplifies the process of calculations itself; however, these methods are more slowly convergent than the Newton-Raphson method.

2.2. Physically non-linear issues

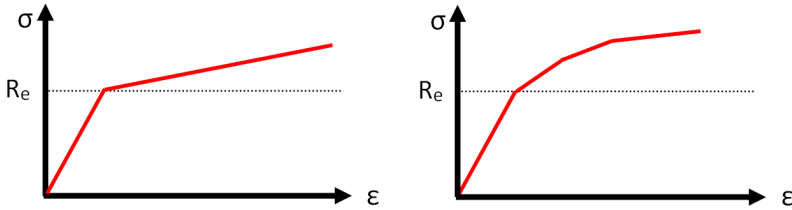
In physically non-linear issues, constitutive equations describing relations between stresses and deformations are non-linear. We deal with the issues of this type in the case of occurrence of large deformations in the flexible scope after crossing the boundary of proportionality, achieving plastic deformations, and also while considering the phenomena of crawling.

Analysis of many sets requires allowing for changes of features of material after crossing the boundary of plasticity. In analyses concerning the resistance of construction, the most frequently used non-linear models of materials are various kinds of flexible-plastic models, in which transforming of material from flexible state into the plastic state occurs. In flexible-plastic materials, beside flexible deformations, permanent deformations also occur, which one may note as:

$$\{\varepsilon\} = \{\varepsilon_s\} + \{\varepsilon_{PL}\} \quad (9)$$

Thus, full deformation is the sum of flexible deformation $\{\varepsilon_s\}$ and plastic deformation $\{\varepsilon_{PL}\}$.

The simplest model of flexible-plastic material is the material of bilinear characteristics, made of two segments of different angle of gradient towards the axis of deformations ε – pic. 2.2a.



Pic. 2.2. Model of flexible-plastic material: a) bilinear characteristics, b) multi-linear characteristics

Model of material of bilinear characteristics is usually used for initial flexible-plastic calculations, in which we want to get information concerning the zones of construction plasticity fast. In the case of a necessity of gaining more precise calculations, i.e. approaching to real (usually experienced) characteristics of material, one uses the model of flexible-plastic material of multi-linear characteristics – pic. 2.2b.

3. Examples of FEM modeling in the ABAQUS® program

The ABAQUS program of Dassaults Systemes company (www.simulia.com) is a commercial calculation package using the finite element method. It enables realization of complex issues of solid state mechanics, heat transmission, mechanics of liquids and coupled analyses in linear and non-linear scopes. In the Mechanics Department of Lublin University of Technology the ABAQUS program is used in didactic process both in the scope of subject classes and in transitional works, engineer and MA theses and also in scientific activity of the workers of Mechanics Department. With regard to the above, in the present chapter the examples of numerical simulations of FEM of chosen engineer issues will be presented, with the use of the ABAQUS programming packet.

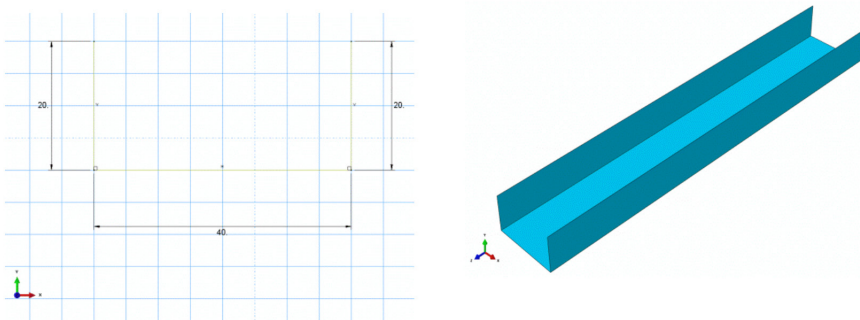
3.1. Analysis of linear statics of a thin-wall U-shaped profile put under axis squeezing

The issues connected with marking critical load for static buckling are based on solving own issue. In the case of finite elements method, solving the issue of static buckling of a construction is realized on the basis of so-called limited approach to bifurcative loss of statics, allowing to mark the values of critical load and form of buckling with the use of linear flexible analysis. In solution of the issue, there are conditions for extreme of potential energy [1]. This means that for sequences of static character, the second variation of potential energy has to be positive-marked.

In the present work, the critical state analysis was conducted with the use of linear analysis of statics, the so-called *buckling analysis*, allowing to mark critical loads of squeezed U-shaped profile an respective to them forms of construction's buckling. The considered U-shaped profile is an example of typical thin-wall pole constructions which one discretizes with finite element method with the use of beam or layer elements.

The preparation stage of numerical model includes in this case working out of geometrical model, definition of model's material, and also specification of boundary conditions and the way of loading, put down to the geometrical model (independent on finite elements grid). The last stage is generation of FEM grid, based on discretization of the geometrical model, with the use of taken parameters of discretization process, which are included in as density and kind of finite elements grid, type of finite element method and level of taken function of element's shape.

Geometrical model of the profile of U-shaped profile should be made as a three-dimension layer part (3D,Shell), the solid of deformable features (Deformable) should be made with the stretch method (Extrusion) of profile section, of which geometrical parameters are presented in the pic. 3.1a. The length of profile $L = 250$ mm was measured and the thickness of wall $g = 1$ mm.



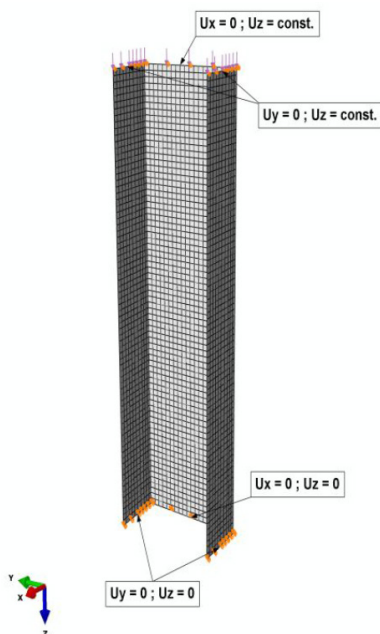
Pic. 3.1. Geometrical model of U-shaped profile: a) profile section, b) 3D model

In calculations one should assume that the profile is made of aluminum alloy, for which there will be a model of material defined, of linear-flexible characteristic.

(Mechanical/Elasticity/Elastic), by giving two independent material parameters, the Young's module $E = 70\,000\text{MPa}$ and the Poisson's number $\nu = 0.33$. The defined model of material is a physical linear issue in conducted calculations.

Numerical analysis will be conducted in the scope of calculations of own issue, concerning the statics of construction. For this purpose one has to define the type and parameters of calculations in the Step module, specifying the analysis as Linear Perturbation with the Buckle option – own issues, geometrically linear.

Formulated boundary conditions for numerical model correspond to realization of articulating support of end sections of a profile. The definition of boundary conditions should be made through specification of translative and rotary levels of latitude in proper knots of the model, or through coupling of levels of latitude based on definition of the condition of constant, generalized knot dislocations. A scheme of definition of boundary conditions is presented in the pic. 3.2.



Pic. 3.2. Discrete model of U-shaped profile, with proper boundary conditions and loads

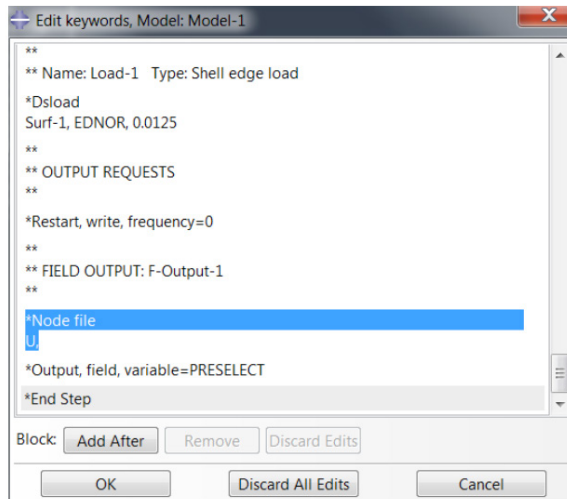
Realization of the above boundary conditions is conducted through giving zero-dislocations to the knots lying on the boundaries of upper and lower sections of the profile, respectively on the directions perpendicular to the surface of each wall (dislocations $ux=0$ i $uy=0$). Additionally, the possibility of dislocations in

perpendicular direction ($u_2 = 0$) should be blocked for knots belonging to the edge of upper end of the profile; the knots belonging to the edge of upper end should be put down with equal dislocation $u_2 = \text{const.}$ through coupling of dislocations in axis direction of the profile – *Interaction, Create Constraint – Equation* module. Boundary conditions should be defined in the module *Load* in the stage *Step: Initial*, choosing the procedure of blocking of latitude levels in the *Displacement/Rotation* knot.

The load of the model will be realized by loading all of the edges of the upper end of the profile, providing its even squeeze in perpendicular direction – the *Load* module, the kind of load *Shell edge load*. The value of total loading of the model is 1N, that is why each current millimeter of the edge will be loaded with the outlay of 0,0125N/mm. Taking of a unit load of construction in the issues of statics leads to acquirement of an own value corresponding directly to critical load.

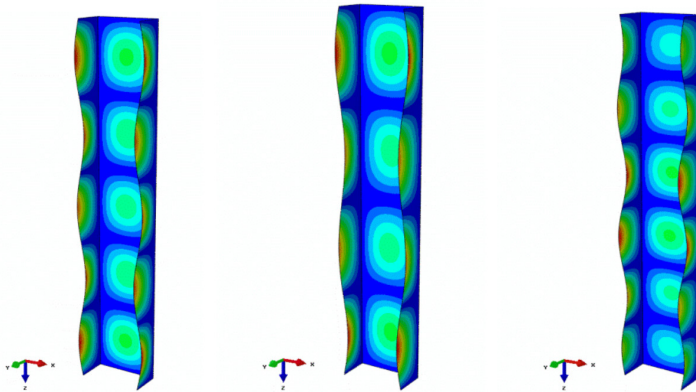
In the process of discretization of geometrical model (the *Mesh* module), layer finite elements of the SHELL type will be used, each of them having six levels of latitude in each knot. The type of finite element taken for the construction of a discrete model is an eight-nodal layer element with reduced integration of the *S8R* marking, having the shape function of the second level. In the worked discrete model one should take even density of the grid of finite elements of the dimensions characteristic for a single element 2x2mm, which will provide an even separation of respective walls of U-shaped profile with a grid of constant density. As a result of the used method of discretization, one got a numerical model of the dimensions equaling 5000 elements, which will provide the possibility of precise observation of the forms of construction's buckling, while keeping the acceptable 'costs' of numerical analysis (the time of calculations' lasting).

For providing additional possibilities of the further numerical analysis describing the work construction in post-critical state, one should note the results concerning knot dislocations in a special file having the format *.fil. For this purpose, one should choose the option *Model/Edit Keywords* in the upper menu of the program. After editing a text file consisting of the data of model in the area concerning entering of results *OUTPUT REQUESTS*, one should add the verses of command in the way presented in the pic. 3.3:



Pic. 3.3. Edition of results of knot dislocations to the *.fil file

The solution of own issues concerning the linear statics of construction are the own values which are directly the values of critical load and correspondent to this forms of statics loss, by the taken unit load of the model. In the pic. 3.4 three initial forms of U-shaped profile's buckling are presented, corresponding to the three initial own values.



Pic. 3.4. Forms of U-shaped profile's buckling: a) first form $P_{kr} = 9068 \text{ N}$ ($m=5$), b) second form $P_{kr} = 9217 \text{ N}$ ($m=4$), c) third form $P_{kr} = 9478 \text{ N}$ ($m=6$)

While evaluating the results one may state that with regards to the proportion of U-shaped profile's dimensions towards the length of the whole profile, the buckling of construction has the character of a local buckling of respective walls

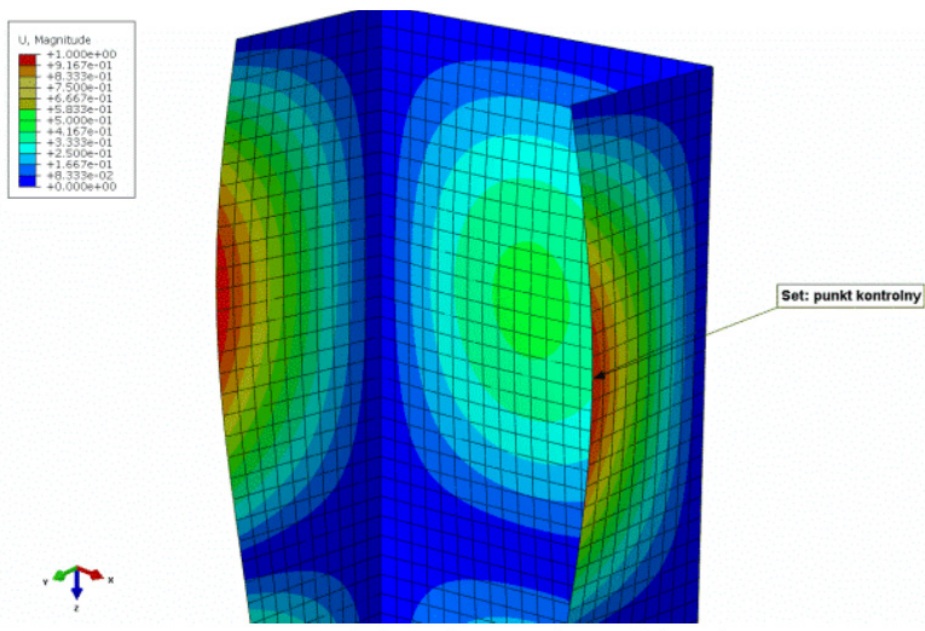
of the profile, which is evinced by creation of a specified number of half-waves in longitudinal direction of the profile. A practical meaning in this case has the first form of statics loss, corresponding to the lowest own value. This means that in the case of losing the statics of the profile, as a result of static squeezing, the construction will undergo the buckling of the value of load $P_{kr} = 9068\text{N}$, experiencing the deformation which causes local folding of walls and web of profile according to the gained form corresponding to the lowest value of critical force of the half-waves amount $m=5$ – pic. 3.4a.

3.2. Analysis of post-critical states of thin-walled U-shaped profile, put to the axis squeezing

Thin-walled constructions are characterized by the possibility of work after losing the statics in the so-called post-critical flexible state [9,10]. In order to describe the work of construction in post-critical state, it is necessary to make a non-linear numerical analysis allowing for big dislocations of a construction – non-linear geometrical issue [1-3,5]. The solution of non-linear statics issue allows to specify full description of the state of deformations and stresses of a construction after crossing the value of critical load. Such calculations are led on discrete models, with implemented geometrical imperfection corresponding usually to the lowest own value, marked in linear analysis of own issue. The description of construction's work in the post-critical state is usually made on the basis of so-called post-critical path of balance, presenting the dependency of the load P on the folding U of chosen knot of a model, located most frequently in the area of the biggest folding of a construction. Calculations of non-linear statics will be made on discrete model used for own issue, in which indispensable modifications will be made, while keeping the same grid of finite elements. It is a necessary condition, because the results of knot dislocations were derived for the knots of the model in the *.fil file. In order to work out a discrete model allowing to lead non-linear analysis, one should copy a present model in the CAE base, with the use of a command from the upper menu of the program – *Model/Copy Model*. The following modifications will be made in the copied model:

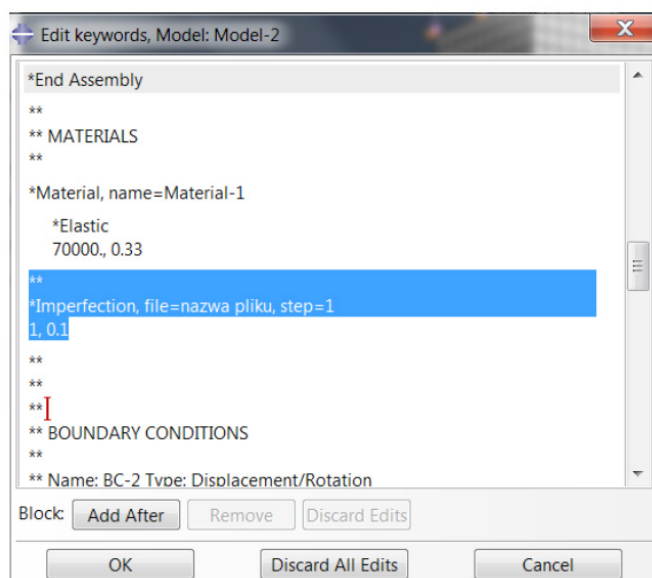
- *Step* module:
 - one should change the type of analysis from the analysis of own issue Buckle into non-linear static analysis Static General, with the option NLGEOM on, which allows for geometrical non-linear issue (big dislocations in this case); as a value of an initial increment of load, one should take *Initial increment size* = 0.1,
 - in order to mark post-critical path of balance in the knot on the wall of profile in the area of biggest folding, one should create Set with the

name 'control point' (the command from the upper menu: Tools/Set/Create), and then derive results in the form of graph with the use of the tool Create History Output by choosing the option Set: control point, for which one should make the graphs of displacements Displacement in the function of construction's load – pic. 3.5,



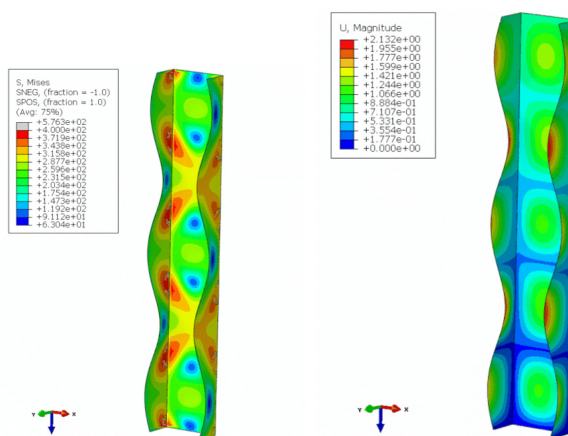
Pic. 3.5. *Post-critical path of balance – control point*

- Load module: one should change the value of load Shell edge load from the unit one (0,0125N/mm) into the value correspondent e.g. to $150\%P_{kr}$ equaling 170,025 N/mm,
- In order to implement geometrical imperfections corresponding to the lowest form of buckling, gained in linear analysis of own issue, with the use of option from the upper menu Model/Edit Keywords, after editing text file consisting of data of a model one should add verses of commands presented in the pic. 3.6 (the second line means: 1 – number of buckling form, 0.1 – value of imperfection meaning 0.1 mm),



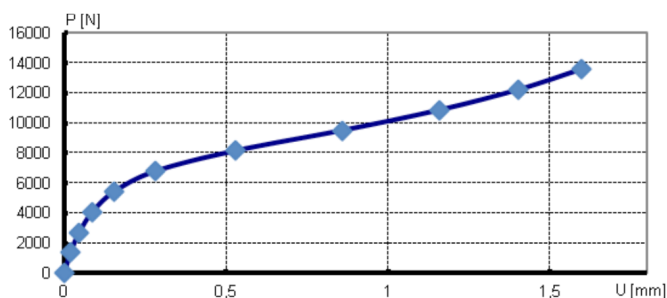
Pic. 3.6. Import of introductory information corresponding to the lowest own value

Solution of the issue of non-linear statics gives total information allowing to make qualitative and quantitative evaluation of construction's work in post-critical state. Analysis of the gained results will be made on the basis of the distributions of reduced stress, which are marked by the Huber-Mises-Hencky's (H-M-H) resistance hypothesis and displacements of U-shaped profile's knots – pic. 3.7.



Pic. 3.7. Results of calculations a) distribution of stress H-M-H, b) map of profile's folding

We'll get the state of deformation of construction being in post-critical state; it stands the deepening of initial deformations harmonious with the implemented form buckling. Map of distribution of reduced stress H-M-H allows to evaluate the level of construction's exertion and to identify the areas of the highest levels of stress. As the most strained zones in the case analyzed, one should consider the boundary areas of the profile. The specified post-critical path of balance $P-U$ allows to make evaluation of construction's stiffness in the full scope of the load pic. 3.8. In the case analyzed, the gained characteristics keeps the static character, i.e. the increment of construction's folding is possible only by the increase of external load. It confirms the legitimacy of the taken plate model for analysis of post-critical states of the thin-wall construction examined.



Pic. 3.8. *Post-critical characteristics of the $P-U$ construction*

4. Summary

The analysis of static issue of the squeezed thin-wall section of U-shaped profile, presented in the chapter, is an example of the use of finite element method in engineering issues. The presented numerical analysis concerns very essential issues connected with designing thin-wall constructions, exposed to the loss of statics in the scope of exploitation loads. Such phenomena, despite being observed in real structures, e.g. aviation ones, are useless with regard to i.e. exhaustion resistance or aerodynamic characteristics of a structure. Thus, the abilities of describing and analyzing of the problem of statics loss and the work of construction in the post-critical scope belong to unusually important issues in thin-wall constructions designing. Effective tools allowing to make this type of analyses are currently the numerical programs using the finite element method. As it was shown in the example of squeezed thin-wall U-shaped section, making numerical simulations with FEM method makes the solution of non-linear statics issue possible, while providing a great deal of important information allowing to describe the work

of construction in the full scope of load. The applied way of proceeding leads to specification of the value of critical load, the form of statics loss, and also to specification of stiffness characteristics of construction in post-critical state. The non-linear incremental-iterative (the Newton-Raphson method) procedures used in the process of calculation allow to analyze the issues with taking into consideration big displacements for which one should allow i.e. the loss of thin-wall constructions' statics.

The conducted numerical analysis of thin-wall construction stands an example of solution of a classic engineering issue allowing in qualitative and quantitative way to mark stiffness and resistance characteristics of constructions. The gained results of numerical analyses provide a lot of important information allowing to make current verification and optimization of constructional parameters, yet in the stage of designing of a construction. It confirms very considerable usefulness of finite element method in solving engineering issues, frequently very complex ones.

Literature

1. Rusiński E., Czmochoński J., Smolnicki T., *Zaawansowana metoda elementów skończonych w konstrukcjach nośnych*, Oficyna Wydawnicza Politechniki Wrocławskiej, Wrocław 2000.
2. Bąk R., Burczyński T. – *Wytrzymałość materiałów z elementami ujęcia komputerowego*. WNT, Warszawa 2001.
3. Rakowski G., Kacprzyk Z.: *Metoda Elementów Skończonych w mechanice konstrukcji*, Oficyna Wydawnicza PW., Warszawa 2005.
4. Niezgoda T. – *Analizy numeryczne wybranych zagadnień mechaniki*. WAT, Warszawa 2007.
5. Osiński J.: *Obliczenia wytrzymałościowe elementów maszyn z zastosowaniem metody elementów skończonych*, Oficyna Wydawnicza PW., Warszawa 1997.
6. Abaqus HTML documentation.
7. Kleiber M., *Metoda elementów skończonych w nieliniowej mechanice kontinuum*. PWN, Warszawa-Poznań 1985.
8. M. Kleibera (red.), *Komputerowe metody mechaniki ciał stałych*, w ramach serii Mechanika Techniczna t. XI, Wydawnictwo Naukowe PWN, Warszawa 1995.
9. Waszczyszyn Z. i inni, *Metoda elementów skończonych w stateczności konstrukcji*, Arkady, Warszawa 1990.
10. Zaráj J., Królak M., Kotelko M.: *Metody doświadczalne wyznaczania obciążeń krytycznych i analizy zachowania się elementów konstrukcji w stanie zakrytycznym*. X Krajowa Konferencja Wytrzymałości Materiałów i Badania Materiałów, Kudowa-Zdrój 20-22 wrzesień, 2006 (wersja elektroniczna).

Chapter IV

Modern techniques of production accelerating

Techniques shortening the time of designing and producing

Features influencing product's development [1,4,7]

- Short time of products' life, forcing shortening of their cycles of developments and production implementation
- Increasing number of products' variety
- Frequent changes and modifications of products, focused on addressees tastes,
- New and original pattern lines of products,
- Decreasing amounts of production series
- Producing of short series and unit products to special order of a customer,
- Minimization of production costs, which is their price.

Thus, in the process of designing one should examine many different solutions and next create fast a prototype. One may do it thanks to computer techniques shortening the time of designing and producing (Time Compression Technologies – TCT).

Techniques of accelerating production [1,4,7]:

- Virtual prototyping (Virtual Prototyping) – examination of prototype existing in computer),
- Fast production of real prototypes of machines and devices (Rapid Prototyping),
- Fast serial production (Rapid Manufacturing)
- Fast production of tools (Rapid Tooling),
- Backward engineering or in other words – reverse engineering (Reverse engineering) – creating solid model in computer on the basis of a real object.

Virtual prototyping (Virtual Prototyping) is creation and examinations concerning the 'virtual' prototype, which is a fake creation existing only in computer. It includes [1,4,7]:

- Computer design of an object
- Simulation of the process of creation (e.g. casting or mechanical working)
- Simulative examinations of features, e.g.:
 - Resistance (analysis with Finite Element Method and others)
 - Functional (kinematics, dynamics, ...)
 - Ergonomic (service)
 - Possibilities of recycling
 - And so on

Researches on virtual object, which is a computer model, may include [1,4,7]:

- Checking of many variants of solutions
- Checking of feasibility (on numerical machine tool)
- Simulations of casting process
- Checking of possibilities of montage and collisions identification
- Resistance examinations (FEM – DEM) – static and dynamic
- Marking of heat transformation and distribution of temperature
- Simulation of work: kinematic (movement) and dynamic (movement + forces, moments, friction, ...)

Computer programs for virtual prototyping

‘Virtual prototyping’ programming allows to build a realistic model of moving prototype and to conduct examinations on it, which concern kinematics of movement and also dynamics with taking into consideration masses, forces, frictions, repressions, deformations, stresses, vibrations etc., allowing at the same time to optimize a project before real construction of a prototype. Example systems for modeling and simulating examinations: Working Model – simulation of two-dimension objects, Visual Nastran – simulations of three-dimension objects, ADAMS (analysis of kinematics and dynamics), ADINA, ABAQUS (linear and non-linear, static and dynamic analysis with finite element method). FLUENT (analysis of transmissions), MATLAB + SIMULINK (modeling and simulation of dynamic sequences – including sequences of steering) [1]. Other programs which one should enumerate here are e.g. CATIA, Solid works, Mechanical Desktop, Inventor.

1. Fast production of prototypes – Rapid Prototyping

Systems of fast production of prototypes (RPS) is a group of devices and technologies included in CAM – (Computer Aided Manufacturing), which is computer-aided production.

It is automatic production of machine elements or other objects, with the aid of devices steered from computer on the basis of the solid model worked before.

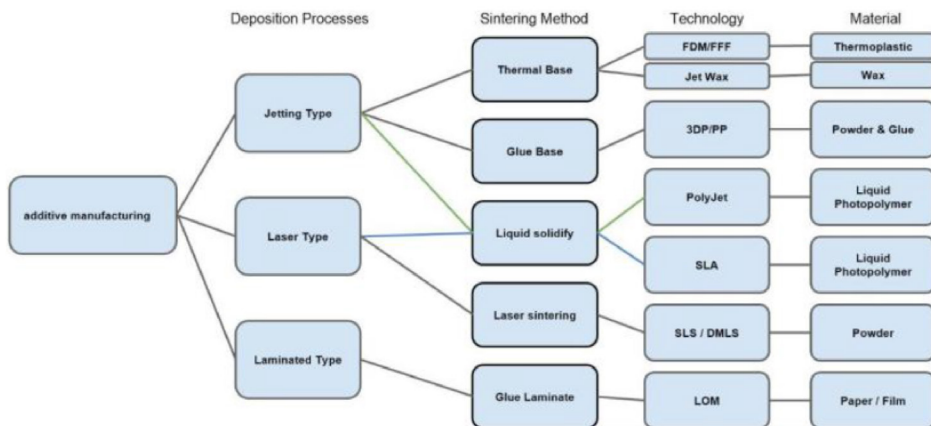
Contrary to the deficit methods used by working machines, ***RP methods are additive (incremental)*** – it means that they are based on step-by-step putting (adding, gluing) layers of material by gluing, fusing, fritting or hardening of various materials with the aid of laser or other radiation beams.

Thus: Rapid Prototyping = Generative, incremental, additive technologies.

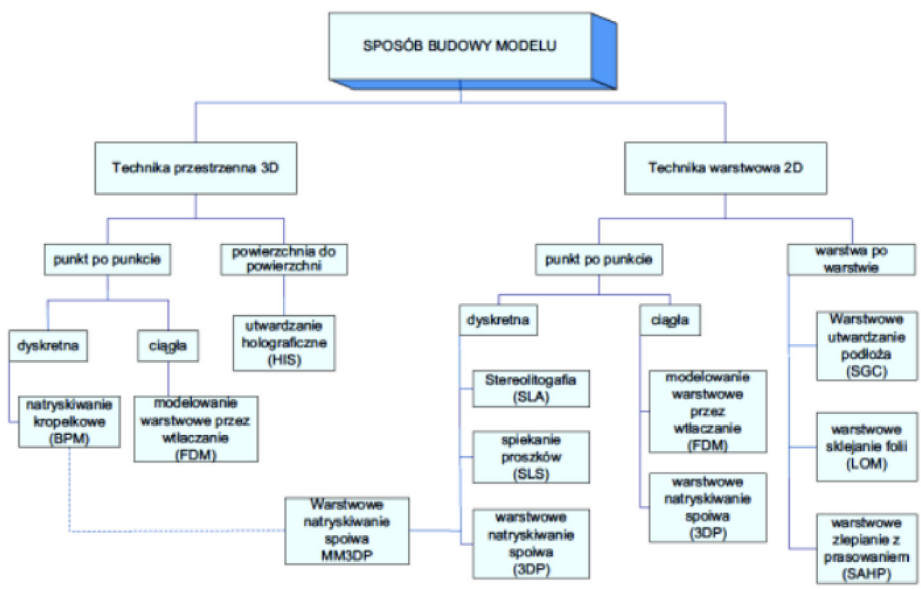
In other words, RP is process of building physical models of plastic, metal, ceramics or paper, based on virtual 3D models, consisting in computer-steered layer merging of materials in the form of liquid, powder, or sheets [14].

Also the name Solid Freeform Fabrication (Formless Production of Permanent Shapes) is used [23].

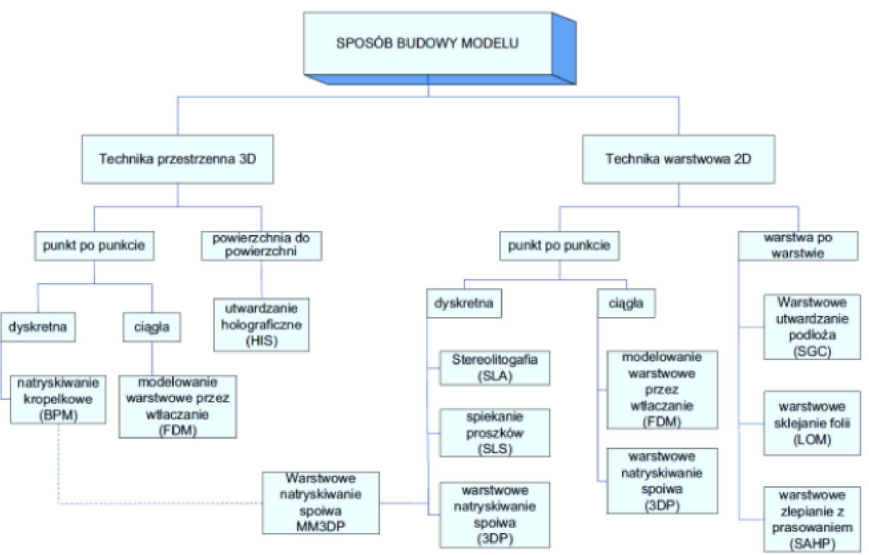
a)



b)



c)



Klasyfikacja metod RP z uwagi na sposób budowy modelu

Pic. 1.1. Division of RP techniques [8](b,c)

Technological possibilities of fast prototyping systems

- Fast production of prototypes, ready-made products and tools for their production
- Possibility of market verification of a product, without engagement of costs in preparation of tools for production of trial series
- No technological limits in free shaping of products' geometry, and at the same time widening of market products patterning
- Minimization of the risk of putting products on the market, while not meeting customer's expectations

Tab. 1.1. *Materials processed in chosen RP processes [7]*

RP method	Form of initial material	Binding method	Processed materials
SLS Selective Laser Sintering	powder	sintering	Wax, thermoplastics, ceramics, metals
3DP 3D Printing		bonding	Ceramics, metals
SLA StereoLithography	liquid	Polymerization	epoxy resins and acrylic
SGC Solid Ground Curing			
FDM Fused Deposition Modeling		melting and curing	Wax, thermoplastics
BPM Ballistic Particle Manufacturing			
MM3DP Model Maker 3D Plotting			
LOM Laminated Object Manufacturing	Solid object	adhesive bonding	Paper (plastics)
LOM - SAHP Selective Adhesive of Hot Press			

First RP systems were introduced in 1980s, initially only for prototyping production, now they find wider and wider use, also in production of tools or short series of high-quality elements.

The word 'fast' means in practice the period of at least tens of hours, depending on method, used devices and complexity of a model. One also use various materials, e.g.: high-temperature-melting for final product and low-temperature-melting as fillings separating respective parts.

Multiple production and correcting of physical models prototypes has been possible thanks to the invention and use of fast fabrication technologies of prototyping in the production (eng. Rapid Prototyping – RP) and fast fabrication of tools, which are casting forms for short informative series (eng. Rapid Tooling – RT).

The fundamental aim of the uses of these technologies is physical modeling (geometrical, functional, visual, assembly models, technical prototypes) on the basis of 3D computer objects, mainly aiming at evaluation of usable functions, aesthetics of products and marketing evaluation [1].

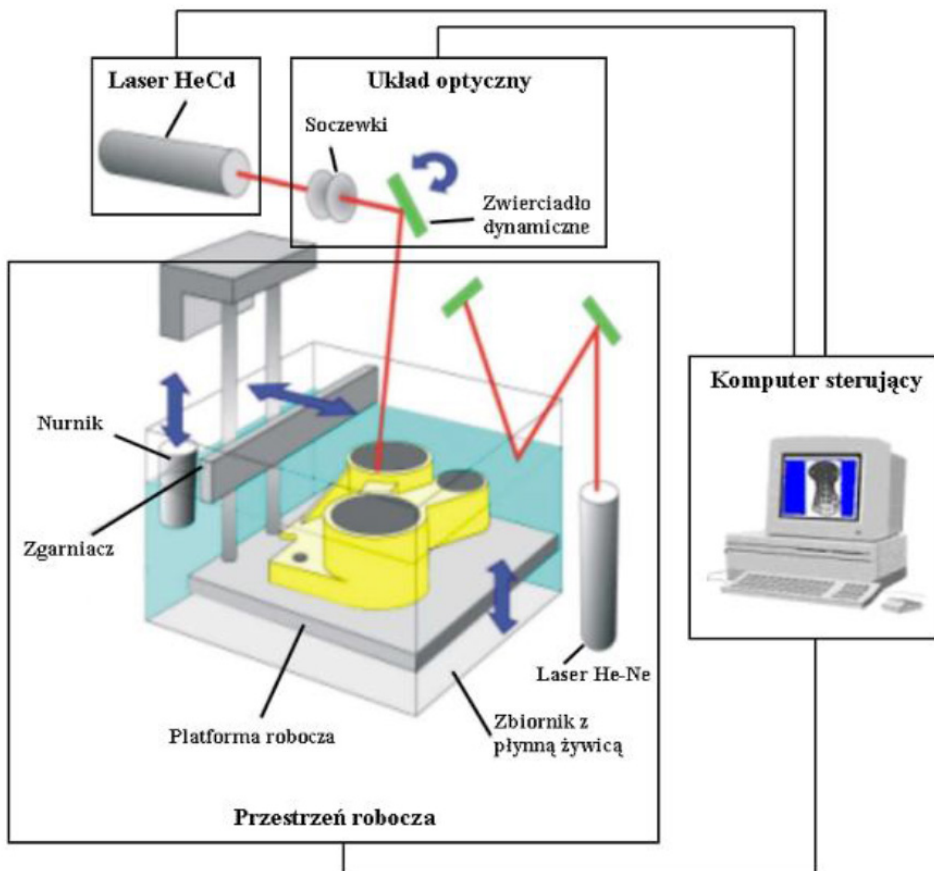
The disadvantage of prototypes made with RP and RT techniques is the fact that they don't correspond fully to the requirements concerning functionality, shape or quality of a real product. Their main task is marking of weak places in products development, whose elimination without these technologies would entail considerably higher costs than the costs incurred in the case of making prototypes with RP and RT methods [1].

Tab. 1.2. *Rapid Prototyping methods – technology*

Stereolithography	SLA	1986	utwardzanie fotopolimeru za pomocą lasera UV
Fused Deposition Modeling	FDM	1989	wtapianie porcji wypełniacza plastikowego lub drutu metalowego
Selective Laser Sintering	SLS	1986	spiekanie za pomocą lasera cząstek plastiku, metalu, ceramiki lub szkła
Electron Beam Melting	EBM	1993	stapianie warstw metalu w komorze próżniowej za pomocą wiązki elektronowej
Laminated Object Manufacturing	LOM	1996	sklejanie profilowanych arkuszy plastiku, papieru lub metalu
Single Jet Inkjet	Inkjet		natryskiwanie roztopionego wosku, metalu lub materiału utwardzanego optycznie
Three Dimensional Printing	3DP	1989	sklejanie materiału proszkowego za pomocą natryskiwanego kleju

Process of fast fabrication of physical models with the use of stereolithography method (SL).

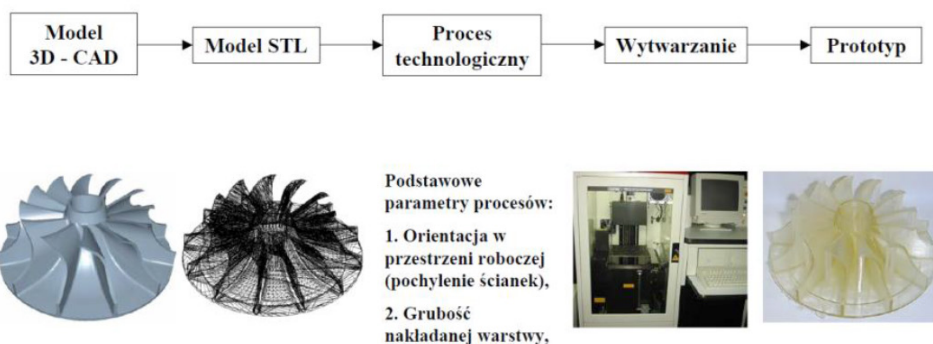
The process of stereolithography, use e.g. in the SLA machine consists in local change of phase state of homogenous center (change from liquid into solid) under the working of UV laser. The process of change of resin from liquid into the solid one, under the influence of UV radiation, bears the name of photopolymerization. The essence of initiating of polymerization consists in creation of polymerization's radicals by the light of laser, which react mutually on monomers' molecules and then they initiate the increase of polymeric chains. The path of laser's beam is steered by dynamic mirror through the computer which also steers the work of stereolithographic machine. Polymerization occurs only in the area of lightening with laser's beam, in a precisely specified capacity. That is why this method is characterized by comparatively high precision.



Pic. 1.2. *The idea of prototypes fabrication process with the method of stereolithography [4,13]*

A typical process of prototype fabrication with the method of stereolithography may be divided into the following stages [4,7]:

- Creating of geometrical model in CAD system,
- Approximation of solid model with STL format,
- Preparation of technological process, used for fabrication of physical prototype (model) on the machine, which is connected with:
 - Verification of data correctness saved in the STL format
 - Orientation of the model in labor space of machine
 - Creating of supports for the fabricated prototype
 - Specification of technological parameters of the process, which is:
 - Thickness of the layer which is put
 - Compensation of layers' 'overexposure'
 - Compensation of width of laser's beam
 - Number of transitions and speed of scraper's movement
 - Style of layers' building
- generating of files which steer the process of fabrication and sending them to the sequence of machine's steering
- creation of prototype – physical model in resin



Pic. 1.3. Stages of fast fabrication of prototype with the method of stereolithography (SLA) [7]

Creation of geometrical model in CAD system

The first and basic condition of fabrication in RP technology is gaining of three-dimensional solid model in CAD system. Solid model ensures that geometry of the model is always closed. However, such certainty is not provided by surface model [7].

A model may be built of rectilinear solids (cylinder, cube, rectangular prism etc.) It may also be made with the use of standard editing tools, such as: pulling out, rotation, cutting off, phasing, rounding etc., by gaining through coordination

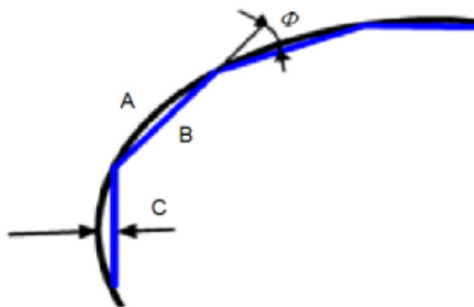
measuring with measuring machines or 3D laser scanners, of the cumulus of points, which allows to get solid model of the measured object, when processed properly.

A certain kind of this method of measuring is the dimension with the use of e.g. techniques know to medical diagnostics, which is Roentgen computer tomography or magnetic resonance. A proper processing of medical images allows to distinguish contours of interesting areas which, while covered with layer parts, make gaining the solid model possible.

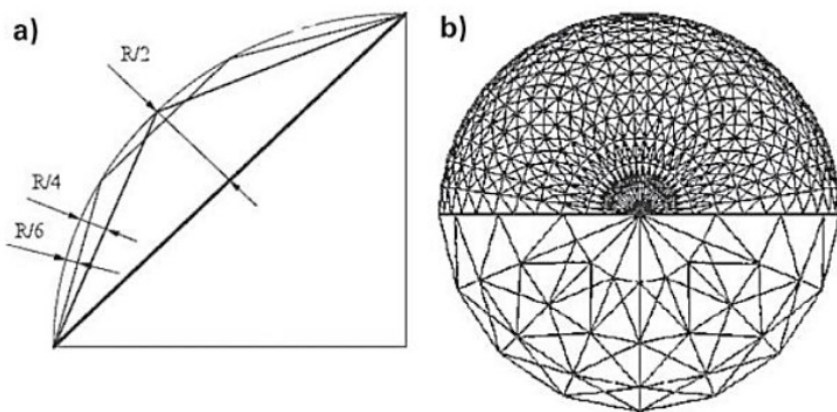
A solid model may have various level of complexity. One of constraints for stereolithography method is the thickness of model's wall which cannot be smaller than the diameter of laser's beam.

Approximation of solid model with STL format

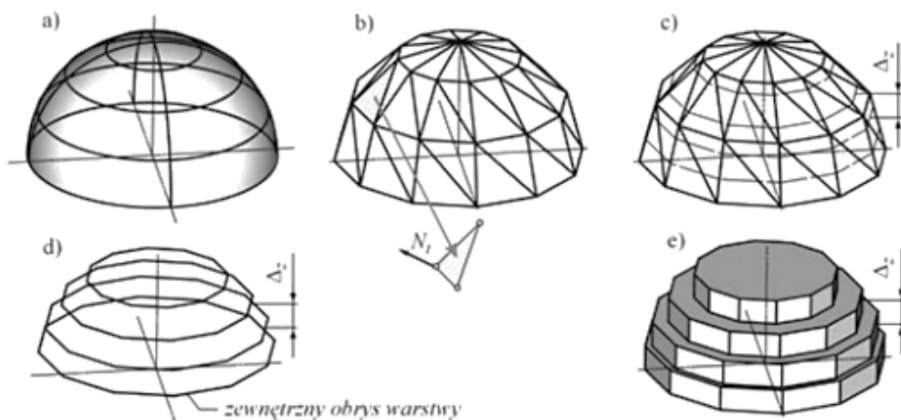
The 3D solid model got in CAD system is approximated with triangular elements connected with each other in the peaks. A characteristic trait of such approximation is change of flexures (lines) of external contours and internal walls, through the chords which are sides of triangular elements. While noting contours, the distance between its curvature and chord is marked. Also the angle which is made by both sides of triangle, i.e. (chords). The smaller are numeral values given to this parameters, the higher number of triangular elements will the model be described with. At the same time it boils down to increase of the size of data file. Coordinates of peaks and normal vector elements, specifying orientation (swelling) of wall, are saved in this file.



Pic. 1.4. A – opening surface, B – triangulation surface, C – tolerance, Φ – angle of elements divergence [4]

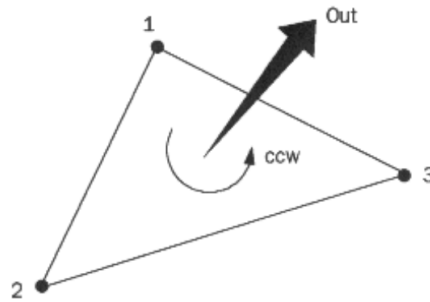


Pic. 1.5. Secant error in approximation of circle with secants (a) and influence of triangular amount on sphere patterning (b) [18]



Pic. 1.6. Process of stereolithographic model fabrication: a) CAD model, b) STL model, c,d) division of STL model into layers, e) ready-made SLA model, Δz – thickness of separate layer of SLA model, N_i – normal vector [11]

Triangulars in STL file have to provide proper fitting with other triangulars in the area of peaks and one should provide their proper orientation, so as to specify which side of the triangular includes the interior of model. Orientation of surface is specified by the turn of normal vector and normal order of knots (right-turn sequence), in which peaks are enumerated (pic.).

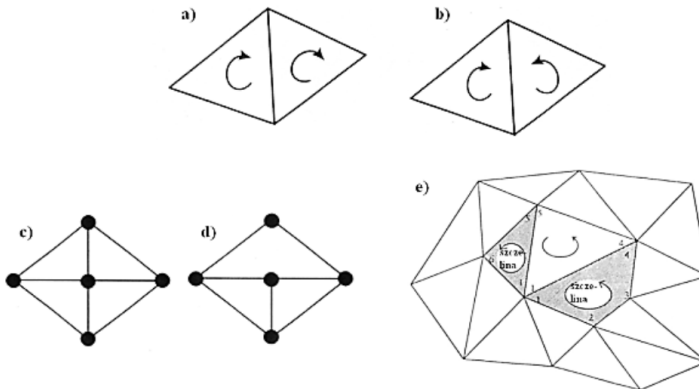


Pic. 1.7. Orientation of STL element's surface

In the taken procedure, the rule 'vertex-to-vertex' is binding – each triangle has to have only two mutual peaks with each neighboring triangle.

Errors connected with construction of approximated geometrical models in STL format:

- turns of normal vectors, harmonious with general direction of triangle pieces generation
- opposite turn of one normal vector towards the direction of generated grid, of triangle pieces
- correct assignment of the edges of triangle pieces
- incorrect assignment of the edges of triangle pieces
- spaces in approximated surface of a virtual model



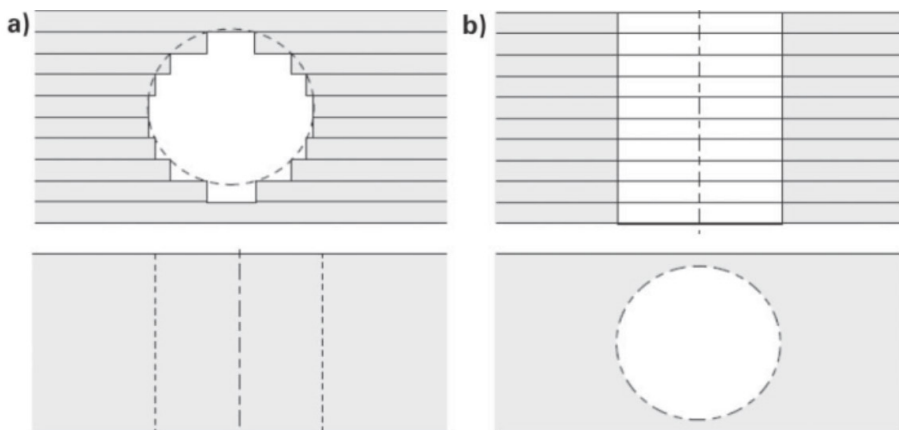
Pic. 1.8. Errors connected with construction of approximated geometrical models in STL format:

- turns of normal vectors, harmonious with general direction of triangle pieces generation
- opposite turn of one normal vector towards the direction of generated grid, of triangle pieces
- correct assignment of the edges of triangle pieces
- incorrect assignment of the edges of triangle pieces
- spaces in approximated surface of a virtual model [4]

A huge part of search engines is able to read STL files so as to put them to analysis and if need be correction, control of coherence, and procedure of gaps identification in three-dimension environment made of triangles. This process is fully automatic.

While creating models with techniques of fast prototyping, one should allow for the following rules:

- in the case of elements in which details are comparative to the thickness of the put layers of material, one should expect that they will undergo deformations
- the level of details deformations is hard to specify, because it depends mainly on the placement of triangles grid which creates structure of surface in *.stl format, towards the layers of the built model
- proper placement of an object during its fabrication may influence on precision of a model's details production (pic. 1.9)



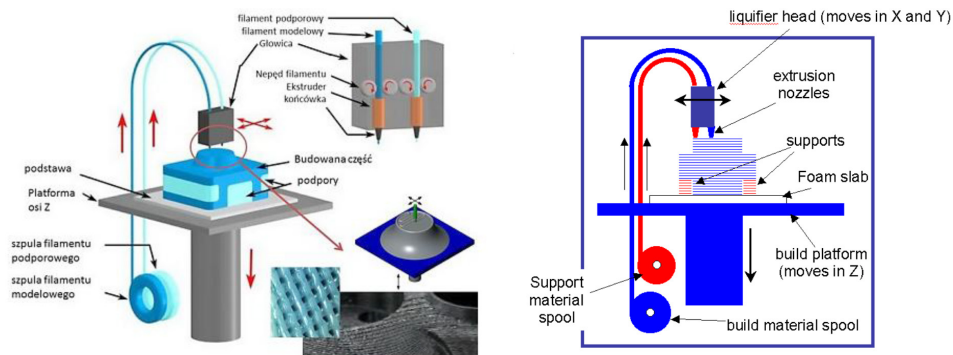
Pic. 1.9. Possibilities of reconstruction of parallel (a) and perpendicular to the layers (b) axis in SL technology [16]

The course of typical process of fast prototyping in FDM method – Fused Deposition Modeling – extrusion settling of the fused material

Realization of the process of fast prototyping proceeds in the stages [1,7]:

- creating of geometrical model of an object in CAD system or alternatively–digitalization of existent physical solid,
- saving of file in STL format,
- transfer of the file in STL format to the programming of the machine for fast prototyping,

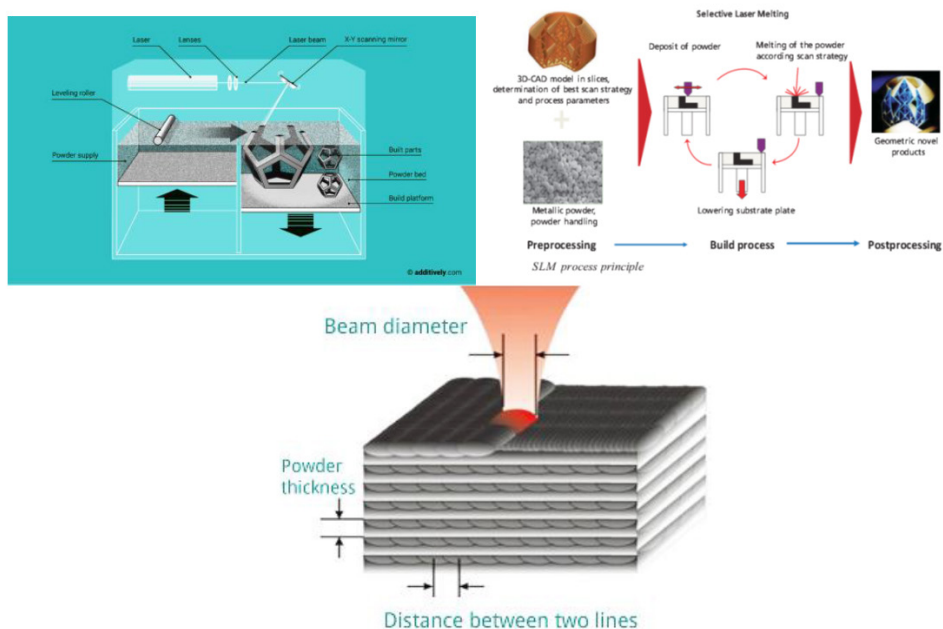
- division of an object into profile sections of which product will be built, and arranging of processing parameters: thickness of layer, width of layer etc.,
- automatic creation of supporting constructions,
- building of the product, consisting in distribution of fluidized material in the form of thin 'thread', in turn on each layer (layers connect with each other, creating a complete model),
- removing of supporting constructions, and finishing treatment (if need be) of the created model.
-



Pic. 1.10. Idea of FDM technology [8,17,20]

SLS (Selective Laser Sintering) method, SLM (Selective Laser Melting) – sintering (melting) of powdered material

The rule of models building in SLS/SLM method is a mixture of SLA technology (stereolithography) and 3DP (3D Printing). STL file is divided by machine's programming into bitmaps and it is sent layer by layer to SLS device. A layer of powder is put on the base of chamber, which is fused from the above with a beam of laser of 30-100W power, according to the presented before bitmap. After fusing the layer, the next layer is put on it and the process repeats from the beginning.



Pic. 1.11. Idea of models fabrication with the SLS method – a) [19], and SLM method – b,c) [18]

Similarly to 3DP technology, the support and the element separating respective parts from each other is unsintered powder. After printing out, one should clean the model of the powder remained and the piece is ready for use. Depending on the kind of selective sintering system, the most frequent thickness of the put layer is 100 microns (0,1 mm). It allows to gain the precision of models of the sequence from 0,1 to 0,2 mm, which is the precision efficient both for creating prototypes and unit ready-made products. Depending on the kind of powder and the thickness of the used sintered layer, one may create models of more than 99% of density.

The companies, which produce SLS systems, use various kinds of materials. Polyamide powders prevail – clear and with addition of glass fibre or coal fibre. One may also use the powders basing on polystyrenes which work very well as masers for the method of lost model. Designers who need the look reminding of metal will be interested in the powder with addition of aluminum. All of the powders are characterized by very good mechanical and physical features, owing to which one can create not only testing model, but also a ready-made product used as final product.

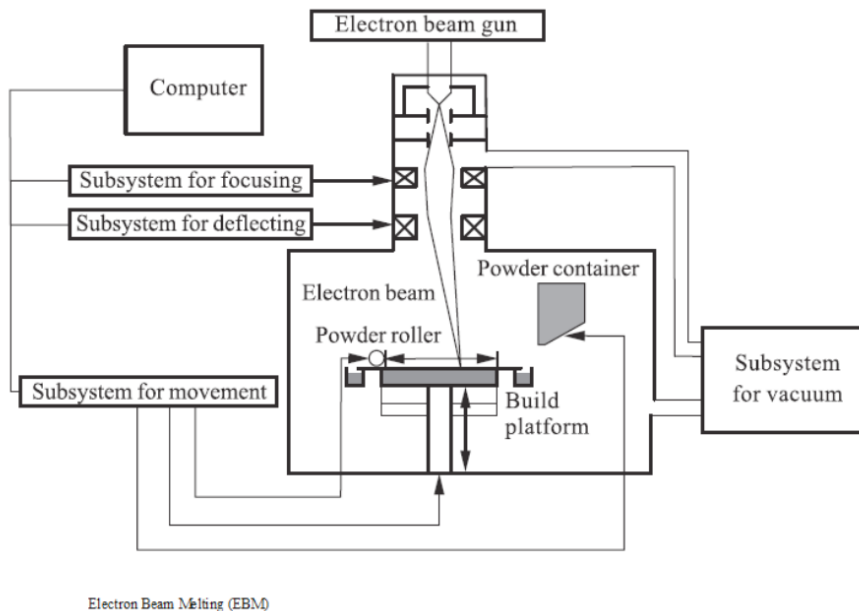
SLS systems are used practically in each branch of industry (functional, ergonomic, fit prototypes). Pieces created with the aid of sintering with laser are exploited in motorization, aviation, packaging industry or industrial patterning.

Thanks to the possibility of sterilization of a ready-made product, SLS spreads also in medicine – as pieces of medical equipment.

The variant of these technologies is also **DMLS – Direct Metal Laser Sintering** –*technology of direct fusion of metals' powders*.

Electron Beam Melting (EBM) – electron, selective melting (of powder)

Building of models proceeds through putting layers of metal powder on lowering platform, and next melting of each of layers with the aid of concentrate beam of electrons in the way in which actual layer is fully melted and permanently joined with the previous one. The process takes place in vacuum chamber, because otherwise atoms of gas would disperse the electron beam. Owing to high vacuum with minimal participation of helium, EBM machine can produce details with complicated spatial structures, keeping at the same time the highest standards of cleanness of melted metal alloys. Mainly because of high density and cleanness of metal structure, Electron Beam Melting has found its use in implants production, consisting of porous structures and making osteointegration easier, which are impossible to be made with cutting treatment. EBM is also much faster technology than the DMLS and SLM ones; however, it offers much lower precision of the built elements and worse quality of surface, which causes that most of engineering pieces require additional processing with cutting.



Pic. 1.12. Scheme of EBM working [source – Internet]

Additive technologies based on powdered metals located in tank chambers ('Powder bed fusion'):

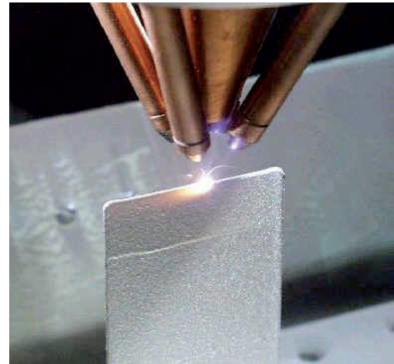
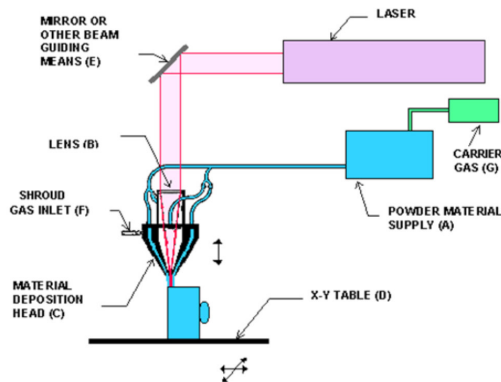
- Direct metal laser sintering (DMLS)
- Selective laser melting (SLM)
- Selective laser sintering (SLS)
- Electron beam melting (EBM) .

Additive technologies based on powdered metals, given with the use of nozzles (e.g. with the use of compressed gas) in the zone of melting and settling ('Blown powder')

- Direct metal deposition (DMD)
- Laser Metal Deposition (LMD), Direct Laser Deposition (DLD)
- Laser Engineered Net Shaping (LENS)

Laser Engineered Net Shaping (LENS)/ Direct Metal Deposition (DMD)

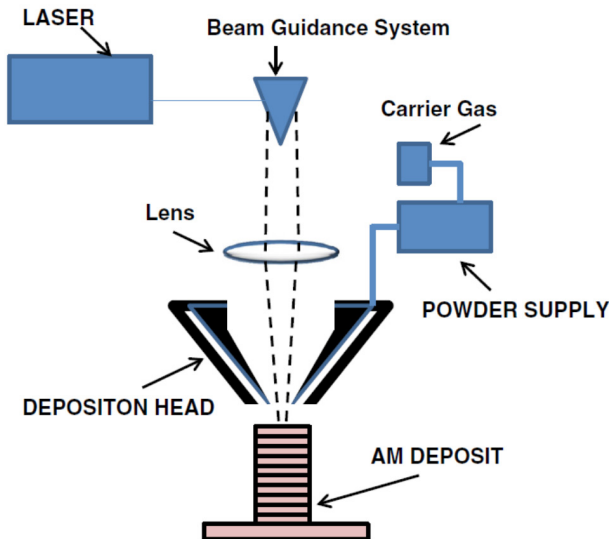
The method is based on dosing a proper amount of powder, along with immediate melting of it, directly on the built model. Laser of high power (from tens of watts to 20KW) melts the provided coaxial powder with the beam of laser through dosing head, on the model.



Pic. 1.13. *Idea of LENS technology [8,22]*

The dozed powder is gravitationally or under the pressure of carrying gases. The environment of these gases is used for protection of melted material from atmospheric environment, aiming a better control of features, and in order to provide a better adherence between the alternate layers. Gases are, however, used also in the cases when dosing of material doesn't require it, but in order to provide better features and parameters, they are exploited. The fabricated models may be already treated as the final ones; however, mechanical processing is advisable. They

are characterized by a good grain structure, and by parameters similar or even better than the proper materials [8].



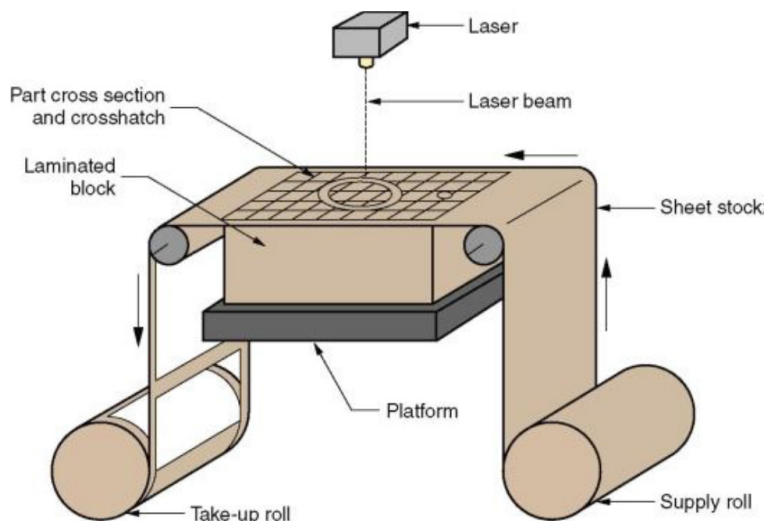
Pic. 1.14. *The rule of EDM working [24]*

Theoretically, the material used in sintering technologies with laser may be each metal, which can be powdered. Currently, there are dozen or so of the powders adapted to DMSL – from simple metal powders, through stainless steel, to titan powders, clean or with additions. In general uses, stainless steels and alloys of various metals (e.g. cobalt with chromium) are most frequently used ones. For medical uses, the possibility of melting pure titan was worked out and implemented, owing to which one can make e.g. implants [2].

Laminated Object Manufacturing (LOM) – Layer fabrication of objects [8]

It consists in setting of material which has the form of foil, in stack or most frequently in gluing them with the aid of laser or heated shaft. Opening material may be unrolled from the roll or it may have the form of sheets. It is covered with glue from the bottom, one-sidedly. The first layer of the foil is a cut shape, corresponding to a proper profile section of the fabrication. One make it with the aid of laser or in certain kinds of LOM, called in short from English SAHP, with the aid of numerically-steered knife. After cutting the shape, the stack lowers with the thickness of further layer, and another layer is put on the previously put one. It is pushed to the bottom layer with the aid of heated shaft, and in the next stage the

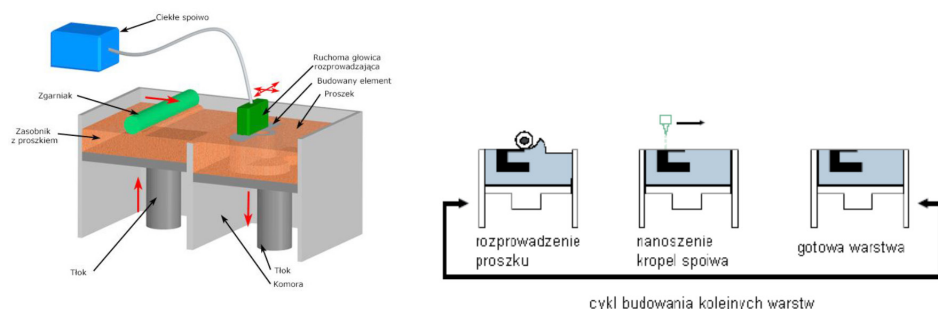
shape of profile section is cut out, but this time it corresponds to the new layer of the future fabrication. The cycle repeats, until the whole model is built.



Pic. 1.15. *The rule of LOM working [25]*

3DP – three-dimensional printing

3DP (Three Dimensional Printing) is a technology of three-dimensional printing enabling to use powders from polymeric, through ceramic, to metal ones. Solids built in that way have huge porosity and they sometimes require fulfillment of free spaces with enforcing material. There is no problem with porosity if liquid labor material is used for building. The benefits of 3DP are: inconsiderable sizes, quiet work, low costs and very fast work.

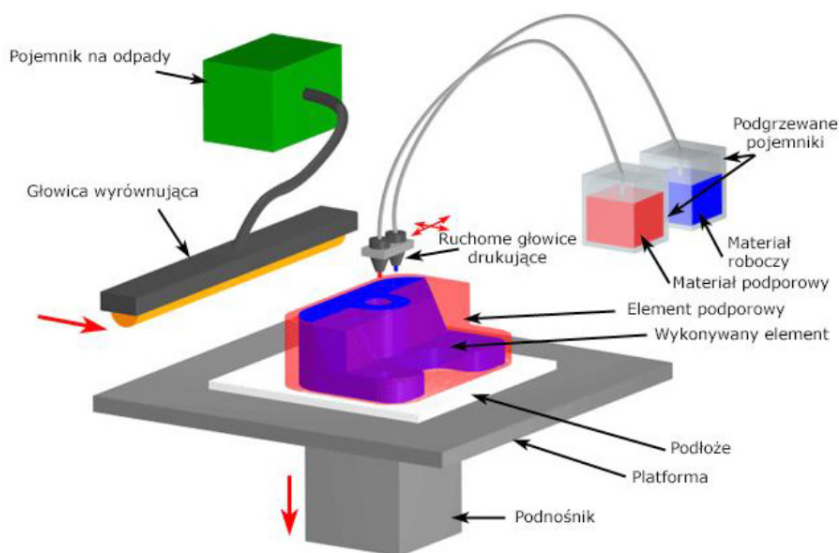


Pic. 1.16. *The essence of 3DP technology [8,17]*

Spraying of material's cement is used for local transmission of glue, so the connections of powders locally. Usually, two containers are used, the container in which product is shaped and an additional box with fresh powder. A huge advantage of this technology is the fact that all kinds of powder can be exploited. It is easy to add color to the printed final products.

IJP – Ink Jet Printing

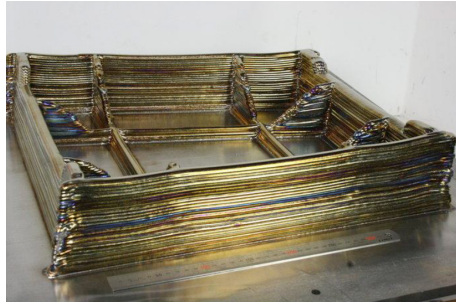
It is a technology belonging to the RP methods which patterns surface well and it is characterized by a good print resolution. Not only labor material (thermoplastic material) is put on the layer, but also aiding substance, the so-called supporting (wax), providing stability of solid while printing it.



Pic. 1.17. *The rule of IJP printing method working*

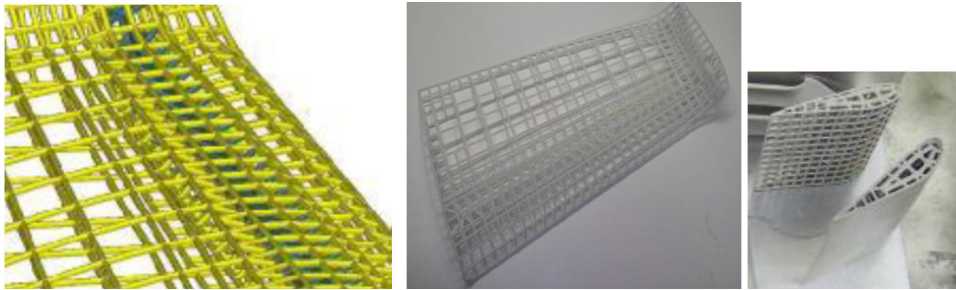
Possibilities and areas of use of generative technologies

In recent years, one observes an intense development of RP technologies, both in the area of their technical possibilities and also in the area of use. That is why one is saying rather about the third technical revolution. Cosmic technique, aviation industry, medical technologies are the fields in which this advance is the most intensive one. Thus, e.g. zero-waste technologies, possibility of producing advanced technologically metal products of the materials which may endure temperature to 3500°C are being tested (pic. 1.18).



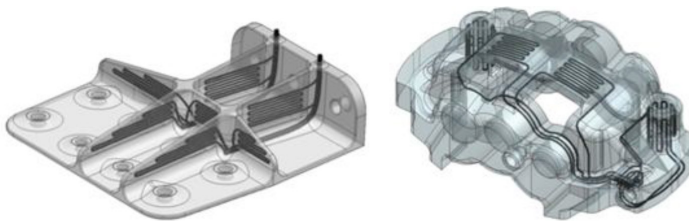
Pic. 1.18. *Example of production of titan powders, of ribbed element used in aviation technique [26]*

The next group of issues concerns possibilities of building of crafts wings' elements, as also whole objects (e.g. drones), with the use of RP technology and industrial robots.

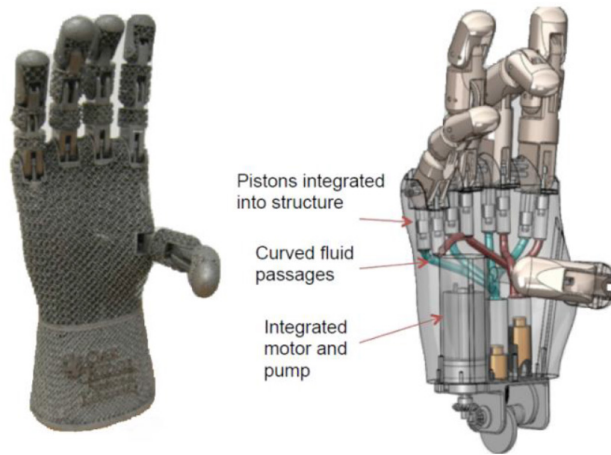


Pic. 1.19. *Fabrication of airplane's wings' construction with the use of RP technology [12]*

Possibilities of fabricating multifunctional material systems in which functional integration of the built in the structure: sensors, electric circuits, elements producing and cumulating energy, tracks of communication occurs are tested (pic. 1.20, pic. 1.21)

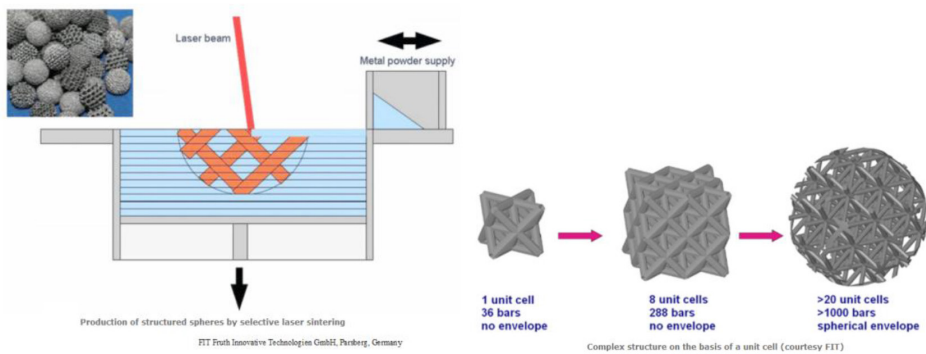


Pic. 1.20 *Building of elements with optimized internal cooling, contours (geometry) of details impossible to be gained with traditional methods of shaping, decreasing of costs by maximization of efficiency [27]*

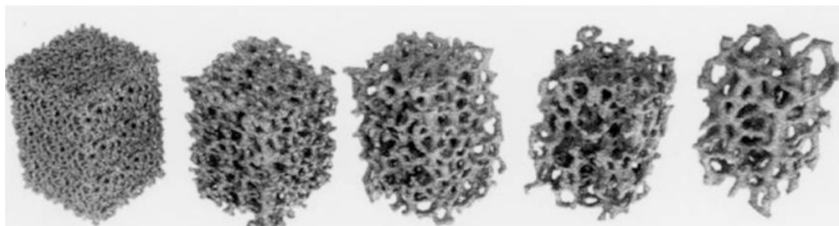


Pic. 1.21. *Engine and pump, wires and pistons integrated with grid structure for decrease of mass of humanoid robot's grab [6]*

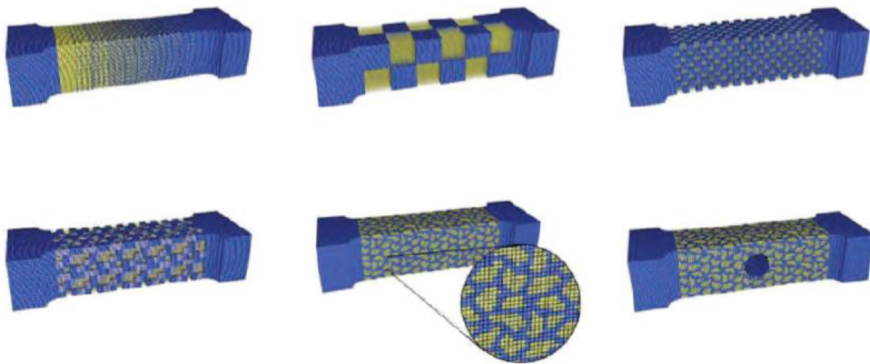
The emergent field – numerical designing and producing of gradient materials and structures, ultra-light, of programmed porosity and mechanical parameters (pic. 1.22, pic. 1.23, pic. 1.24).



Pic. 1.22. *Sintering of round structures of programmed porosity of material*



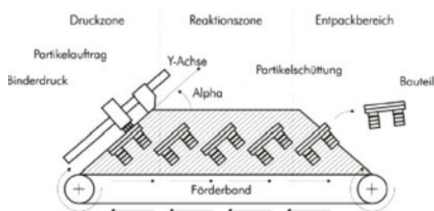
Pic. 1.23. *Building of tructures of programmed porosity with RP methods*



Lipson, H., & Kurman, M. (2013). *Fabricated: The New World of 3D Printing*. Indianapolis, Indiana: John Wiley and Sons, Inc.

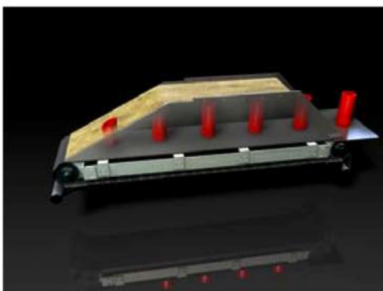
Pic. 1.24. *Materials of discrete structure and mechanical features gained in generative technologies*

They are undertaken in a wide scope of trials of systems (pieces) building of multi-materials, e.g. steel, bronze (CuSi3%), and in the scope of massive production of elements in RP technologies trials of automation of these processes are undertaken – of constant fabrication (pic. 1.25).



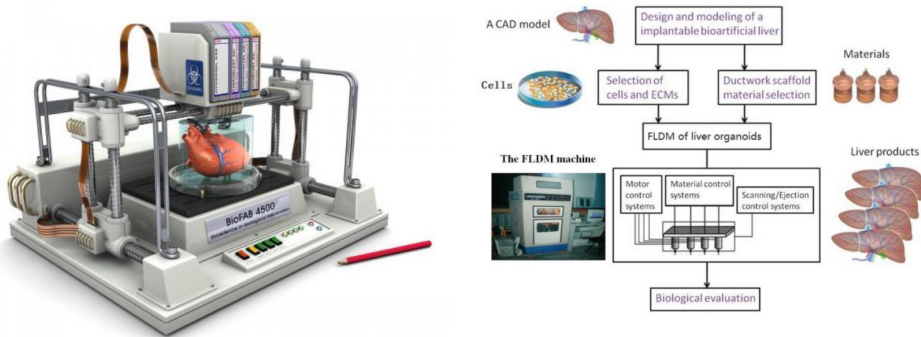
Neu: Endlos 3D Drucker

v·xeljet



Pic. 1.25 *The device for serious production of elements in RP technology [28]*

In the area of medical technologies, generative technologies are tested i.e. in the scope of possibilities and fabrication of e.g. implants and also so-called 'bio-printing' of human organs (pic. 1.26.).



Pic. 1.26. 3D printer for building of human organs – a) [29], and example of integration of materials in RP in intelligent fabrication of human organs [30]

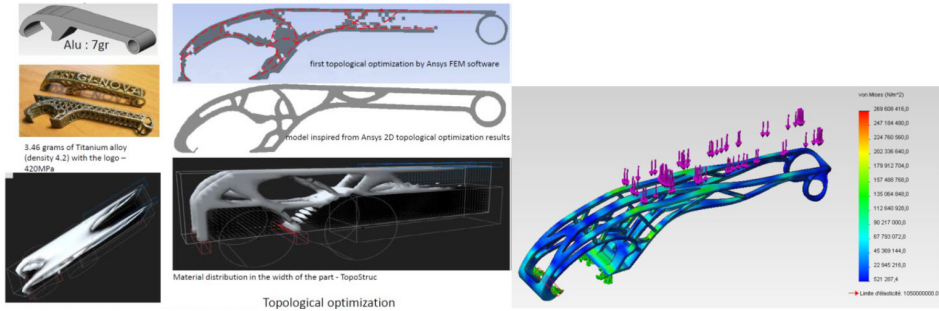
Optimization in techniques of fast prototyping

Development of RP technology has proved that an especially important issue is optimal designing both of construction and the process of fabrication itself. It is reflected in mass, stiffness of construction and also in the costs and time of metals fabrication. An especially important is a proper use of methods of construction's optimization, including topological optimization.

A typical optimization issue, independently from chosen algorithmics, consists of the following elements:

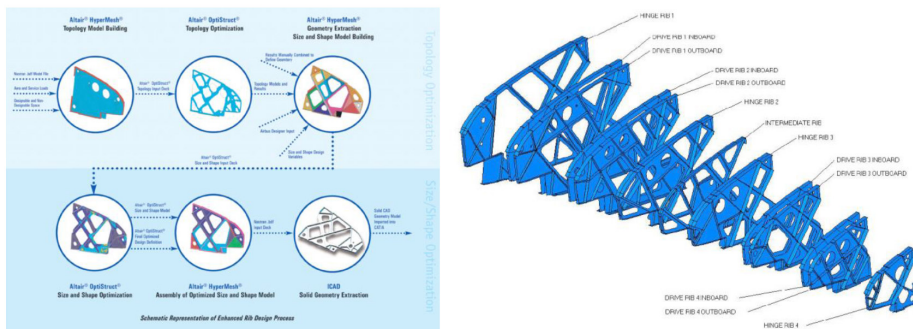
- The MES model along with any number of loads states: resistance, vibration, heating, and also acoustic; under certain conditions one may also define non-linear issues,
- Set of designing variables: material, topological, of shape, of dimension,
- The function of purpose which is usually minimization of mass or reduction of vulnerability,
- Scalar limiting conditions; usually it is about not crossing permissible stresses and keeping of proper folding, or definition of boundary frequencies of own vibrations,
- Technological conditioning; HW/OS can force spatial repetition of found distribution of masses, and also taking into consideration the kind of fabrication process,
- Additional options, e.g. max. number of iteration or level of the so-called discretition of target construction in topological optimization.

The use of topological optimization in designing allows to restrain considerably e.g the mass of detail (of construction), time of fabrication and energy inputs, which is especially important, particularly in designing of crafts or cosmic constructions. The idea of such optimization is illustrated in the pic. 27.



Pic. 1.27. The essence of topological optimization with the limit of mass details of titan alloys [31]

Topological optimization uses most frequently the discretization of construction space with the use of finite element method. Algorithm of optimization assigns the parameter of density η , called pseudodensity, to each of finite elements of the construction. This parameter may change during optimization in the range $<0,1>$. It is treated here as decisive variable. For each finite element the value 0 is equivalent to its remove from the construction, which is connected with reduction of an object's mass. The criterion of finite element remove may be connected with e.g. elimination of the least deforming elements or the least swollen ones. Most frequently the function of purpose for the problem of topological optimization is minimization of the mass by limitations connected with the taken parameter of state (stress or deformation. Searching of e.g. maximal stiffness of construction and maximal frequency of vibrations are also possible [15].



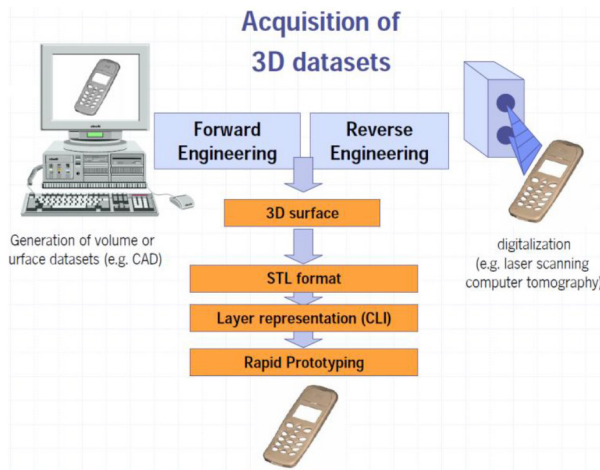
Pic. 1.28. Example of shape's optimization procedure, the size and mass of elements of a plane's wing, fabricated in RP technology [32]

2. Reverse engineering

The reverse engineering (RE, eng. Reverse Engineering) is a technology allowing to reconstruct construction rules of already existent objects. It is used for the aim of recognition of rules, according to which an object has been designed and then projected. In fabrication industry it consists in reconstruction of product's geometry, the rule of working and sometimes materials of which the object has been made. Reverse engineering is also used in other fields, e.g. in IT, in which it consists in analysis of existent program aiming at understanding of its work and/or reconstruction of its source code [8].

Reverse *engineering in reference to industry is most frequently identified with digitalization of physical objects geometry*. Its result is a numeral form of model, being the basis of further construction works, computer analyses (e.g. with finite element method) or comparisons of physical models with the computer one. Gaining of numeral form of model allows also to use these data directly in wider and wider used technologies of computer aided fabrication (deficiency processing on machines steered numerically, fabrication with incremental method in Rapid Prototyping, Rapid Tooling and Rapid Manufacturing methods etc.

Reverse engineering techniques are more and more widely used in industry, not only as tools of development and products designing, but also as the systems of production supervising. They provide a fast control dimension of practically each produced fabrication. Such examination lasts from a couple to dozen or so seconds and it consists in digitalization of chosen fragments or the whole surface of a fabrication, in comparison of the gained in that way data to a computer model. A typical programming used in Reverse Engineering technologies (RE) are: Magics, Mimics, Geomegic Studio etc.



Pic. 2.1. RP technology in the use of classic methods and RE [33]

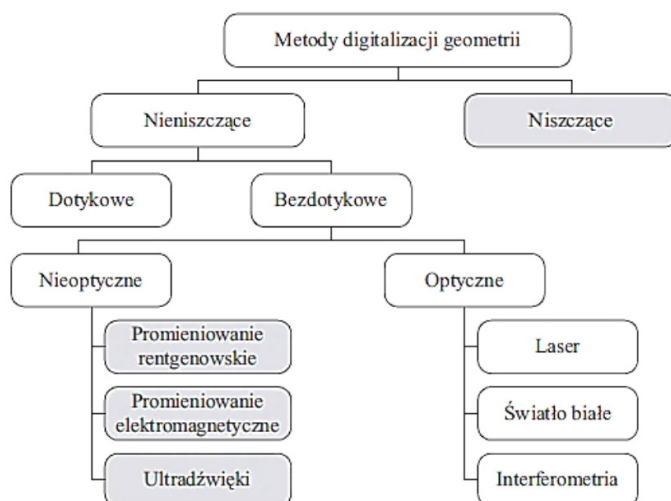
Uses of reverse engineering in the industry

The process of objects geometry patterning finds its use in the tasks as:

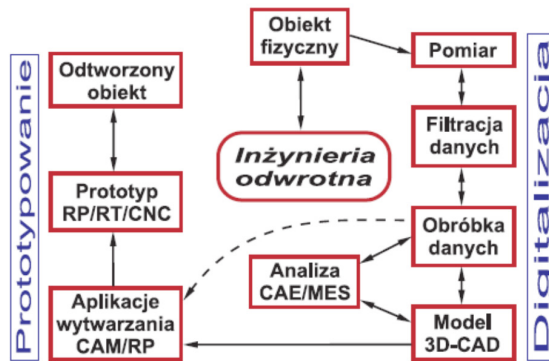
- Implementation of changes to prototypes or already produced elements,
- Working out of production technology of fabrication on the basis of unified product,
- Quality control of the elements produced,
- Reconstruction or generation of documentation of a respective product.

Digitalization methods [8]

Techniques of gaining information on 3D geometry are different with the way of dimension and sometimes with the kind of data which are gained as a result of their use. Taking into consideration the level of automation, the dimension can be made in by-hand, half-automatic or automatic mode. The by-hand mode requiring steering of dimension device by a user is used for reading dimensions of the models of relatively simple geometry, most frequently the prism ones whose models may be created from the bases in CAD system. In half-automatic mode, a measuring device saves chosen by a user fragments of geometry of an examined object, which requires initial definition of dimension area. In the case of dimension of the whole object, scanning in few clampings may be required, and next connecting of respective fragments of scanned surface in one numeral model. In automatic model geometry of the whole examined object may be intercepted without necessity of manual interference of a user in the process of digitalization, and the initial data reflect the full three-dimensional model of an examined object.



Pic. 2.2. *Methods of digitalization*



Pic. 2.3. Procedure of reverse engineering process [36]

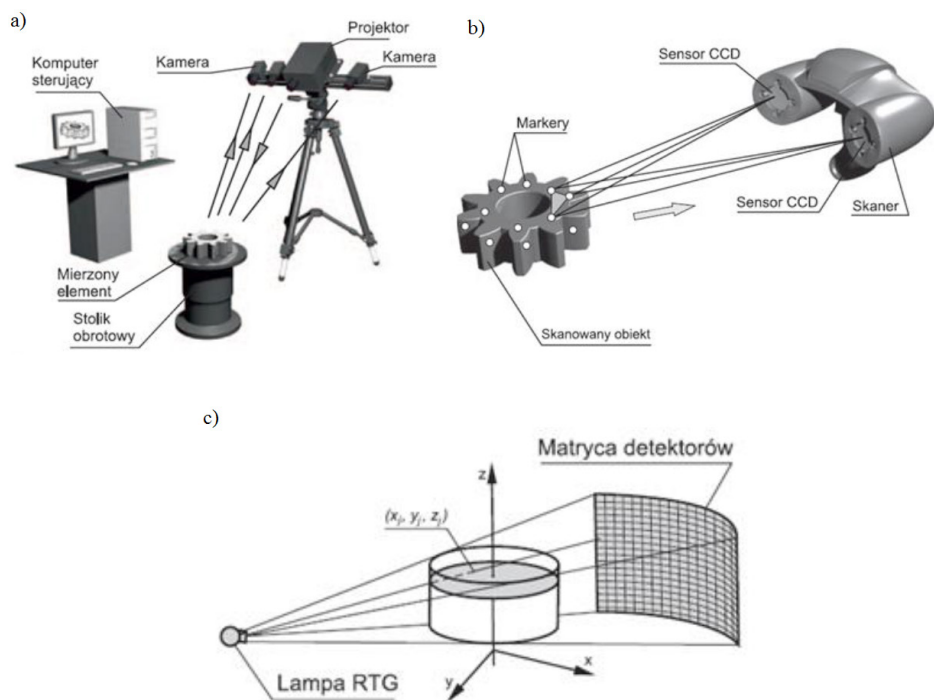
Data processing – digitalization of object [36]

In each RE method problems connected with specification and processing of data occur, e.g. hums, unimportant and incomplete data. Usually one cannot make a full dimension of an object. The provided data are then irregular and burdened with dimensionment error. The processing of large amount of dimensionment data is program- or device- limited. That is why dimensionment data are put to the process of reduction or filtration. They are the basis of approximation with curves (e.g. B-spline) and stretching of surface (e.g. Beziera, B-spline or NURBS). In the final stage, geometrical data are exported from 3D-CAD program (e.g. to IGES, STP, STL format) and used in fabrication process (CNC or RP).

Currently, one uses two fundamental ways of virtual element's model fabrication of complicated shape in RE process:

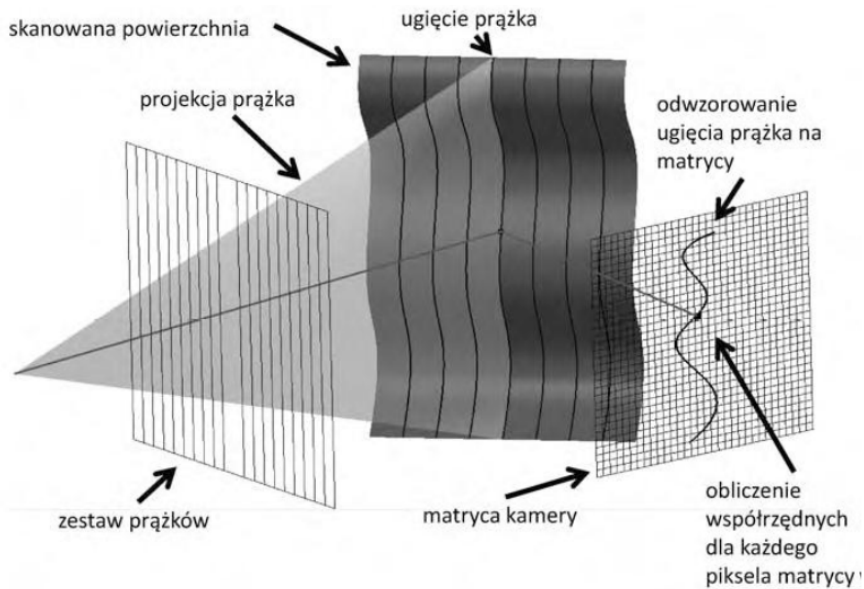
- Processing of given model to the set of mathematical equations describing modeled surface
- Creating of model with interactional ways of processing of physical object dimensionments results; one marks coordinates of points in 3D space, next one uses proper algorithms connecting the points gained as a result of scanning dimensionments.

The surface of examined model is usually an unknown surface. For its diagnosing one may use the approach of surface (flat) digitalization. The digitalized surfaces are divided into paths which are flat curves created by surfaces cutting through each other (digitalization surfaces) – curves are marked with paths of digitalization.



Pic. 2.4. Typical devices used in contactless methods of digitalization: a) optical 3D scanner, b) laser scanner, c) computer tomograph [36]

One of the most frequently exploited types of scanners in reverse engineering are optical scanners based on the projection of structural light, so-called ridge scanners. The projector of a scanner makes projection of a set of ridges of known density, on an examined object. Straight lines undergo deformation adequate to the size of deformation of object's surface; this image is registered by matrices of cameras. Using initial data (structure of light, image registered by the camera and its calibration parameters, angle between direction of projection and direction of readout) and mathematical equations coordinates for each pixel of the camera are calculated. The result of a separate dimensionment is the cloud of points whose number is dependent directly on resolution of the used cameras [35]. Using the initial data (structure of light, image registered by the camera and its calibration parameters, angle between direction of projection and direction of readout) and mathematical equations, coordinates for each pixel of the camera are calculated. The result of a separate dimensionment is the cloud of points which number is dependent directly on resolution of the used cameras (pic. 2.4).



Pic. 2.5. *The rule of ridge scanner working [35]*

The use of reverse engineering methods allows to:

- Interoperate – possibility of evaluation of machine's pieces cooperation, e.g. provided by many producers
- Reproduction of device documentation, of which it doesn't have (loss of documentation occurred or a producer hasn't made it available)
- Analysis of an object as an aim of components structure specification, approximation of costs or claiming of patents breaking
- Control revision of an object as regards keeping and maintenance of geometrical dimensions
- Duplicates creating
- Building of models aiming at numerical analysis of their work, resistance and behavior of their elements, groups or whole objects

Literature:

- [1] Rudnicki Z.: Nowoczesne techniki przyspieszające wytwarzanie. <http://www.kkiem.agh.edu.pl/dydakt/Wyklady/RapidProt12.pdf>
- [2] Katarzyna Chojnowska: Potencjał rynku Rapid Prototyping. Mat. rekl.: BIBUS MENOS Sp. z o.o.
- [3] Chlebus E.: Innowacyjne technologie rapidprototyping- rapidtooling w rozwoju produktu. Wrocław, Oficyna Wykładnicza politechniki Wrocławskiej, 2003.
- [4] Laboratorium Szybkiego Prototypowania – Politechnika Warszawska, Instytut Mechaniki i Poligrafii. Zakład Konstrukcji Maszyn i Inżynierii Biomedycznej. http://imik.wip.pw.edu.pl/kmib/index.php?option=com_content&task=view&id=55
- [5] Chlebus E. „Techniki komputerowe Cax w inżynierii produkcji” WNT, Warszawa 2000.
- [6] Lonnie J. Love: Emerging Manufacturing Technologies and Their Impact on Fluid Power, http://www.nfpa.com/events/pdf/2012_eehpc/ppt/17_nfpa%20manufacturing.pdf
- [7] Haraburda M.: Techniki szybkiego prototypowania w zastosowaniach przemysłowych. Wydział Inżynierii Produkcji, PW, Klub Innowacyjnych Przedsiębiorstw, Warszawa 27.04.2005.
- [8] Mechatronika Moduł 9: Szybkie Prototypowanie podręczniki, ćwiczenia, i rozwiązania. Edward Chlebus (i inni). http://www.adam-europe.eu/prj/3810/prd/1/5/Modul%209_polnisch_komplett.pdf, www.minos-mechatronic.eu
- [9] Carsten Tille & Hermann Seitz : 3D-Printing and Stereolithography –powerful manufacturing tools for textured or high-precision 3D city models. http://www.ikg.uni-bonn.de/fileadmin/nextgen3dcity/pdf/NextGen3DCity2005_Tille.pdf
- [10] <http://www.additive3d.com/publ.htm>
- [11] G. Budzik , M. Sobolak, D. Kozdęba: Wykorzystanie technologii rapid prototyping w odlewnictwie precyzyjnym. Archiwum odlewnictwa, Rok 2006, Rocznik 6, Nr 18 (2/2), PAN – Katowice. PL ISSN 1642-5308
- [12] Brett Lyons: Additive Manufacturing in Aerospace; Examples and Research Outlook. Frontiers of Engineering 2011, Additive Manufacturing. <http://www.naefrontiers.org/File.aspx?id=31590>
- [13] Skalski K., Haraburda M.: Generatywne techniki wytwarzania w rozwoju innowacji.
- [14] Chlebus E.: Zawansowane technologie dla lotnictwa. Centrum Zaawansowanych Technologii Wytwarzania – CAMT/FhG PC Politechnika Wrocławska, Wrocław 11 września 2014
- [15] Mrzygłód M., Michalik M: Optymalizacja topologiczna z ograniczeniem naprężeniowym konstrukcji pojazdu. PAK, Vol. 54, nr 7/2008.
- [16] Gebhardt A.: Rapid prototyping. Carl Hanser Verlag, Munich, 2003

- [17] CUSTOMPART.NET: <http://www.custompartnet.com/>
- [18] Simon Merkt, Christian Hinke, Mohammad Dalaei, Antti Salminen, Tuomas Purtonen, Jan Bültmann: Compressive behavior of lattice structures in solid shells manufactured by SLM. NOLAMP 14, Gothenburg, August 26-28, 2013
- [19] <https://www.additively.com/en/learn-about/laser-sintering>
- 20 <http://www.przyrostowo.pl/technologie/fdm>
- [21] Gareth Bradshaw: Non-Contact Surface Geometry - Dimensionment Techniques. <https://www.cs.tcd.ie/publications/tech-reports/reports.99/TCD-CS-1999-46.pdf>
- [22] Rapid Prototyping (RP) - Michell Griffith, John Lamancusa <http://www.slidefinder.net/r/rapidprototyping2/rapidprototyping2/27961318>
- [23] Laser freeform manufacturing. DPM WORKSHOP November 13-14, 2012. <http://www.rpmandassociates.com/RPMILaserDepositionTechnology.aspx>
- [24]. William E. Frazier: Metal Additive Manufacturing: A Review. Journal of Materials Engineering and Performance. (2014) 23:1917–1928.
- 25] M P Groover: Fundamentals of Modern Manufacturing. John Wiley & Sons, Inc. 2007
- [26] 3D-printed aeronautics demonstrator. http://www.esa.int/spaceinimages/Images/2013/10/3D-printed_aeronautics_demonstrator
- [27] Sue Dunkerton: Integrating materials and processes to manufacture new products. Industrial Technologies 2012.
- [28] Gideon N. Levy : Additive Manufacturing in Manufacturing: A future oriented technology with high degree of innovation potentials- are we ready? Challenges and Chances to handle. 18th edition of the AEPR forum 24 -27 June 2013. https://csissaclay.files.wordpress.com/2013/10/aepr_2013_levy.pdf
- [29] Mary-Ann Russon: 3D Printers Could be Banned by 2016 for Bioprinting Human Organs. <http://www.ibtimes.co.uk/3d-printers-could-be-banned-by-2016-bioprinting-human-organs-1434221>
- [30] Xiaohong Wang, Jukka Tuomi, Antti A. Mäkitie, Kaija-Stiina Paloheimo, Jouni Partanen and Marjo Yliperttula: The Integrations of Biomaterials and Rapid Prototyping Techniques for Intelligent Manufacturing of Complex Organs. Materials Science » Biomaterials » “Advances in Biomaterials Science and Biomedical Applications”, book edited by Rosario Pignatello.
- [31] Pierre Marie Boite: De l'imprimante 3D à la fabrication additive. Les ateliers de l'information. Mardi 15 Avril 2014. <http://cyan1.grenet.fr/podcastmedia/ateliers-info-BUsciences/20140415-AT71-impression-3D.pdf>.
- [32] Fred van Keulen, Matthijs Langelaar: Engineering Optimization. Concepts and Applications
- [33] Carsten Tille & Hermann Seitz : 3D-Printing and Stereolithography –powerful manufacturing tools for textured or high-precision 3D city models.
- [34] Wyleżoł M. : Inżynieria odwrotna w doskonaleniu konstrukcji. Mode-

lowanie Inżynierskie. 32, s. 485-490, Gliwice 2006. http://www.kms.polsl.pl/mi/pelne_1/wylezol.pdf

[35] Kowalski M., Kowalski M., Paszkiewicz R., Kuczko W. , Wichniarek R., Zawadzki P.: Automatyzacja procesu skanowania na podstawie danych pozyskanych z pomiarów fotogrametrycznych. Postępy Nauki i Techniki NR 7, 2011.

[36] Budzik G. , Pająk D. : Metody inżynierii odwrotnej. Nowe technologie. Listopad-grudzień 2010 r.